ENHANCING THE EFFICIENCY OF INJECTION MOLDING AND IMPROVING THE QUALITY OF AUTOMOTIVE PARTS BY MEANS OF THE INDUCTION HEATING TECHNOLOGY

SINEENAT TONGJOY

A THESIS SUBMITTED IN PARTIAL FULFILLMENT
OF THE REQUIREMENT FOR THE DEGREE OF
MASTER OF ENGINEERING IN AUTOMOTIVE ENGINEERING
(INTERNATIONAL PROGRAM)
INTERNATIONAL COLLEGE
KING MONGKUT'S INSTITUTE OF TECHNOLOGY
LADKRABANG
2015

KMITL-2015-IC-M-004-05

THESIS TITLE	ENHANCING THE EFFICIENCY OF INJECTION MOLDING AND IMPROVING THE QUALITY OF AUTOMOTIVE PARTS BY MEANS OF THE INDUCTION HEATING TECHNOLOGY
STUDENT NAME	MS. SINEENAT TONGJOY
STUDENT ID	56610004
DEGREE	MASTER OF ENGINEERING
PROGRAM	AUTOMOTIVE ENGINEERING (INTERNATIONAL PROGRAM)
YEAR	2015
THESIS ADVISOR	ASST.PROF.DR. PREECHAR KARIN DR. PATCHAREE LARPSURIYAKUL PROF. ISAO SATOH ASSOC.PROF. TAKUSHI SAITO

ABSTRACT

Injection molding is a popular process in the automotive part industry because of its advantages such as short cycle times, high production rate, high quality of part surface, easy to produce the complex geometry parts, good mechanical properties and low cost. Although injection molding has many advantages, some defects frequently occur in the molded parts such as weldline, surface gloss, and flow mark, etc. Heat and Cool technology has been recently used to improve the surface appearance and quality of molded parts due to capability in thermally cycling the mold surface temperature. Induction heating is the interesting technique that can rapidly heat and cool the mold surface and is most likely to save the cost.

This study is the examination of the influence of induction heating system on the injection molding process before applying this technique to further produce the real automotive parts. The experiments were divided into two main phases. The first phase is preliminary study of induction heating system, which matches the types of mold inserts, process parameters, and induction coil. To investigate the influence of induction heating, a new special mold insert was designed and produced namely test

mold. The experiment results showed that mold insert which is SKD61 with heating power and coupling gap of 80% and 17.5 mm provided the best heating rate at about 10°C/s. This condition was used as the induction heating condition for test mold injection in the second main phase. The second phase is the main experiment of test mold which study the influence of process parameter including induction heating for injection molding on the properties of molded parts. This phase includes the design of experiment by Taguchi method, injection, property testing of molded part, result analysis by regression analysis, and validation. There are three different material used as molding materials: PC, PC/ABD and PA6GF30, and four process parameters: injection speed, packing pressure, heating temperature by the induction heating or the mold surface temperature before the filling stage, and water temperature were studied the effect on five properties: weldline, surface gloss, flexural strength of weldline, surface roughness and warpage, based on Taguchi experimental layout. From the results, it was found that the induction heating successfully improved the surface appearance such as weldline, surface gloss, and surface roughness of molded parts especially on the elimination of weldline. However, the induction heating did not enhance the warpage and mechanical property like flexural strength of weldline.

ACKNOWLEDGEMENTS

This thesis was successfully completed with assistance and kindness of many people

Firstly, I would like to express my sincere gratitude to my researcher-advisor, Dr.Patcharee Larpsuriyakul for providing the main idea of this research and also her invaluable and constructive suggestions during the planning and development of this research. Also I would like to sincerely thank Asst. Prof. Dr. Preechar Karin for his great support and suggestion. In addition, I really appreciate Prof. Isao Satoh and Prof. Takushi Saito from Tokyo Institute of Technology for their kind suggestion and kindness.

My grateful gratitude are also extended to Mr.Dumrong Thanomjitr for his guidance and help in injection molding process, to Mrs.Natcha Prakymoramas and the staff members of polymer laboratory, for their support in doing the experiments.

I would like to thank National Science and Technology Development (NSTDA) which provided the golden opportunity and full scholarship for studying in the master program. This research would have been impossible without the support of National Metal and Materials Technology Center (MTEC), T. Krungthai Industries Public., Ltd. and NSTDA-University-Industry Research Collaboration.

Finally, I wish to thank my parents for their great support and encouragement throughout my study.

SINEENAT TONGJOY

TABLE OF CONTENTS

LIST OF TABLES

LIST OF FIGURES

CHAPTER 1
INTRODUCTION

1.1 Background And Problem Statement

Nowadays plastics have been being popular in a wide variety of industrial applications including the automotive parts. Many plastic automotive parts, i.e. dashboard, door trim, assist grip, headlight covers, and tonneau cover etc., are manufactured by the injection molding technology. Injection molding is one of the most widely used process for manufacturing plastic products because of its advantages such as short cycle times, high production rate, high quality of part surface, easy to produce the complex geometry parts, good mechanical properties and low cost. Although injection molding has many advantages, some defects frequently occur on the injection-molded parts such as weldline, surface gloss, and warpage etc. These problems result in a lower quality of product, both in terms of strength and cosmetic appearance. The aesthetics of injection molded products can be solved by secondary operations such as spray painting, polishing, etc., which make the cost higher.

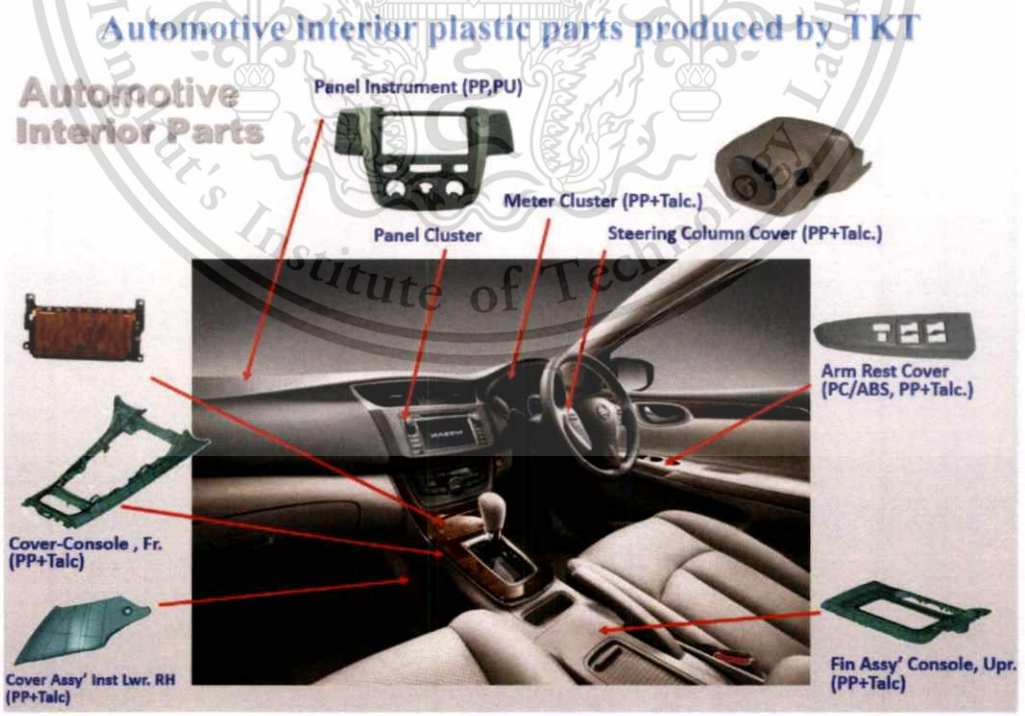

Figure 1.1 The automotive interior plastic parts produced by T.Krungthai Industries Public Company Limited (TKT).

T.Krungthai Industries Public Company Limited (TKT), which is a Thailand-based company, is the marketing leader in service of production of automotive plastic part and concern industry with quality and service. The automotive interior plastic parts as shown in Figure 1.1 produced by the company also encounter the injection molding defects. These defects cause the high rate of waste and more production process leading to the uncertain quality of plastic parts. Hence, the production process improvement is required to keep the production stable and quality. With this solution, TKT engineers have considered that applying Heat and Cool technology to the problematic molded plastic part likely cause the production stability and the same quality level. Therefore, TKT Company had decided to research and develop Heat and Cool technology by working together with National Metal and Materials Technology Center (MTEC) of which is a public organization operating under the National Science and Technology Development Agency (NSTDA). There are various types of Heat and Cool technology, so the preliminary study were conducted. It was found that Surface Heat & Cool technique by Induction Heating is probable technique with the least cost such as mold production cost, invested tool cost, and running cost. With these advantages, TKT Company and MTEC had decided to study and improve Heat & Cool by Induction heating with test mold part which is the new designed-part for this case. If this phase is achieved with using induction heating, the shifter trim plate as shown in Figure 2.2 is further molded by means of induction heating. The problems of shifter trim plate required to be improve are weldline, sink mark / flow mark and warpage.

Therefore, this study is a part of collaborative project between TKT Company and MTEC. The focuses on the effect of induction heating and other processing variable on the injection molded part.

1.2 Objective Of The Study

1.2.1 To enhance the efficiency of productivity and solve the defects of automotive parts by means of the induction heating technology.

1.2.2 To study the injection molding control parameters with induction heating to get process stability and quality part.

1.2.3 To apply knowledge of this research as guideline to solve quality defects of other industrial parts.

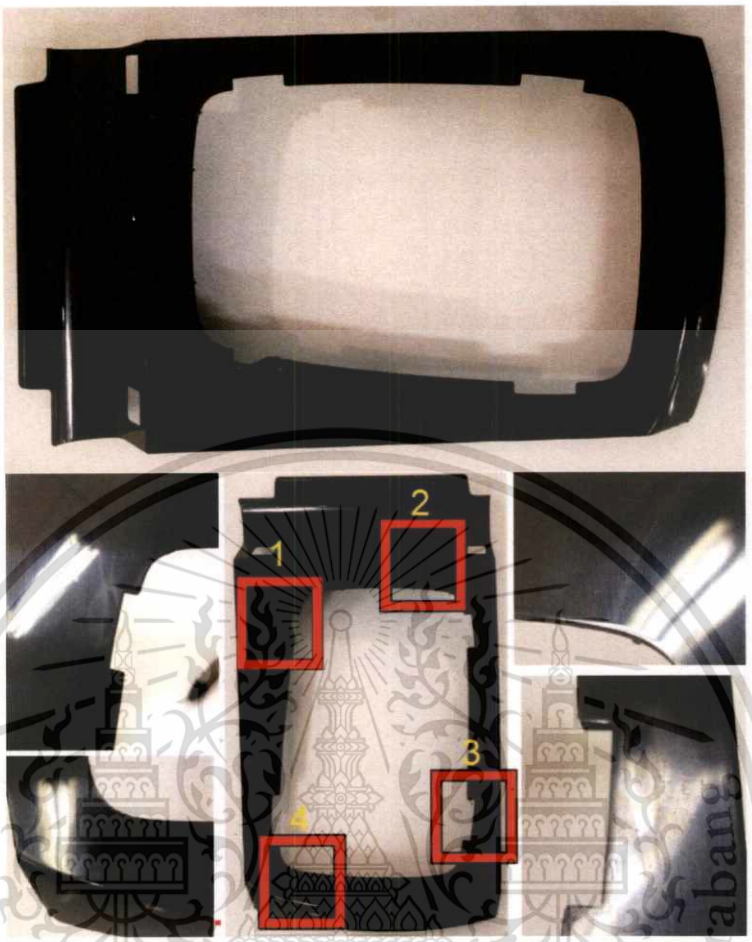

Figure 1.2 Shifter Trim Plate for injection molding by aid of induction heating

1.3 Hypothesis To Be Tested

1.3.1 Productivity and defect parts can be improved with technology induction heating.

1.4 Scope Of the Study

1.4.1 The induction coil in this study was designed by Taiwan consultant.

1.4.2 The test mold parts were examined for five properties such as weldline, gloss, flexural, roughness, and warpage.

1.4.3 The optimal processing parameter of each material and the ranking of each parameter affecting the interested property were determined by the coefficient values obtained from the regression analysis.

1.5 Expected Benefits

1.5.1 Enhancing the potential of student in the task of improving the quality of plastic parts using induction heated mold technology.

1.5.2 Developing the injection molding process by means of induction heating technology.

1.5.3 Understanding the term and concept of design of experiments using the taguchi approach.

CHAPTER 2
LITERATURES REVIEW

This chapter describes the related theory and research to this study.

2.1 Theory

2.1.1 Plastic Injection Molding

In injection molding, a plastic is heated and molten as polymer melt and then injected with high pressure into a mold through sprue, runners and gate to fill the all cavities. After the cooling stage, the molded parts are ejected from the mold at the end of the injection molding process.

Injection molding is one of the most widely used process for manufacturing plastic products (from the smallest component to entire body panels of cars). Its advantages and disadvantage are as follows [1]:

- **Advantages**
  1.) Short cycle times
  2.) High production rates
  3.) High quality of part surface
  4.) Easy to produce the complex geometry parts
  5.) Good mechanical properties
  6.) High tolerances are repeatable
  7.) Wide range of materials can be used
  8.) Low labor costs
  9.) Minimal scrap losses
  10.) Little need to finish parts after molding

- **Disadvantages of Injection Molding**
  1.) Expensive equipment investment
  2.) Running costs may be high
  3.) Some defects frequently occur in the molded parts.
  4.) Parts must be designed with molding consideration

2.1.1.1 Injection Molding Machine

Generally, the injection molding machine consists of two principal components are described below.

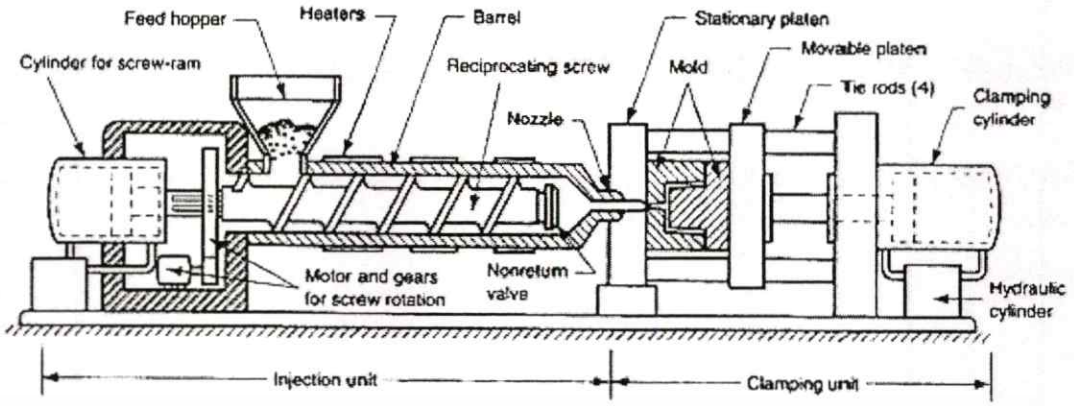

Figure 2.1 Structure of the injection molding machine [2]

1) Injection Unit

The injection unit is unit where is responsible for all injection activities. The function of the injection unit is to receive the plastic resins from hopper, heat and melt them to a uniform and homogeneous melt, convey the melt to the nozzle and then inject them through the nozzle into the cavity of mold. The injection unit includes the hopper, barrel, heater bands, rotating screw with non-return valve, hydraulic cylinder and pistol and drive motor. Figure 2.2 illustrates the schematic drawing of the elements of an injection unit. The unit may be a ram fed or screw fed.

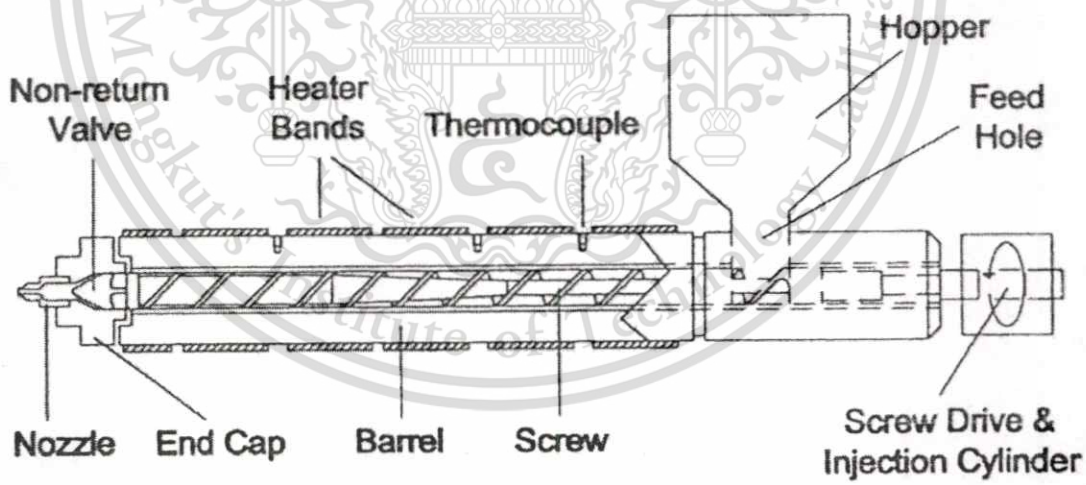

Figure 2.2 Elements of an injection unit of an injection molding machine [3]

2) Clamping Unit

The clamping unit is involved with the performance of the mold. Its function is to hold the two halves of mold together in appropriate alignment and slide the half of the mold or the moving platen forward and backward for the mold opening and closing. It provides a sufficient

clamping force to resist the injection force to keep the mold closed during the melt is injected, cools down and ejects the molded part. The clamping unit consists of two platens, a stationary platen and a moving platen, tie bars, and ejection system as shown in Figure 2.3.

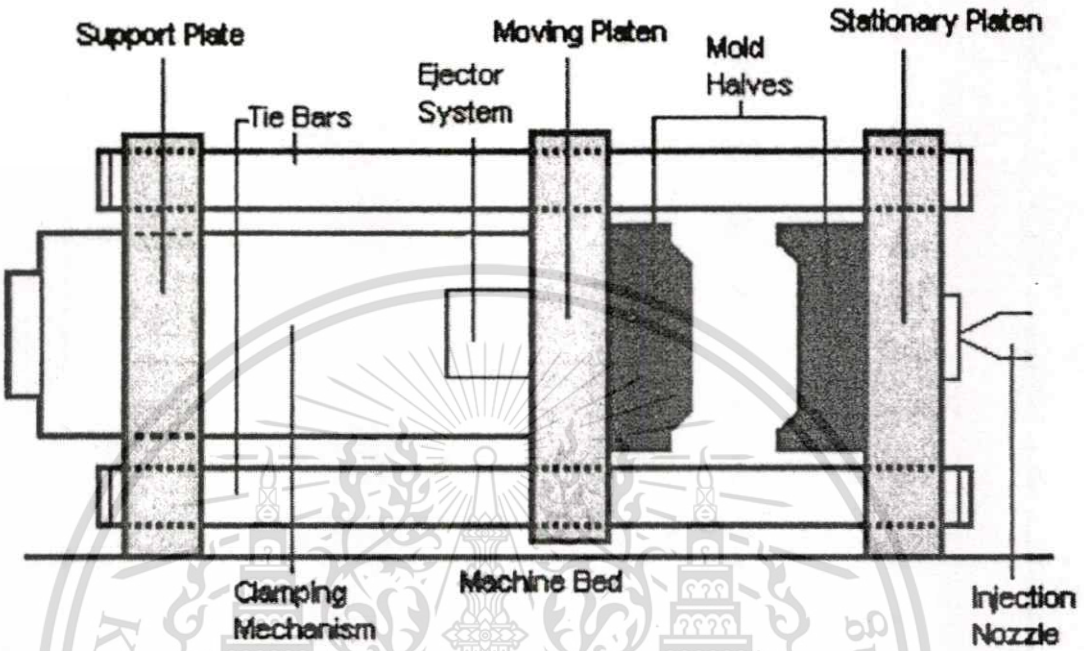

Figure 2.3 Elements of a clamping unit of an injection molding machine [3]

2.1.1.2 Stages Of Injection Molding

The process of injection molding can be divided into six major separate stages: mold close, filling or injection, packing and holding, cooling, mold open, and finally ejection. The total amount of time to perform all of the stages in producing an injection molded part is called the cycle time. That is the time from mold close to mold open. Among these stages, the cooling stage takes up 50 to 80 percent of the cycle time [4]. Figure 2.4 illustrates the basic molding process components and chart of cycle time. The operation of an injection molding machine and the cavity pressure versus time profile during the process are illustrated as Figure 2.5(a) and Figure 2.5(b), respectively.

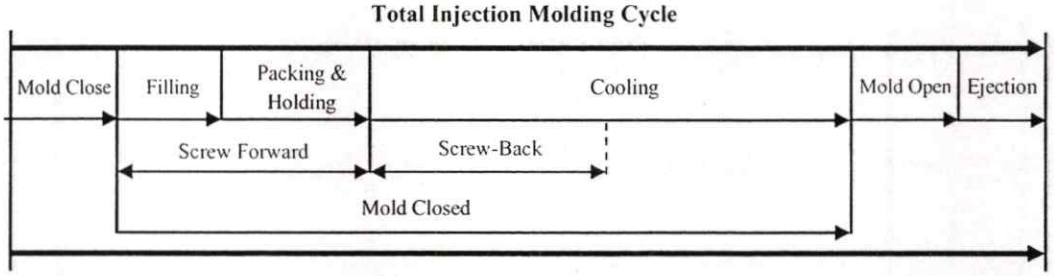

Figure 2.4 Major stages of the injection molding cycle and its cycle time.

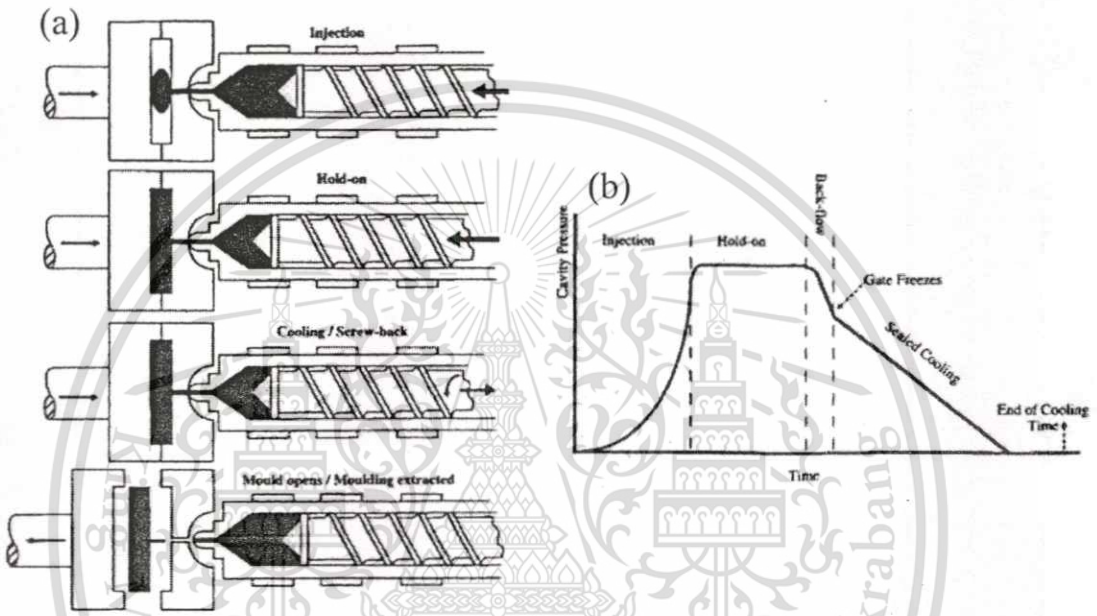

Figure 2.5 The operation of an injection molding machine is demonstrated as (a) the schematic of injection molding process and (b) the schematic of cavity pressure versus time profile [5].

The details about six major stages of injection molding process are described below.

1.) Mold close

The moving platen mold slides toward the stationary platen to close the mold and is locked the mold halves together securely to prevent the mold open due to the resistance force inside the mold.

2.) Filling

The inject unit moves to the mold until touches the sprue bushing. The melt is quickly injected to fill the mold cavity.

3.) Packing and holding

In packing phase, the additional melt is further injected into the cavity in order to compensate for the part thermal shrinkage. This phase is

switch from velocity control to pressure control which typically takes place before the cavity is filled. Holding pressure is then applied to keep the melt in the cavity till the gate has frozen or solidified. After the gate freezes off, the part continues to shrink without melt compensation.

4.) Cooling

Once the holding is over, the cooling starts to solidify the molded part. At that time, the injection unit retracts from mold to prevent lowering the nozzle temperature as the melt solidifies that can cause the melt in front of nozzle is too viscous until cannot flow. Screw-back occurs during the cooling time and is the plastication or preparation of the melt for the next shot. The mold is still closed until the end of the cooling time. This step take the longest time within an injection molding cycle.

5.) Mold open

The mold is opened at the end of the cooling step.

6.) Ejection

When the mold is completely opened, the injection molded part is ejected from the mold.

2.1.2 Heat & Cool Technology

Rapid heat cycle molding (RHCM) is an injection molding technology, which the mold is heated and cooled rapidly. In one molding cycle, RHCM process can be divided into four stages: heating, high temperature holding, cooling and low temperature holding according to the mold temperature state. Figure 2.6(a) illustrates the principle of the rapid heating cycle in the injection molding process. Before the filling or injection stage, the mold is heated above the melt's glass transition temperature (Tg) to a preset high temperature. When the mold temperature reaches the preset high temperature, the heating stage is over. Then, the high temperature holding stage starts and keeps up during the filling and packing. It is completed after the end of packing and the process goes into the cooling stage. In this stage, the mold and melt are rapidly cooled down to the low temperature by cooling water as coolant to solidify the melt in the mold cavity. After the cooling stage is finished, the mold is opened for part ejection with the low temperature holding stage begins. That is RHCM injection cycle. For the next RHCM injection cycle, the mold will be heated again.

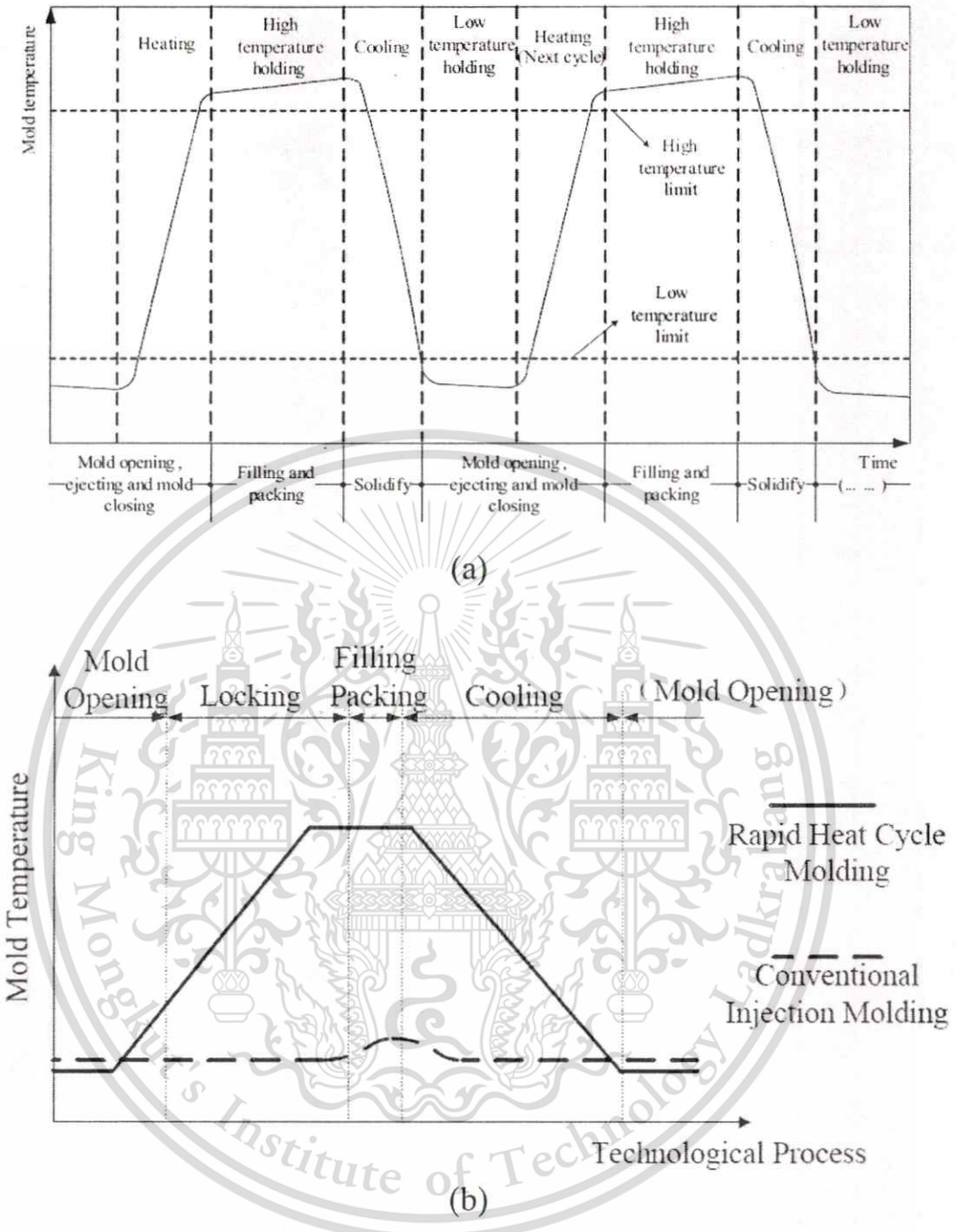

Figure 2.6 Schematic of (a) the mold temperature changing curve during the RHCM process [6] and (b) the difference of mold temperature changing curve between RHCM and conventional injection [7].

With RHCM, the cavity surface prior injection is higher temperature level than that in conventional injection molding (CIM) as shown in Figure 2.6(b). It prohibits or slows down the phenomenon of premature freezing of the polymer melt during filling stage and results in preventing the frozen

layer that occur in CIM that decreases viscosity of the melt and helps the melt can easily flow into the cavity [8]. Figure 2.7 demonstrates the frozen layer occurs in CIM and disappears from RHCM. For this reason, RHCM can solve the molding defects in CIM such as short shot, weld line, flow mark, jetting mark, and warpage. One of RHCM techniques is induction heating which described in more detail in the next section.

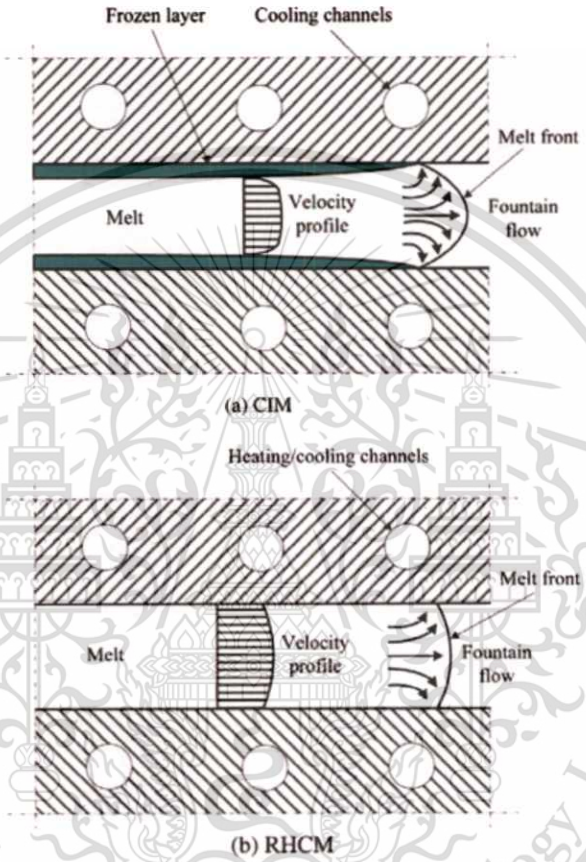

Figure 2.7 Schematic of the filling process of the polymer melt in CIM and RHCM [9].

2.1.3 Induction Heating

Induction heating is a non-contact heating process. It is a rapid, precise, repeatable, safe and efficient approach of electrically-conductive object heating. The high-frequency alternating current is applied to the induction coil to heat the electrically-conductive materials. The heat is generated within the workpiece by eddy current which differ from other heating methods where heat is generated in a heating element or flame and is then applied to the workpiece.

2.1.3.1 Principle Of Induction Heating

The induction heating system comprises of an alternating-current (AC) power supply, induction coil, water cooling and workpiece. Due to a great number of current is provided to the induction coil, the water cooling is required to remove the waste heat from coil.

Induction heating can generated heat within a part by two mechanisms of energy dissipation. These mechanisms are eddy current heating and hysteretic heating.

Eddy current heating is caused from the resistance to the flow of electricity in the metal part called workpiece that results in power losses in the form of heat according to the law of conservation of energy. With this law, eddy currents produce heat in workpiece by Joule effect: P = I2R, where I is the amount of current, and R is the resistance. Figure2.8 illustrates the principle of induction heating that induce eddy current within workpiece. All electrically conductive metals have the resistance to the flow of electricity. Eddy current heating can occur in both nonmagnetic and magnetic materials. For nonmagnetic materials such as copper, steel, and aluminum at above the Curie temperature, there is only mechanism of eddy current heating. This mechanism is the primary mechanism in ferromagnetic materials such as steel, and nickel at below the Curie temperature. The alternating electric current passed through the induction coil causes the nonuniform current distribution in the cross section of coil. The maximum current density will be on the surface of coil as shown in Figure2.9. This is called "skin effect". It is also found in the workpiece heated by induction coil. The AC current generates a time-variable magnetic field surrounding the coil which has the same frequency as the current of coil. When the coil is placed near the workpiece, this magnetic field induces an equal and opposing electrical current known as eddy currents flowing in closed loops within workpiece. The skin effect causes these currents are most concentrated at outer surface of workpiece as a thin skin. Thus, the heat is limited to workpiece's surface or localized areas that adjacent to the induction coil. The heated depth from the skin effect, is called penetration depth. It is also named as reference depth or skin depth. The penetration depth is mainly dependent upon the frequency of AC field the properties of heated workpiece such as the electrical resistivity and the relative magnetic permeability. The penetration depth is defined as the thickness layer or depth from the outside where 87 % of the power (the heat due to the resistance of the current flow) or 63 % of the current density is occurred [10].

Hysteretic heating is caused by the friction between molecules known as magnetic dipoles which occurs only in ferromagnetic materials. The dipoles is regarded as small internal magnets. As ferromagnetic metals

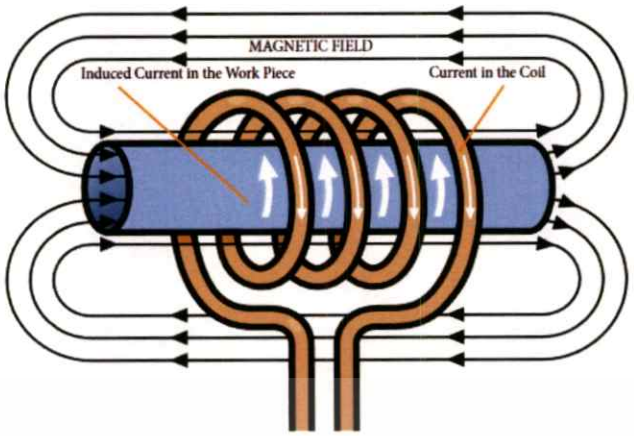

Figure 2.8 Principle of induction heating [11].

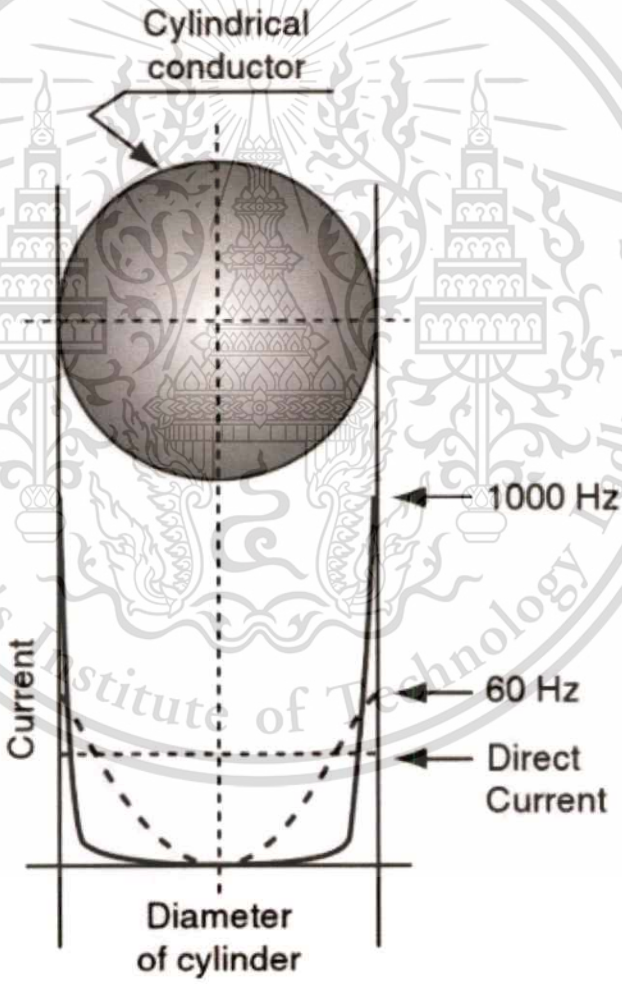

Figure 2.9 Current distribution as function of frequency due to skin effect [12].

are being heated by induction heating from room temperature, the alternating magnetic field created by the coil results in the changing of

magnetic polarity of the material. The energy required to turn the small internal magnets around, which is a sort of friction, is transformed into a minor amount of heat. This is so-called hysteresis losses. Figure2.10 shows the effect of hysteresis on heating rate. Hysteresis heating ends when material is heated above the Curie temperature which it becomes nonmagnetic and the reversal of dipoles does not occur [10].

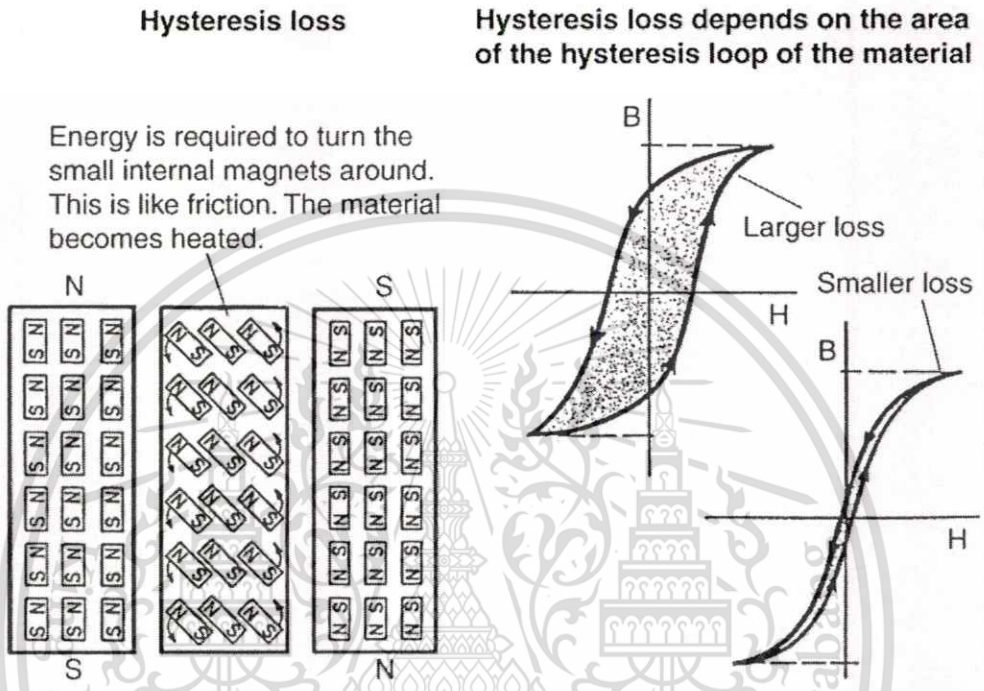

Figure 2.10 Effect of hysteresis on heating rate. N, north; S, south; B, flux density in a ferromagnetic material; H, corresponding magnetic intensity [10].

In induction heating, hysteretic losses is so small compared to eddy current losses that has a much greater impact on overall heat generation. Therefore, hysteretic losses can be ignored.

The heating rate of the workpiece depends on the intensity of the induced current, the frequency of the induced current, and the physical properties of the workpiece which are the electrical resistance, the specific heat, and magnetic permeability. These physical properties are the temperature-dependent properties that change with temperature. The specific heat increases with temperature. This means that when the workpiece is hot, it will need more required energy to heat the workpiece than when it is cold. The resistivity also increases as temperature increases.

2.1.3.2 Coil Design

An induction coil design plays an important role in the efficiency optimization of an induction heating process. Before design the coil, it needs to know where the heat required to be generated on workpiece for the optimization of coil design to achieve the maximum heating efficiency. In the other words, the coils can be designed in the various types and styles depending on the shape of workpiece surface to be heated as shown in Figure 2.11.

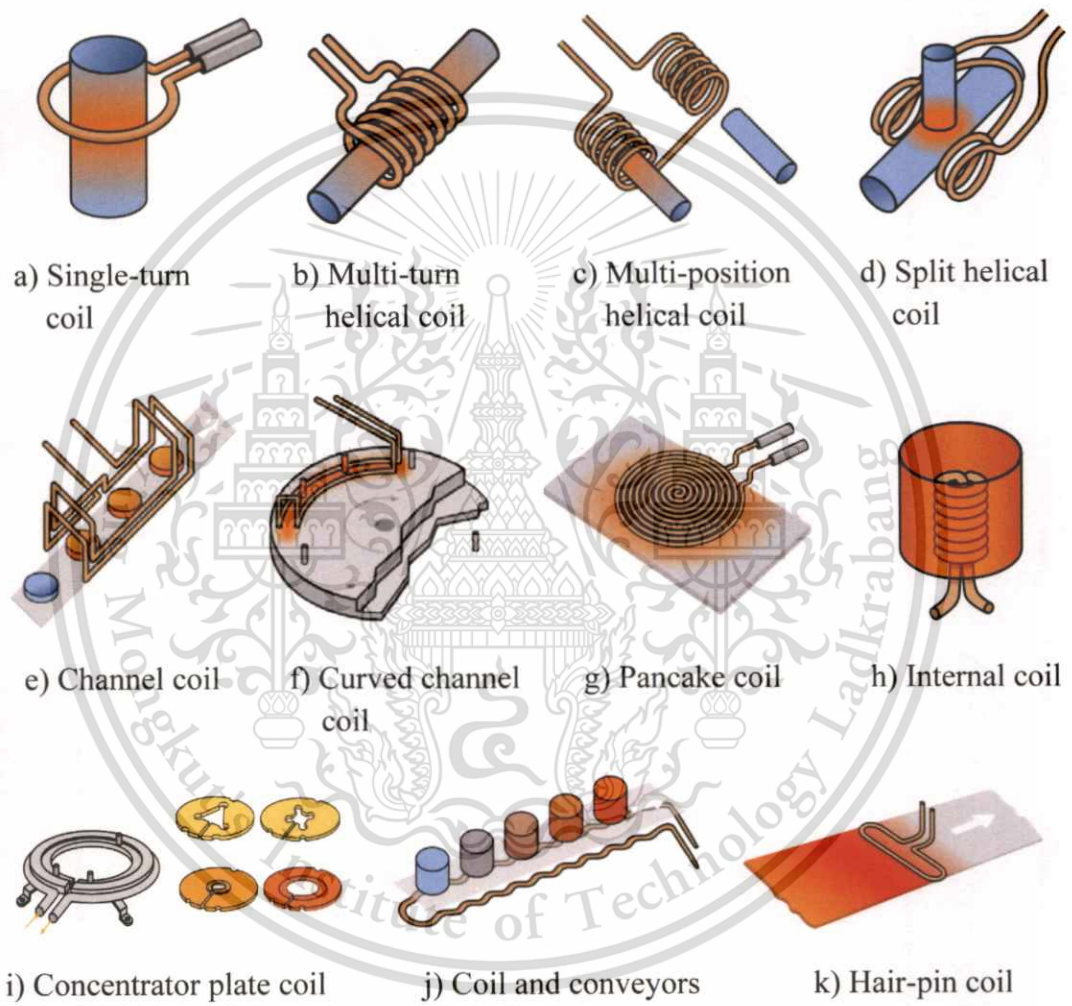

Figure 2.11 Various types of coil design [13].

The magnetic flux lines generated from the induction coil are most concentrated close to the coil turns and weaken when far from the coil. The denser flux lines cause the higher current generated in the heated workpiece that results in higher heating rate. Thus, the coil is required to be coupled to the workpiece as close as possible for maximum energy transfer. The distance between coil and heated workpiece, so-called the coupling gap, is essential to the amount of heat generated in workpiece. In general, the coupling gap from 3/32 inches to 1/8 inches is sufficient for heating the

thin skin of workpiece's outer surface. Matching the coil to the induction power supply is also critical to the coil electrical efficiency. Moreover, the coil design needs to concern about the cancellation of magnetic field. The coil which the opposite sides of inductor are too close results in no inductance as shown in the left of Figure 2.12. It should has a loop in the inductor to cause some inductance. Induction coils are usually made of copper tubing with water cooling flow inside the coils to prevent themselves gets hot or over-heating. Their diameter ranges from 1/8 inches to 3/8 inches [14].

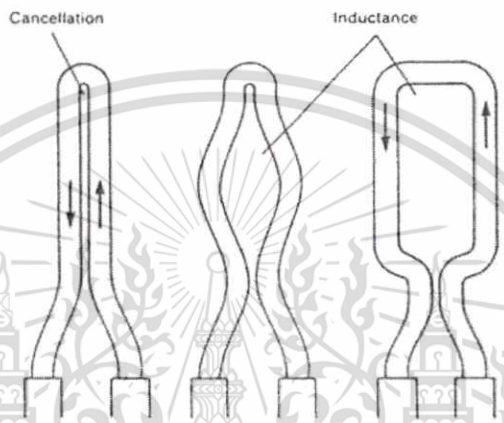

Figure 2.12 Effect of coil design on inductance [15].

- **Calculation of Pancake Work Coil**

With Wheeler's formula, the inductance of flat pancake coil can be calculated as follows [16].

$$L_c\ (\mu H) = \frac{r^2 n^2}{8r+11w} \tag{2.1}$$

Where, r = radius to center of windings (inches)
w = width of windings (inches)
n = number of turns

The number of coil turns depends on the required inductance. Each turn need to be considered separately. The sum of each turn its self and mutual inductance with all other turns is the total inductance.

Determine coil wire diameter (d_w) from rms current rating and outer diameter of induction coil as follows [17];

$$d_w(m) = \sqrt{\frac{4I}{\pi J}} \tag{2.2}$$

$$D_o\ (m) = D_i + (2 \cdot n \cdot d'_w) \tag{2.3}$$

Where, I = rms current rating (Amp)
J = allowable current density (A/m^2)
D_i = inner diameter of induction coil (m)
D_o = outer diameter of induction coil (m)
d'_w = coil wire diameter with insulation (m)

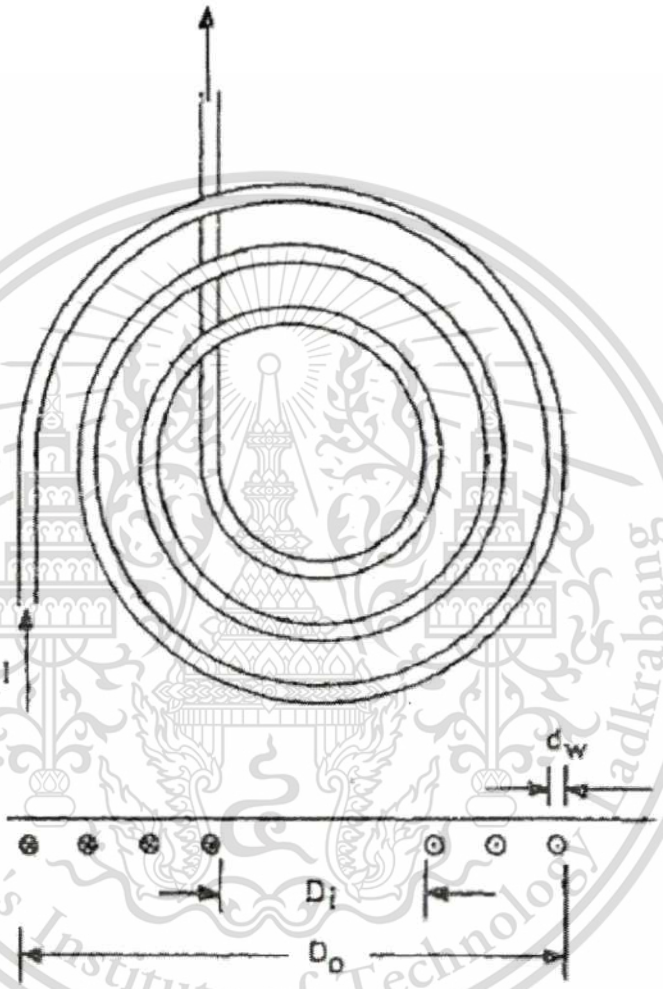

Figure 2.13 A typical pancake coil.

The minimum thickness of coil wire requires to be at least two times of penetration depth or skin depth (δ) of current in coil wire. Thus, the minimum thickness of wire coil is [18]

$$t_c(m) = 2\delta_c \tag{2.4}$$

Which δ is calculated as follows;

$$\delta\ (m) = \frac{1}{\sqrt{\pi f \mu_c \mu_o \sigma_c}} \tag{2.5}$$

Where, f = applied frequency (Hz)

μ_c = magnetic permeability of conductor (H/m)

μ_o = magnetic permeability of free space (H/m)

σ = electric conductivity of conductor (mho/m)

2.1.3.3 Induction Heating In The Injection Molding Process

Generally, the outer surface of product requires the good surface quality. Hence, the induction coil is designed to heat the cavity side of mold. The pancake coil is suitable design to use for heating the flat cavity surface. In the injection molding process, the induction heating is applied to heat the desired mold side to above the glass transition temperature (T_g) of molded material prior the injection stage. Figure 2.13 illustrates the scheme of injection molding by means of induction heating. During the part ejection stage of the molding cycle, an induction coil is moved forward to the cavity side to be heated rapidly when the water cooling is off. After the mold temperature reaches the target, the coil is retracted and the mold then closes to perform the plastic injection as shown in Figure 2.14. The water cooling is on when the packing stage starts.

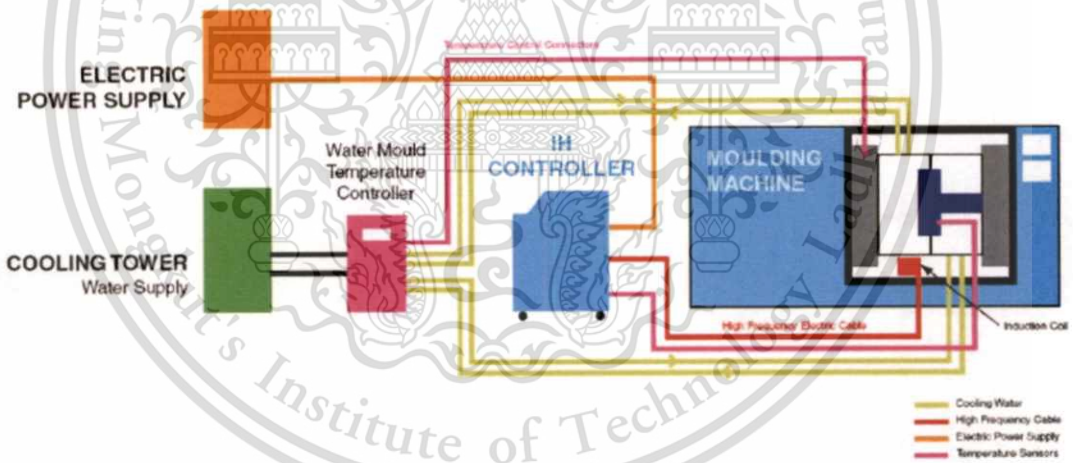

Figure 2.14 Diagram of the injection molding using induction heating system [19].

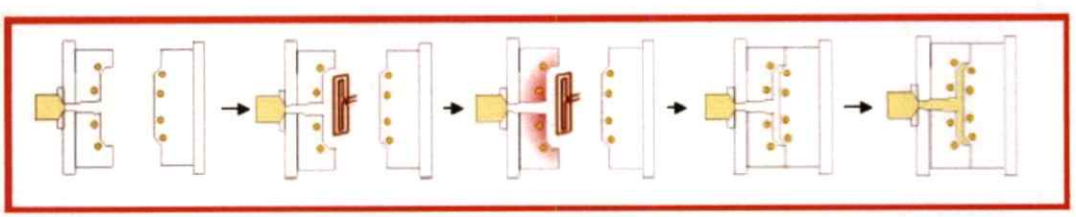

Figure 2.15 Schematic of the performance of the external induction heating used in the injection molding [19].

2.1.4 Taguchi Method

Taguchi method is a form of the design of experiment (DOE) techniques. It is the powerful and efficient technique to optimize the performance characteristic, quality and cost of a process or product by reducing the effect of source of variation to system performance. Taguchi method is the suitable approach to study the effect of several parameters on the desired characteristic. Taguchi method utilizes the specifically designed tables known as "orthogonal array" to design the experimental layout. With the orthogonal array, the number of experimental trials can be reduced to study the entire system. The experimental results based on orthogonal array are converted into a form of signal to noise (S/N) ratio. In terms of S/N ratio, signal or S represents the desired value (mean) from the control factors for the outcome characteristic and noise or N represents the undesired value from uncontrollable factor for the outcome characteristic. S/N ratio can be categorized into three quality characteristic i.e. smaller-the-better, larger-the-better, and nominal-the-best. Calculation of the S/N ratio depends on the desired quality characteristics or experimental objective as follows [20]:

1.) For smaller-the-better:

$$S/N = -10\ log_{10}\left(\frac{1}{n}\sum_{i=0}^{n} y_i^2\right) \tag{2.6}$$

2.) For larger-the-better:

$$S/N = -10\ log_{10}\left(\frac{1}{n}\sum_{i=0}^{n}\frac{1}{y_i^2}\right) \tag{2.7}$$

3.) For nominal-the-best:

$$S/N = 10\ log_{10}\left(\frac{\mu_y^2}{\sigma_y^2}\right) \tag{2.8}$$

where y_i is the measured data or output for the *i*th trial, n is the number of trials, and μ_y and σ_y represent the mean and standard deviation of the response variable Y, respectively.

The larger S/N ratio provides better quality characteristics, regardless of the category of the quality characteristic. Thus, the optimal level of the process parameters is the level with the largest S/N ratio. The S/N ratio for each level of process parameters is calculated based on the S/N analysis. To determine the effect of each parameter and the optimal parameter combination on the output, the signal to noise (S/N) ratio is employed by Taguchi method.

2.2 Related Research

Induction heating has studied for many years. Most of previous studies have studied the effect of process parameters, such as frequency, power, coupling gap, and workpiece thickness on induction heating [21, 22, 23], and the effect of coil such as the number of coil turns, positioning and cross section [24, 25], on induction heating in term of heating rate and temperature distribution. From the studied were found that injection molding is the efficient heating method. To solve the mold temperature issue that can cause the defects on the injection molded part, induction heating is studied, developed and applied for mold surface heating in injection molding process. From the previous studies found that induction heating can rapidly heat the mold surface without an increase in a significant cycle time [21, 26].

Nian et al. [21] studied the effects of the factors, such as workpiece's thickness, pitch of coil turns, induction coil positioning, coupling gap, frequency, and waiting time, on the heating rate and temperature distribution on mold surface of induction heating by single-layer coil. It revealed that the workpiece thickness is essential factor on heating rate. The thicker workpiece has the lower heating rate than the thinner one. In addition, the coil positioning plays a critical role on heating uniformity.

To improve the non-uniform temperature distribution over the cross and depth sections of heated workpiece resulting from proximity and skin effects that caused by using the single-layer coil for induction heating, the multi-layer coil is investigated. Ming-Shyan Huang and Yao-Lin Huang [27] examined the effect of multi-layered induction coils on efficiency and uniformity of surface heating. They found that the multi-layered coil provided more uniform temperature than the conventional single-layer coil as well as heating efficiency.

Using magnetic concentrators is the most common solution to reduce the proximity effect in the single-layer coil. However, its result is not satisfactory due to it still cannot avoid the proximity effect occurring under the coils as in Figure 2.16(a). Nian et al. [28] developed and investigated the performance of ferrite materials as magnetic shield in the separation of opposing magnetic fields arising from the undesired proximity effect on the enhancement of heating efficiency and temperature uniformity. This studied was found that the optimal positioning of ferrite materials on the single-layer coils could achieve the elimination of the proximity effect as Figure 2.16(b). It increased the heating rate and also enhanced temperature uniformity.

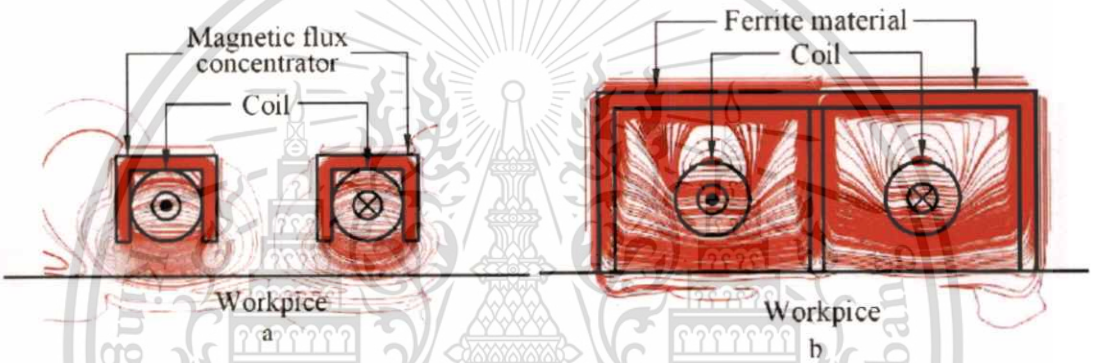

Figure 2.16 Magnetic flux fields of two adjacent opposite current coils: (a) with magnetic flux concentrator; (b) with magnetic shielding material [28].

The effect of induction heating on injection molded part was widely investigated. Chen et al. [29] studied the effect of induction heating on the surface appearance of weld line of injection molded part. It was found that induction heating successfully eliminated weldline and also enhanced the associated weld line strength. Chen et al. [26] examined the effect of induction heating on surface quality of microcellular injection molded parts. Their study showed that induction heating reduced the surface roughness of molded part and removed the flow marks on surface caused by gas bubbles. Kim et al. [30] used induction heating to solve the incomplete filling problem of micron or submicron scale features during injection molding. The results indicated that induction heating achieved the complete filling and material could replicate the nanograting structures.

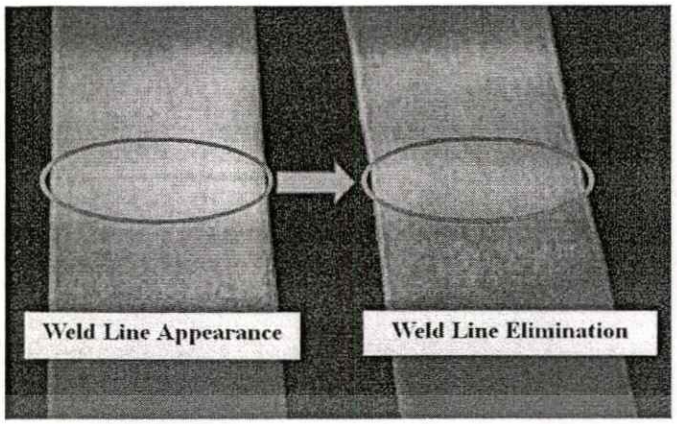

Figure 2.17 Appearance of weldline without induction heating (left). Weld line mark was eliminated (right) by induction heating before to melt injection [29].

From most of previous studies, the common induction heating method using for mold surface heating in injection molding is the use of external induction coil that the robot need to put the coil in front of the cavity surface during the mold opening and part ejection. This results in the longer cycle time. To address this issue, Sung and Hwang [31] proposed the use of an insert type induction heating coil. It was found that the insert type coil could heat the mold with temperature uniformity of about 91 % and provide the heating rate at about 3 °C/s.

CHAPTER 3
METHODOLOGY

3.1 Materials And Equipment

3.1.1 Raw Materials

3.1.1.1 Polycarbonate (PC) (NOVAREX® 7022L1)

3.1.1.2 Polycarbonate/Acrylonitrile Butadiene Styrene (PC/ABS) (Bayblend® T85XF)

3.1.1.3 Nylon 6 with 30% Glass-Fiber Filled (PA6GF30) (Terabo®)

Table 3.1 List of mold materials

Material	Density (kg/m^3)	Thermal conductivity (W/m °C)	Heat capacity (J/kg °C)
M238	7850	33	460
SKD61	7800	25	460
P20	7850	34	460
NAK80	7980	41	460

3.1.2 Equipment

3.1.3.1 Injection molding machine (FANUC ROBOSHOT S-2000i 100B)

3.1.3.2 Induction machine

3.1.3.3 Induction coil

3.1.3.4 Insert mold (M238, SKD61, P20, NAK80)

3.1.3 Characterization Instruments

3.1.3.1 3D Measuring Laser Microscope (Olympus LEXT OLS4100)

3.1.3.2 Gloss meter (KSJ® MG268-F2)

3.1.3.3 Universal testing machine (INSTRON® Model 5967)

3.1.3.4 Surface roughness tester (Mitutoyo®)

3.1.3.5 Laser scanner (ROMER ABSOLUTE ARM, 7-AXIS, 7525 SI)

3.2 Research Plan

The research plan was carried out by two main phases including the preliminary study and main experiment of test mold. Figure 3.1 illustrates the scheme of research plan. More details are described in next section.

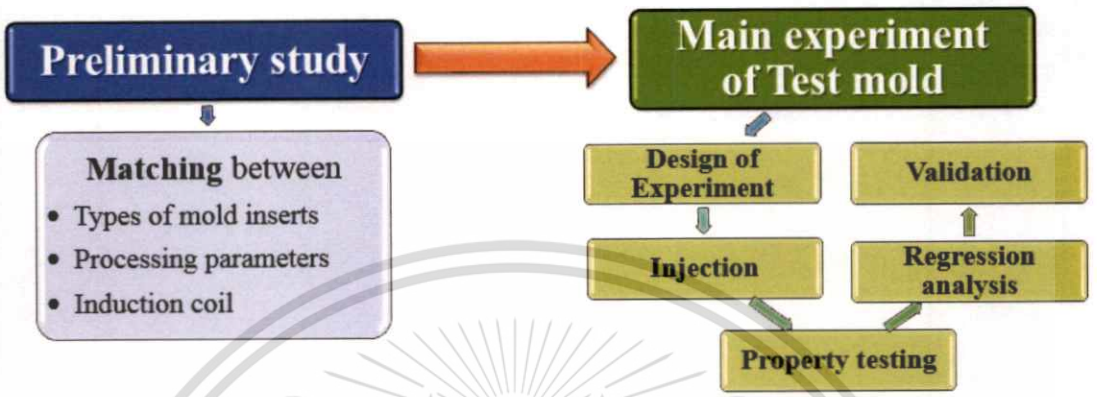

Figure 3.1 Schematic of research plan

3.3 Preliminary Study

Preliminary study is the matching between types of mold inserts (M238, SKD61, P20, and NAK80), process parameters (induction power and coupling gap from center of coil to cavity surface) and single-layer rectangular shaped induction coil to obtain the optimum heating rate. To investigate the influence of induction heating, the special mold inserts of four different materials were designed and made. In this study, this special mold insert is called test mold. Figure 3.2 illustrates the relationship of coil and mold insert. The mold insert that provided the optimum heating rate is selected as the mold insert for the test mold injection. This step is divided into 2 sections as follows:

3.3.1 Induction Power Optimization For Coil And Each Insert Mold

Investigating the optimum power used on each mold insert. Gap between the coil and mold insert surface is fixed at 17.5 mm. Power from the induction machine was varied from 10% to 100% of 45 kW input power. The outputs include mold surface temperature, present power, present current, present frequency were recorded. Mold surface temperature was measured by portable digital thermometer and the rest of outputs were obtained from display of the induction heating machine as shown in Figure3.3.

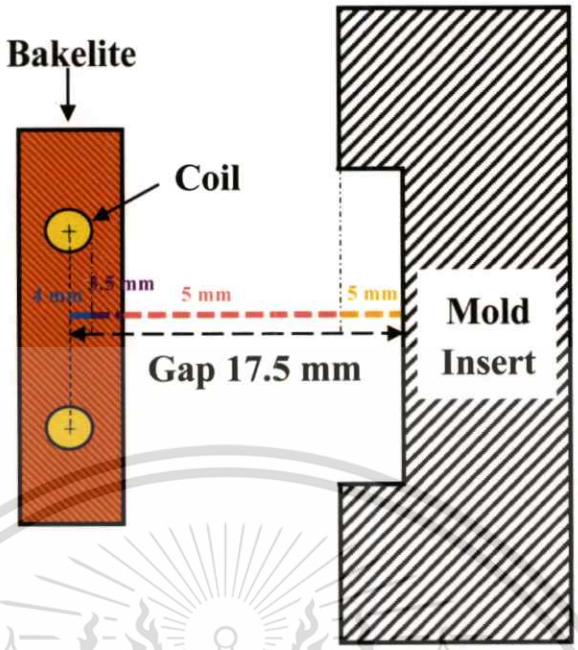

Figure 3.2 Diagram of the distance of gap between the center of induction coil diameter and surface of mold insert.

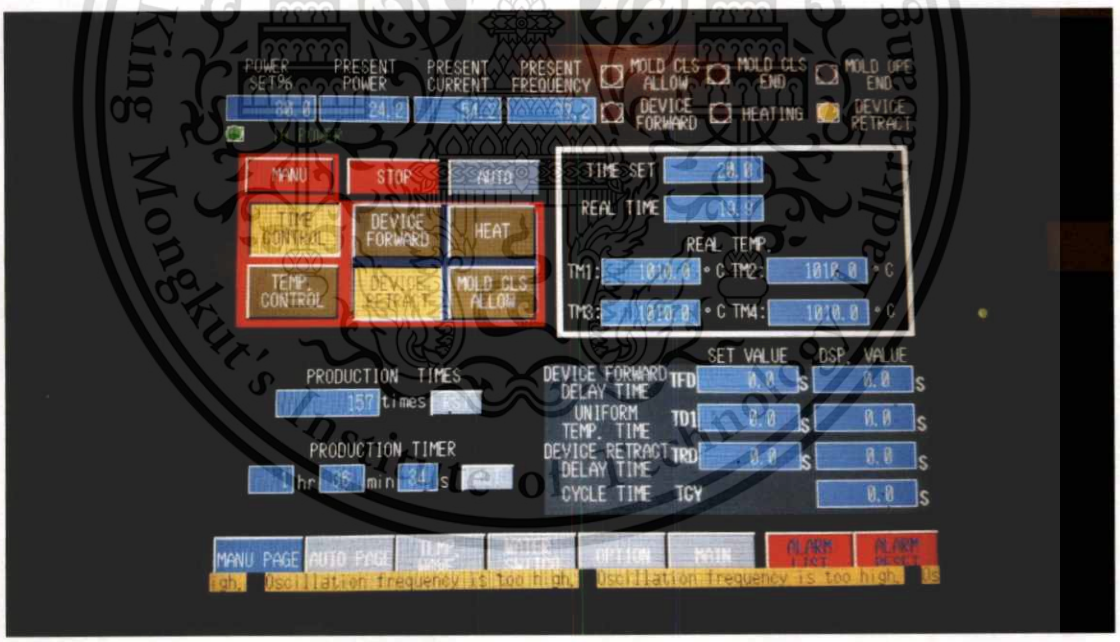

Figure 3.3 Induction heating machine interface.

3.3.2 Induction Heating Coupling Gap Optimization For Coil And Each Insert Mold

Investigating the optimum coupling gap between the coil and mold insert surface for each insert. Power is fixed at the optimal power obtained from 3.3.1. Gap was varied from 12.5 to 19.5 mm. The outputs include mold surface temperature, present power, present current, present

frequency were recorded. Mold surface temperature was measured by portable digital thermometer and the rest of outputs were obtained from display of the induction machine.

3.4 Main Experiment Of Test Mold

3.4.1 Design of Experiment

In this study, the four control parameters: injection speed (A), packing pressure (B), heating temperature by the induction heating or the mold surface temperature before the filling stage (C), and water temperature (D) were investigated the effect on the interested properties of test mold part. Weldline, gloss, flexural strength of weldline, surface roughness, and warpage are the interested properties. The experiment was designed by employing Taguchi method.

3.4.2 Injection

In the injection process, the optimum condition of matching between mold insert, process parameters and induction coil from the preliminary study phase was used as the condition of induction heating for injection molding of test mold part. Figure 3.4 shows the design of induction coil and mold insert. Only cavity side of mold was heated by induction heating as shown in Figure 3.5(a).

(a) (b)

Figure 3.4 The feather of (a) induction coil and (b) mold insert.

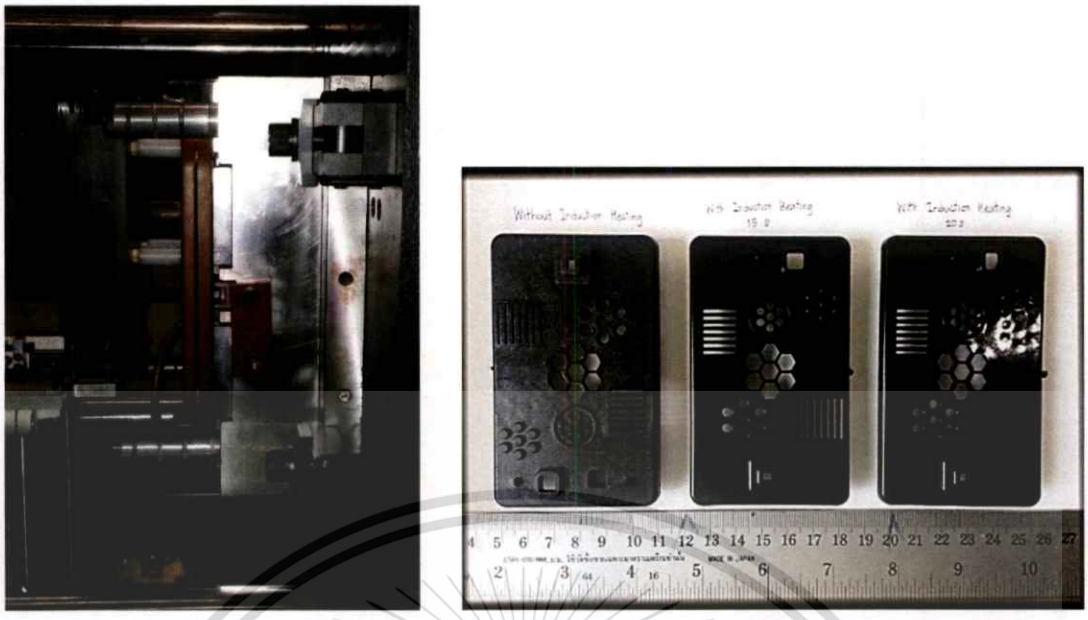

(a) (b)

Figure 3.5 (a) The cavity side of mold was heated by induction heating and (b) the test mold part of PA6GF30 without induction heating and with induction heating 15 s and 20 s, respectively.

3.4.3 Property Testing

The test molded part were tested five properties: weldline, gloss, flexural strength of weldline, surface roughness, and warpage.

3.4.3.1 Weld Line Measurement

The depth and width of a V-notch characterizing the degree of visibility of a weld line were thoroughly investigated by means of the 3D measuring laser microscope (Olympus LEXT OLS4100) as shown in Figure 3.6. Three samples per experiment were analyzed.

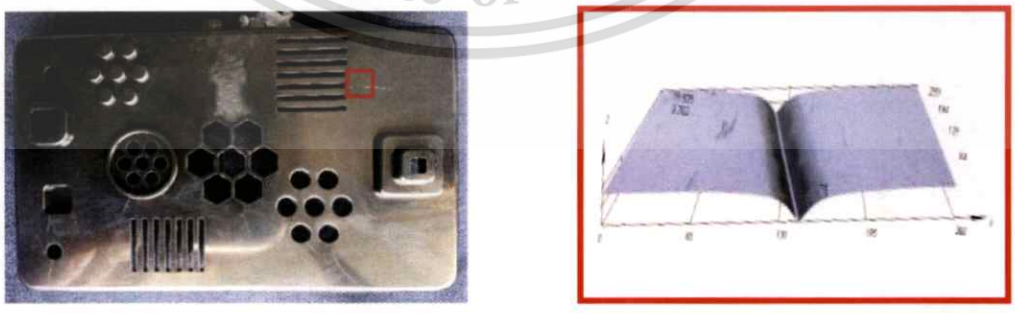

(a) (b)

Figure 3.6 (a) The position of weld line's V-notch and (b) the characteristic of V-notch of weld line investigated by means of the 3D laser measuring microscope

3.4.3.2 Gloss

The specimens are measured the gloss according to ASTM D523 Standard Test Method for Specular Gloss. They are measured the gloss by 60° Angle Gloss Meter (KSJ® MG268-F2) on 9x16 mm^2 of measuring area. The values for gloss measurement are indicated in gloss units (GU) without dimension.

Figure 3.7 The area in the red frame for gloss measurement.

3.4.3.3 Flexural Strength Of Weldline

The molded parts were cut into flexural specimen according to ASTM D790 standards by the wire saw machine. The specimen size is 5 mm x 25 mm x 3 mm. Flexural strength testing was carried out by Universal testing machine (INSTRON® Model 5967) with 30 kN of load cell at crosshead speed of 1 mm/min and support span 20 mm at 21.5°C and 59% humidity.

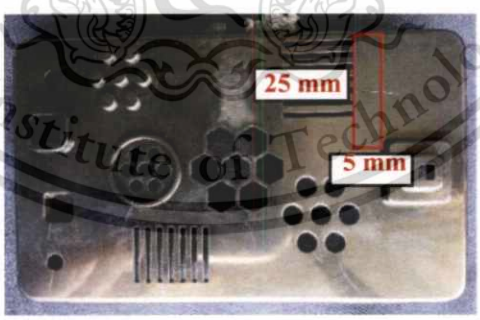

Figure 3.8 The specimen size and position in the red frame for the measurement of flexural strength of weldline.

3.4.3.4 Surface Roughness

The molded parts were measured the surface roughness by surface roughness tester. The stylus of surface roughness tester traverse the sampling length on the surface to measure the surface roughness. The measured values were described as Roughness Average (Ra). Ra is the

arithmetic average height of the individual surface peaks and valleys from the mean line of the profile within the sampling length. The value of Ra is expressed in micrometers (μm). The molded parts were measured the roughness in two direction: parallel and perpendicular to the melt entrance as shown in Figure 3.8. The yellow arrow and red arrow represent the parallel and perpendicular direction to the melt entrance, respectively. Each direction was measured the roughness in three different position. Ra values of these two directions were averaged as the surface average roughness of the molded part.

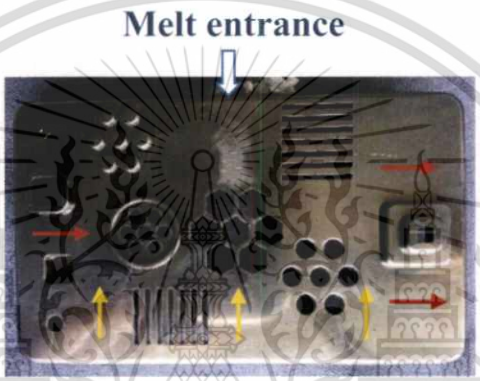

Figure 3.9 The direction of surface roughness measurement which the yellow arrow and red arrow represent the parallel and perpendicular direction to the melt entrance, respectively.

3.4.3.5 Warpage

The test mold part is examined the warpage/shrinkage by laser scanner (ROMER ABSOLUTE ARM, 7-AXIS, 7525 SI). The displacement on Z-axis (Z-displacement) is measured as shown in Figure 3.9. Figure 3.9 shows the measure of Z-displacement on test mold specimen dividing into three lines included of A-line, B-line, and C-line along X-axis which represent the displacement on the edge, middle, and another edge of the specimen, respectively.

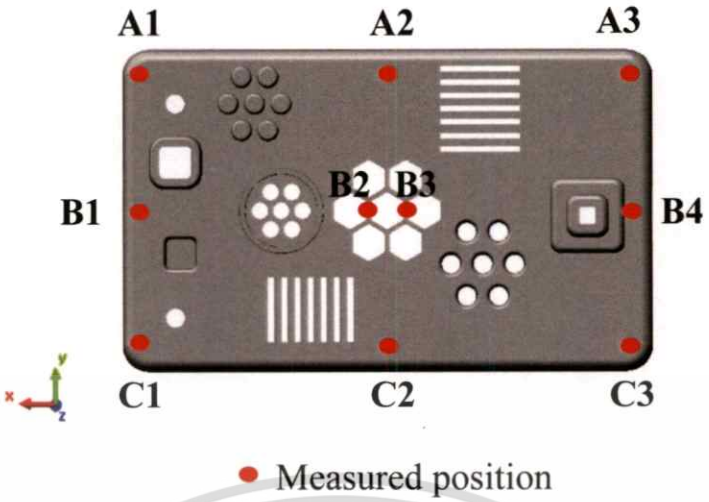

Figure 3.10 The positions for measure displacement on Z-axis (Z-displacement)

3.4.4 Regression Analysis

The measured data were analyzed by the regression analysis to investigate the effect of each molding parameter on that interested property and the best combination of molding parameter setting for each property. The formula of the quality characteristic of S/N ratio for the regression analysis depends on the requirement of that interested property. The ranking of each parameter affecting the interested property is obtained from the difference between the maximum and minimum value coefficient from regression analysis. The effect of each parameter depends on how large that difference value is. In the other words, the parameter with the highest difference value is the most effective parameter affecting that property.

3.4.5 Validation

This stage is the validation of the optimal parameter combination of each property of each material obtained from regression method that it provided the part with the optimal property. The injection molding and property testing were repeated.

CHAPTER 4
EXPERIMENTAL RESULTS AND DISCUSSION

4.1 Effect Of Power And Coupling Gap On Heating Rate For Each Mold Insert

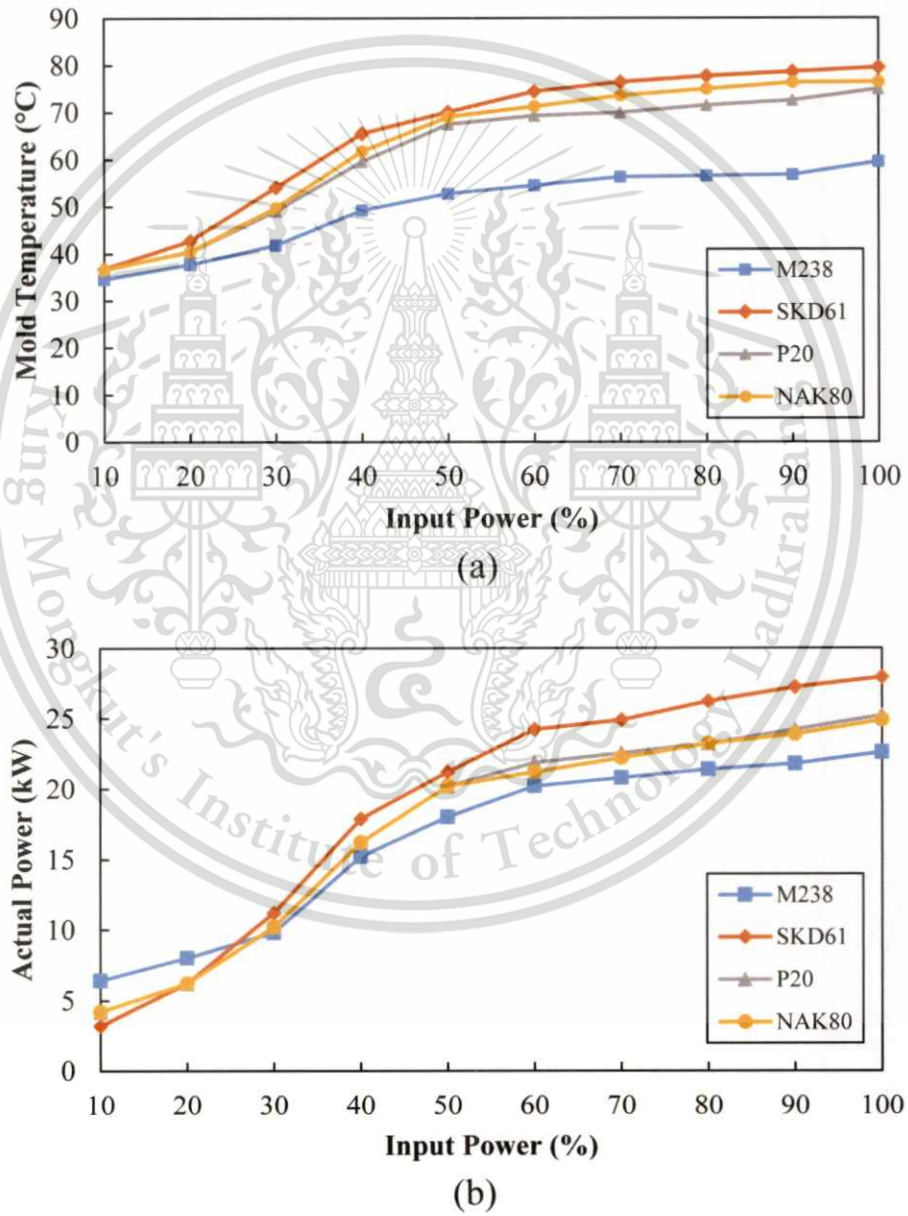

Figure 4.1 The relationship between (a) input power (%) and mold surface temperature (°C/s) and (b) input power (%) and actual power of four different mold inserts.

The optimal power was examined by applying the power of the induction heating machine from 10% to 100% of 45 kW at coupling gap of 17.5 mm. The mold surface temperature and actual power in kW unit as the results of experiment from four different mold inserts were obtained as shown in Figure 4.1. It was found that 80% of power is the power introducing to steady state of the mold temperature for four different mold inserts. In other words, the mold temperature does not significantly

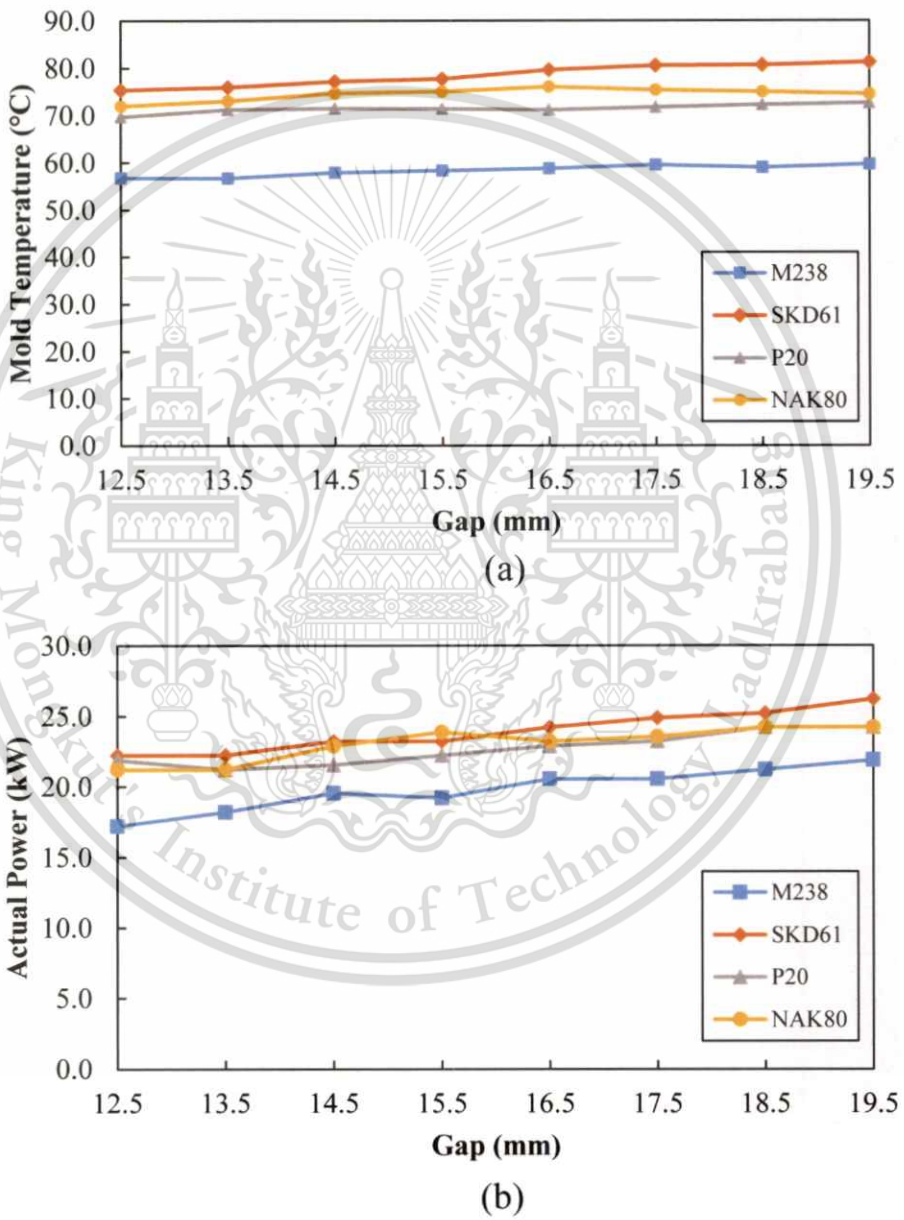

Figure 4.2 The relationship between (a) gap (mm) and mold surface temperature (°C/s) and (b) gap (mm) and actual power of four different mold inserts.

increase when the power is above 80% of applied power. Although applying the more power to coil, that is a waste of electricity. Hence, the power of 80% was applied as the optimal power to investigate the optimal gap which providing the optimal heating rate. It was found that the coupling gap leading into the steady state of the mold surface temperature of M238, SKD61, P20, and NAK80 was 17.5, 17.5, 13.5, and 16.5 mm, respectively, as shown in Figure 4.2.

The results of 4 types of mold inserts showed that SKD61 at condition of 80% of power and 17.5 mm of coupling gap provided the highest heating rate followed by NAK80, P20, and M238, respectively. This is due to SKD61 has least thermal conductivity among the mold inserts, its heat resistance is higher to conduct the heat. That is the capability of heat flowing from the mold surface to the cooling channel surface slower result in the mold surface temperature is still high compared with the mold insert with high conductivity.

Table 4.1 Result of the preliminary study of insert mold.

Mold insert	Power (%)	Gap (mm)	Heating rate (°C/s)
M238	80	17.5	6
SKD61	80	17.5	10
P20	80	13.5	8
NAK80	80	16.5	9

4.2 Experimental Layout For Test Mold Injection Designed By Taguchi Method

Each parameter has two set values (level values) including low and high levels according to Table 4. Thus, the experiments were performed according to Taguchi's 2-level L8 orthogonal array as shown in Table 4.2. Table 4.3 listing 8 experiments based on a L8 orthogonal array was required to further determine the optimum process parameter setting and the influence of parameter on the interested properties. Noted that 'no heating' means the mold surface has relatively the same temperature as the water temperature of each condition used.

Table 4.2 Factors and levels for the Taguchi experiments

Factor	Level	
	1	2
A: Injection Speed (mm/s)	L	H
B: Packing Pressure (kgf/cm²)	L	H
C: Heating Temperature (°C)	L	H
D: Water Temperature (°C)	L	H

Table 4.3 Experimental layout based on a L_8 orthogonal array

Experiment	Parameter			
	A	B	C	D
1	1	1	1	1
2	1	1	2	2
3	2	2	1	1
4	2	2	2	2
5	1	2	1	2
6	1	2	2	1
7	2	1	1	2
8	2	1	2	1

4.2.1 Polycarbonate (PC)

Table 4.4 Factors and levels for the Taguchi experiments of PC test mold part injection.

Parameter	Level	
	1	2
A: Injection Speed (mm/s)	25	75
B: Packing Pressure (kgf/cm²)	1200	1300
C: Heating Temperature (°C)	No heating*	165
D: Water Temperature (°C)	30	80

Table 4.5 Taguchi experiment design for test mold part injection of PC.

Experiment no.	Injection speed (mm/s)	Packing pressure (kgf/cm²)	Heating temperature (°C)	Water temperature (°C)
1	25	1200	30	30
2	25	1200	165	80
3	75	1300	30	30
4	75	1300	165	80
5	25	1300	80	80
6	25	1300	165	30
7	75	1200	80	80
8	75	1200	165	30

4.2.2 Polycarbonate/Acrylonitrile Butadiene Styrene (PC/ABS)

Table 4.6 Factors and levels for the Taguchi experiments of PC/ABS test mold part injection.

Parameter	Level	
	1	2
A: Injection Speed (mm/s)	25	100
B: Packing Pressure (kgf/cm²)	1200	1300
C: Heating Temperature (°C)	No heating*	160
D: Water Temperature (°C)	30	80

Table 4.7 Taguchi experiment design for test mold part injection of PC/ABS.

Experiment no.	Injection speed (mm/s)	Packing pressure (kgf/cm²)	Heating temperature (°C)	Water temperature (°C)
1	25	1200	30	30
2	25	1200	160	80
3	100	1300	30	30
4	100	1300	160	80
5	25	1300	80	80
6	25	1300	160	30
7	100	1200	80	80
8	100	1200	160	30

4.2.3 Nylon 6 with 30% Glass-Fiber Filled (PA6GF30)

Table 4.8 Factors and levels for the Taguchi experiments of PA6GF30 test mold part injection.

Parameter	Level	
	1	2
A: Injection Speed (mm/s)	25	75
B: Packing Pressure (kgf/cm²)	1200	1300
C: Heating Temperature (°C)	No heating*	160
D: Water Temperature (°C)	30	80

Table 4.9 Taguchi experiment design for test mold part injection of PA6GF30.

Experiment no.	Injection speed (mm/s)	Packing pressure (kgf/cm²)	Heating temperature (°C)	Water temperature (°C)
1	25	1200	30	30
2	25	1200	160	80
3	75	1300	30	30
4	75	1300	160	80
5	25	1300	80	80
6	25	1300	160	30
7	75	1200	80	80
8	75	1200	160	30

4.3 Effect Of Processing Parameters On Weldline Property

4.3.1 Polycarbonate (PC)

According to the Taguchi experimental design, the experiments were performed. As observation with naked eye, it could be seen obviously that weldline on test mold part was smaller and less visible when the mold temperature was higher. This was consistent with the results of weldline measurement by 3D Measuring Laser Microscope in Figure 4.3 and as well as the SEM images in Figure 4.4. Figure 4.3 shows the V-notch structure images of weldline of each experiment captured by 3 D Measuring Laser Microscope at total magnification of 50X. These image exhibits the weldline was smaller with the mold temperature rise. With using 3D

Measuring Laser Microscope, the depth and width of V-notch of weldline were obtained as shown in Figure 4.4. It was found that the experiment No.4, with using induction heating to heat the cavity surface temperature up to 165°C, has the smallest depth and width of V-notch which were 0.623 μm and 36.070 μm, respectively. While the experiment No.1, with cavity surface

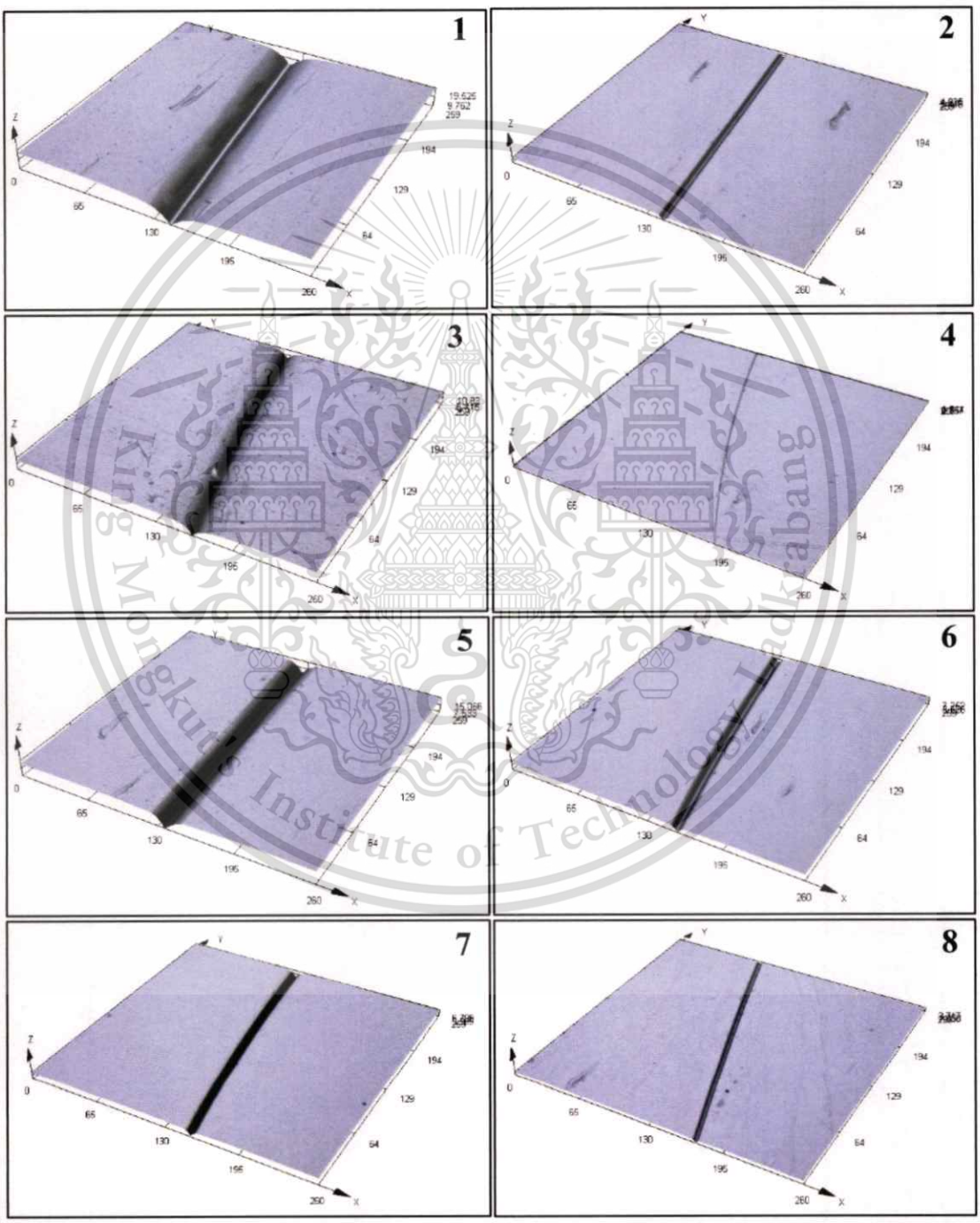

Figure 4.3 The characteristic of V-notch of weld line for each experiment at a total magnification of 50X

temperature at 30°C and without using induction heating, has the largest depth and width of V-notch which were 15.519 μm and 160.62 μm, respectively. The experiment No.5 based on the condition of company using the mold temperature of 80°C, it was found that the depth and width of V-notch are 11.326 μm and 110.582 μm, respectively. The depth and width of V-notch of experiment No.4 is more smaller comparing to experiment No.5 which that of experiment No.4 were improved by 95% and 67%, respectively, as shown in table 4.10. Table 4.10 also shows the S/N ratio that it will be mentioned next.

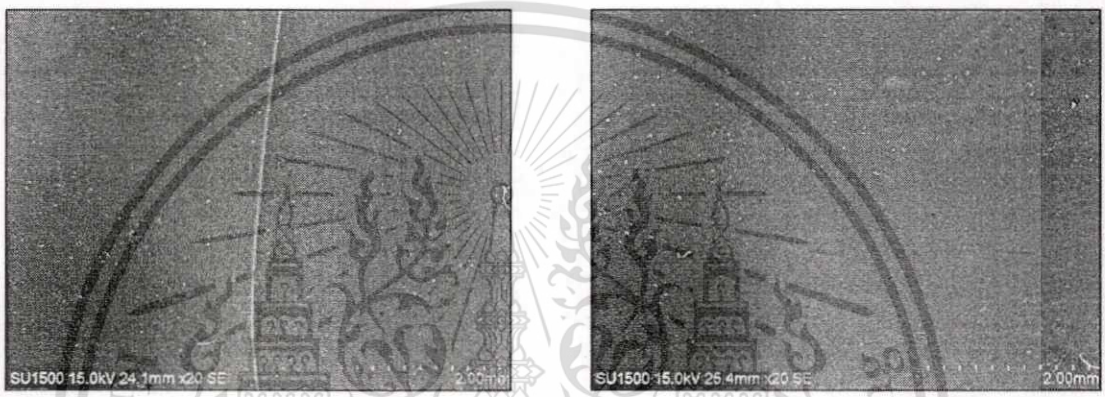

a) Experiment No.1 (without induction heating)

b) Experiment No.4 (with induction heating)

Figure 4.4 SEM images of PC (a) experiment no.1 without induction heating and (b) experiment no.4 with induction heating at the area where V-notch of weld line occur.

To investigate the effect of each molding parameter on the depth and width of a V-notch, the regression analysis was employed to analyze the measured values. Due to V-notch structure of weld lines cause the poor surface quality of the injection-molded parts so the smaller depth and width of V-notch can improve this issue. Therefore, the smaller-the-better quality characteristic of S/N ratio as Eq. 1 is carried out to identify the optimum setting and ranking in eliminating the weld line. The calculated S/N ratios are listed in Table. 4.10. The results of regression analysis showed that the optimum parameter setting of the smallest depth and width can be obtained from the experiment No.4 which is the combination of high injection speed (75 mm/s), high packing pressure (1300 kgf/cm^2), high heating temperature (165°C), and high water temperature (80°C) as Table 4.11. The ranking of

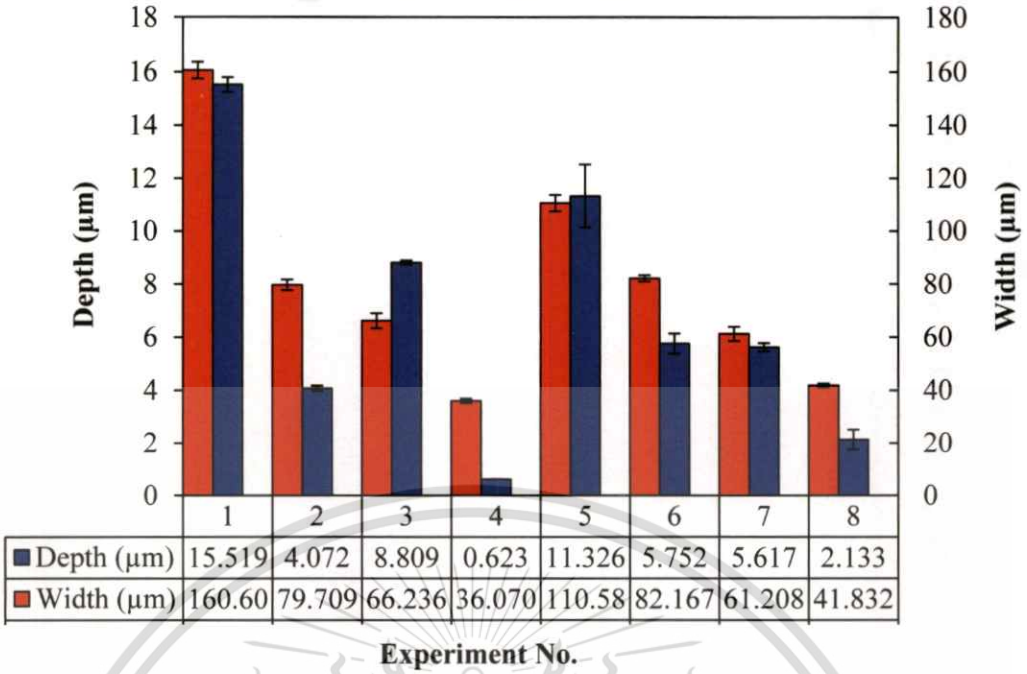

	1	2	3	4	5	6	7	8
Depth (µm)	15.519	4.072	8.809	0.623	11.326	5.752	5.617	2.133
Width (µm)	160.60	79.709	66.236	36.070	110.58	82.167	61.208	41.832

Figure 4.5 The measured depth and width of V-notch for PC

each parameter affecting the weld line visibility is obtained from the difference between the maximum and minimum value coefficient from regression analysis. The effect of each parameter depends on how large that difference value is. In the other words, the parameter with the highest difference value is the most effective parameter affecting the weld line visibility as in Figure4.6. Table 4.11 concludes that the most effective parameter resulting in the smallest depth of v-notch is the heating temperature, followed by injection speed, water temperature, and packing pressure, respectively. It also points out that the most effective parameter promoting the smallest width of V-notch is the injection speed, followed by heating temperature, water temperature, and packing pressure, respectively. This resulted from the high mold surface temperature before the filling stage can prohibit or slow down the freezing of the melt. Consequently, the molecular mobility is higher resulting in the increase in the diffusion of molecules across the weldline interface. The high injection speed result in the heat generated by high shear rate that can prevent the premature melt freezing. It also push the melt to furthest part of mold at shorter time before the freezing of melt. This leads to the smaller depth and width of V-notch.

Table 4.10 Percentage of the improvement and the calculated S/N ratio for the measured depth and width of V-notch on PC specimens.

Exp.	Factor Combination				Depth of V-notch			Width of V-notch		
	A	B	C	D	Average Depth (μm)	Improvement comparing to Exp.5 (%)	S/N ratio	Average Width (μm)	Improvement comparing to Exp.5 (%)	S/N ratio
1	25	1200	30	30	15.52	-37.0	-23.82	160.61	-45.2	-44.12
2	25	1200	165	80	4.07	64.1	-12.20	79.71	27.9	-38.03
3	75	1300	30	30	8.81	22.2	-18.90	66.24	40.1	-36.43
4	75	1300	165	80	0.62	94.5	4.11	36.07	67.4	-31.15
5	25	1300	80	80	11.33	-	-21.13	110.58	-	-40.88
6	25	1300	165	30	5.75	49.2	-15.22	82.17	25.7	-38.29
7	75	1200	80	80	5.62	50.4	-14.99	61.21	44.6	-35.74
8	75	1200	165	30	2.13	81.2	-6.72	41.83	62.2	-32.43

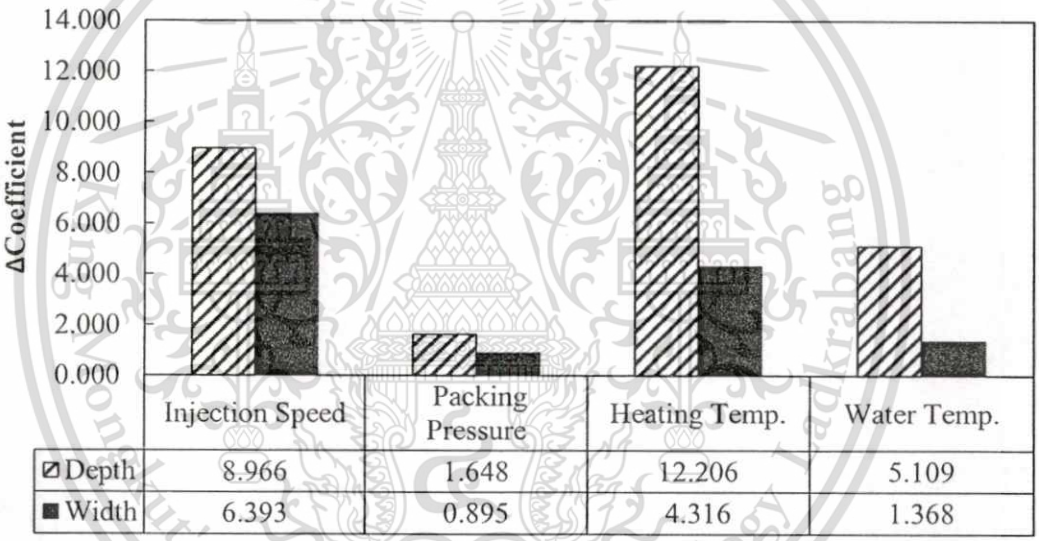

Figure 4.6 The relationship between the difference of regression coefficient values and process parameters affecting on the depth and width of V-notch of PC specimens.

Table 4.11 The best parameter combination and ranking of the effect for producing parts with the smallest the depth and width of V-notch on PC specimens.

Factor	Depth		Width	
	Best Combination	Factor Ranking	Best Combination	Factor Ranking
Injection Speed (mm/s)	75	2	75	1
Packing Pressure (kgf/cm²)	1300	4	1300	4
Heating Temperature (°C)	165	1	165	2
Water Temperature (°C)	80	3	80	3

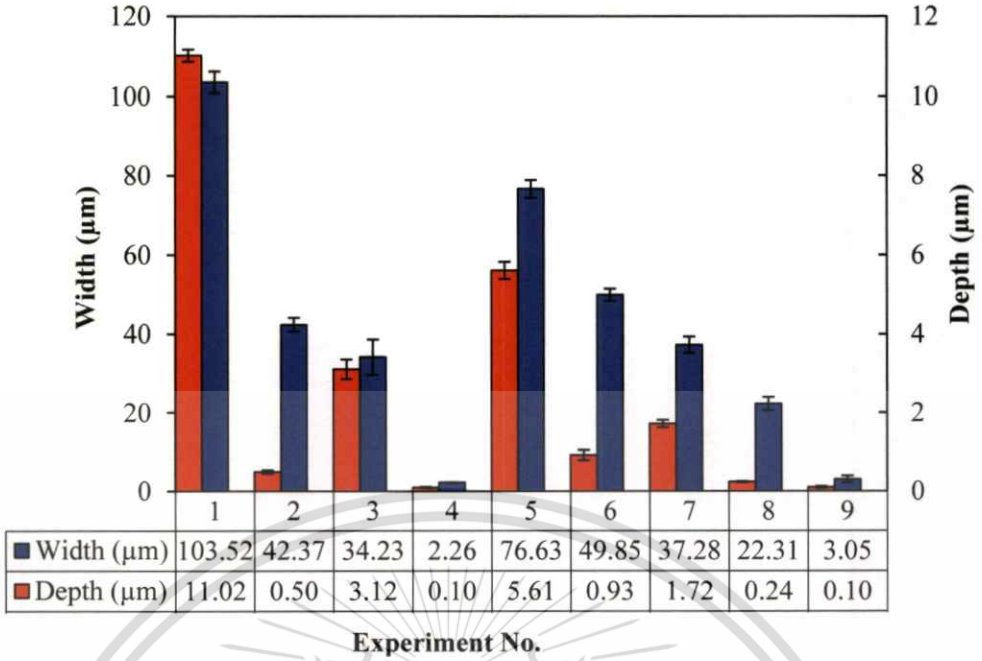

	1	2	3	4	5	6	7	8	9
Width (μm)	103.52	42.37	34.23	2.26	76.63	49.85	37.28	22.31	3.05
Depth (μm)	11.02	0.50	3.12	0.10	5.61	0.93	1.72	0.24	0.10

Figure 4.7 Validation of weldline property for PC

To validate the best combination, experiment No.4 was repeated in the injection molding and weldline property testing. It was found that experiment No.4, as experiment No.9 in Figure 4.7, is still provided the smallest depth and width of V-notch

4.3.2 Polycarbonate/Acrylonitrile Butadiene Styrene (PC/ABS)

As observation with naked eye, it revealed the same results as that of PC specimen. It could be seen obviously that weldline on test mold part was smaller and less visible when the mold temperature was higher. This was consistent with the results of weldline measurement by 3D Measuring Laser Microscope in Figure 4.8 and as well as the SEM images in Figure 4.9. Figure 4.8 shows the V-notch structure images of weldline of each experiment captured by 3 D Measuring Laser Microscope at total magnification of 50X. These image exhibits the weldline was smaller with the mold temperature rise. With using 3D Measuring Laser Microscope, the depth and width of V-notch of weldline were obtained as shown in Figure 4.10. It was found that the experiment No.4, with using induction heating to heat the cavity surface temperature up to 165°C, has the smallest depth and width of V-notch which were 0.096 μm and 2.260 μm, respectively. While the experiment No.1, with cavity surface temperature at 30°C and without using induction heating, has the largest depth and

width of V-notch which were 11.015 μm and 103.52 μm, respectively. The experiment No.5 based on the condition of company using the mold temperature of 80°C, it was found that the depth and width of V-notch are 5.610 μm and 76.630 μm, respectively. The depth and width of V-notch of experiment No.4 is more smaller comparing to experiment No.5 which that

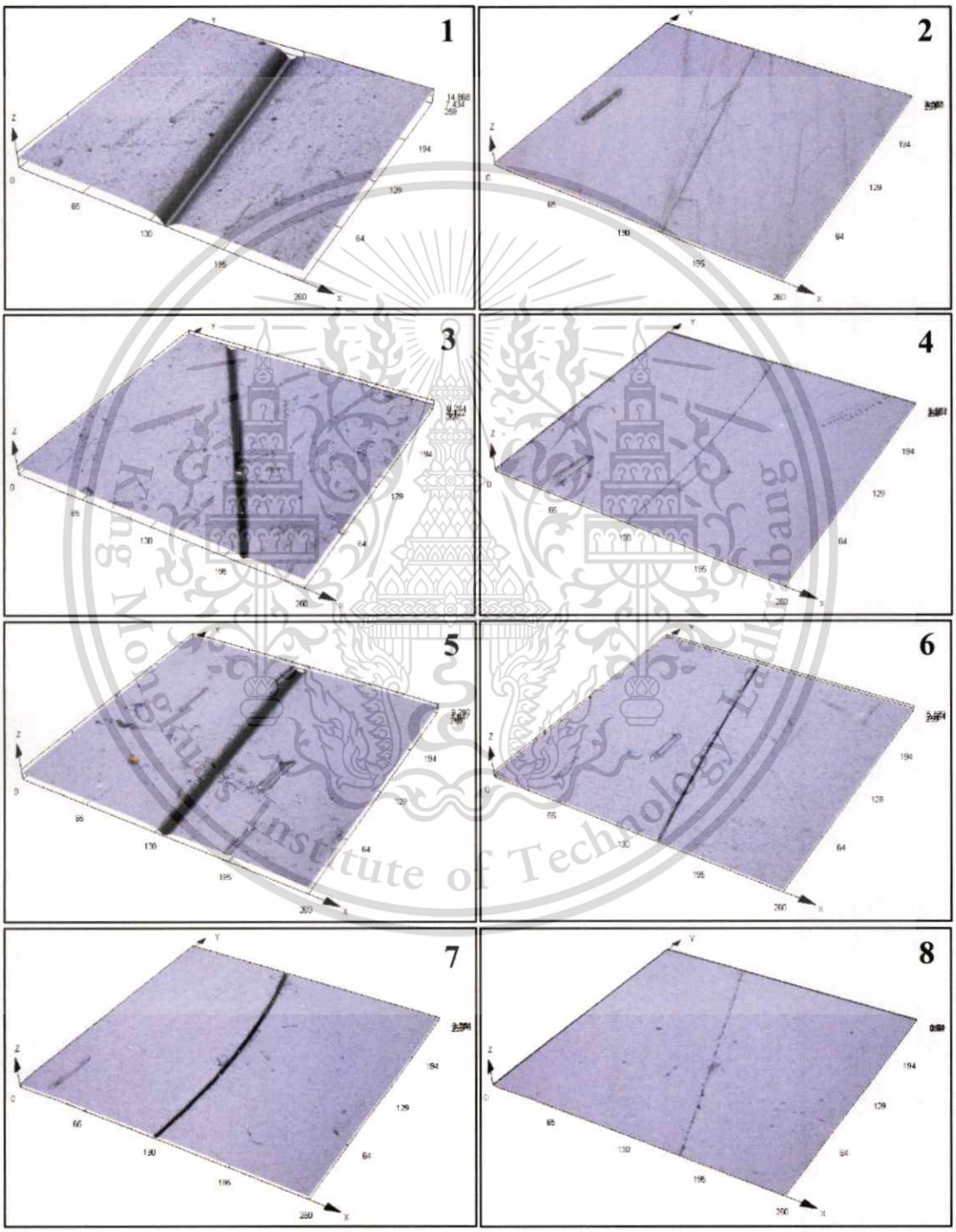

Figure 4.8 The characteristic of V-notch of weld line for each experiment at a total magnification of 50X for PC/ABS specimen.

of experiment No.4 were improved by 98.3% and 97.1%, respectively, as shown in table 4.12.

a) Experiment No.1 (without induction heating)

b) Experiment No.4 (with induction heating)

Figure 4.9 SEM images of PC/ABS (a) experiment no.1 without induction heating and (b) experiment no.4 with induction heating at the area where V-notch of weld line occur.

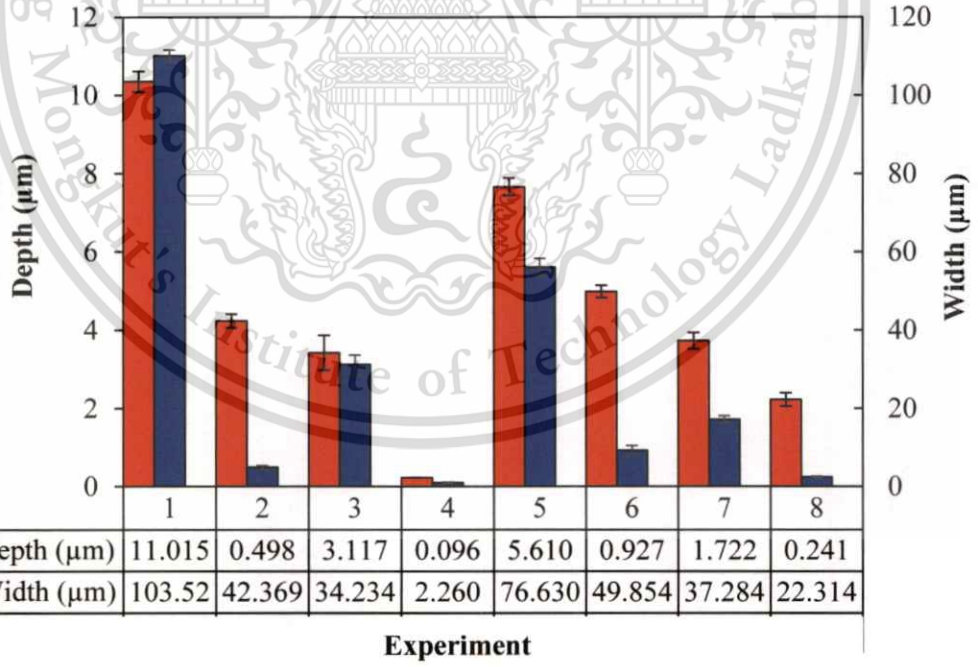

Figure 4.10 The measured depth and width of V-notch for PC/ABS

Table 4.12 Percentage of the improvement and the calculated S/N ratio for the measured depth and width of V-notch on PC/ABS specimens.

Exp.	Factor Combination				Depth of V-notch			Width of V-notch		
	A	B	C	D	Average Depth (μm)	Improvement comparing to Exp.5 (%)	S/N ratio	Average Width (μm)	Improvement comparing to Exp.5 (%)	S/N ratio
1	25	1200	30	30	11.02	-96.4	-20.84	103.52	-35.1	-40.30
2	25	1200	160	80	0.50	91.1	6.02	42.37	44.7	-32.55
3	100	1300	30	30	3.12	44.4	-9.90	34.23	55.3	-30.76
4	100	1300	160	80	0.10	98.3	20.27	2.26	97.1	-7.08
5	25	1300	80	80	5.61	-	-14.99	76.63	-	-37.69
6	25	1300	160	30	0.93	83.5	0.57	49.85	34.9	-33.96
7	100	1200	80	80	1.72	69.3	-4.73	37.28	51.3	-31.44
8	100	1200	160	30	0.24	95.7	12.36	22.31	70.9	-27.00

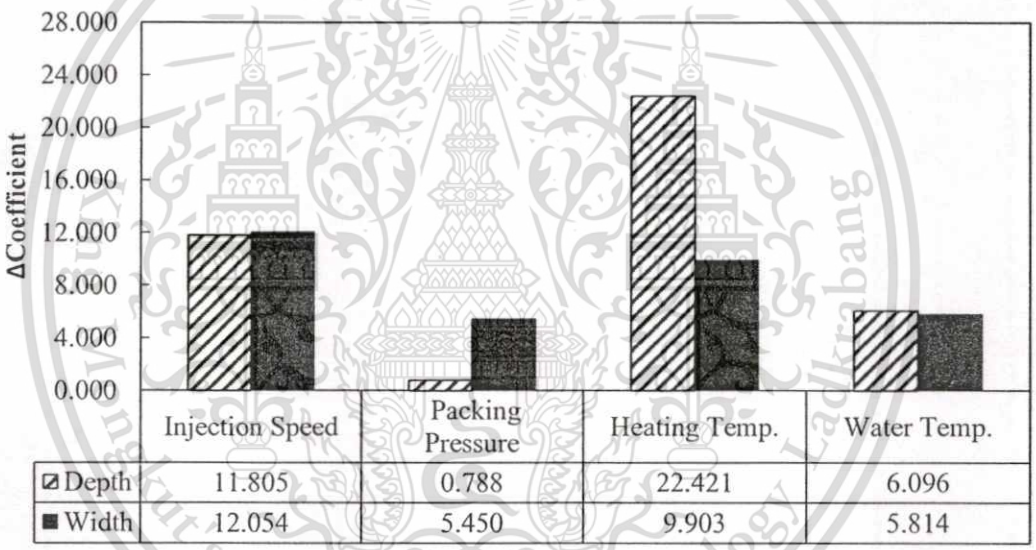

Figure 4.11 The relationship between the difference of regression coefficient values and process parameters affecting on the depth and width of V-notch of PC/ABS specimens.

In regression analysis, the smaller-the-better quality characteristic of S/N ratio as Eq. 1 is carried out to identify the optimum setting and ranking in eliminating the weld line. The calculated S/N ratios are listed in Table 4.12. The results of regression analysis showed that the optimum parameter setting of the smallest depth and width can be obtained from the experiment No.4 which is the combination of high injection speed (100 mm/s), high packing pressure (1300 kgf/cm²), high heating temperature (160°C), and high water temperature (80°C) as Table 4.11. The parameter with the

Table 4.13 The best parameter combination and ranking of the effect for producing parts with the smallest the depth and width of V-notch on PC/ABS specimens.

Factor	Depth		Width	
	Best Combination	Factor Ranking	Best Combination	Factor Ranking
Injection Speed (mm/s)	100	2	100	1
Packing Pressure (kgf/cm²)	1300	4	1300	4
Heating Temperature (°C)	160	1	160	2
Water Temperature (°C)	80	3	80	3

highest difference value is the most effective parameter affecting the weld line visibility as in Figure 4.11. Table 4.13 shows the most effective parameter resulting in the smallest depth of v-notch is the heating temperature, followed by injection speed, water temperature, and packing pressure, respectively. It also points out that the most effective parameter promoting the smallest width of V-notch is the injection speed, followed by heating temperature, water temperature, and packing pressure, respectively. This resulted from the high mold surface temperature before the filling stage can prohibit or slow down the freezing of the melt. Consequently, the molecular mobility is higher resulting in the increase in the diffusion of molecules across the weldline interface. The high injection speed result in the heat generated by high shear rate that can prevent the premature melt freezing. It also push the melt to furthest part of mold at shorter time before the freezing of melt. This leads to the smaller depth and width of V-notch.

To validate the best combination, experiment No.4 was repeated in the injection molding and weldline property testing. It was found that experiment No.4, as experiment No.9 in Figure 4.12, is still provided the smallest depth and width of V-notch.

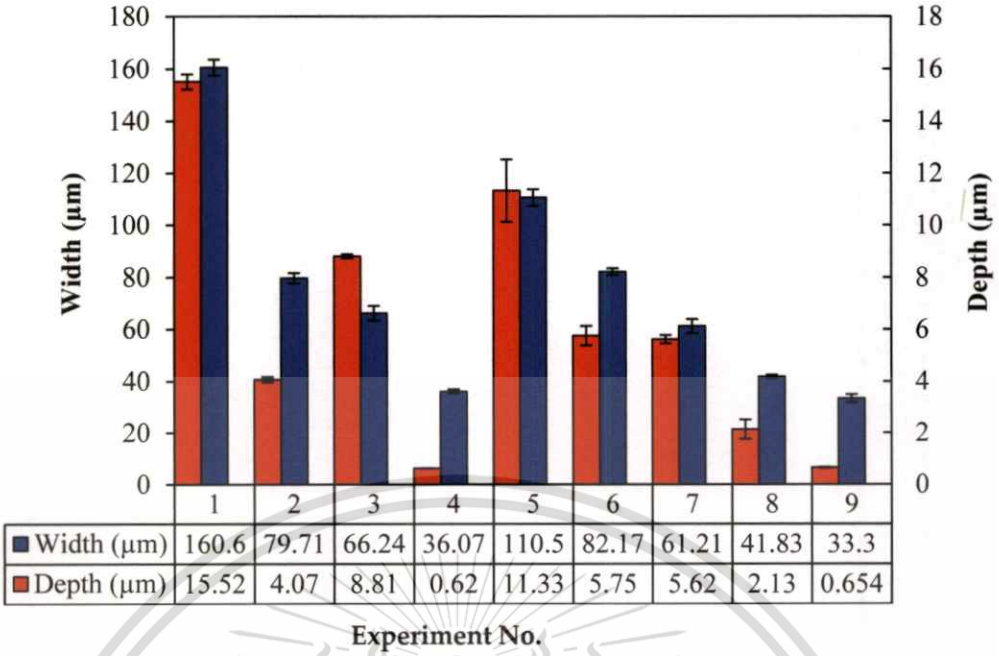

	1	2	3	4	5	6	7	8	9
Width (µm)	160.6	79.71	66.24	36.07	110.5	82.17	61.21	41.83	33.3
Depth (µm)	15.52	4.07	8.81	0.62	11.33	5.75	5.62	2.13	0.654

Figure 4.12 Validation of weldline property for PC

4.3.3 Nylon 6 with 30% Glass-Fiber Filled (PA6GF30)

With observation with naked eye, weldline on PA6GF30 test mold part cannot be seen as well as the results of weldline measurement by 3 D Measuring Laser Microscope and SEM images in Figure4.14. Figure 4.13 shows the weldline images of each condition captured by 3 D Measuring Laser Microscope at total magnification of 20X. However, these image exhibit the specimen surface was smoother when the mold temperature increases resulting from the glass fibers were sink down in the polymer due to the melt has more molecular movability to move along the cavity surface.

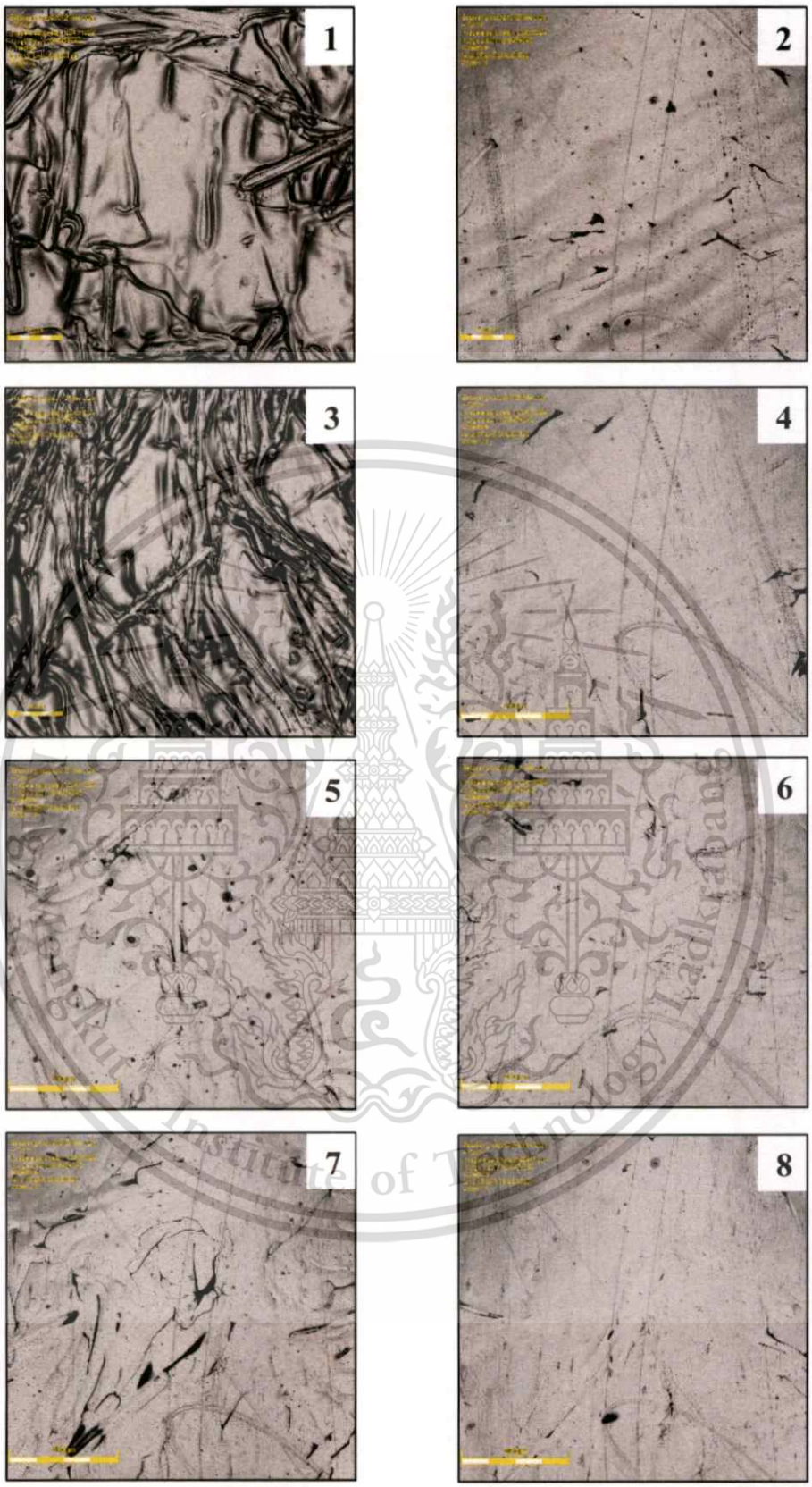

Figure 4.13 The characteristic of V-notch of weld line for each experiment at a total magnification of 20X for PA6GF30 specimens.

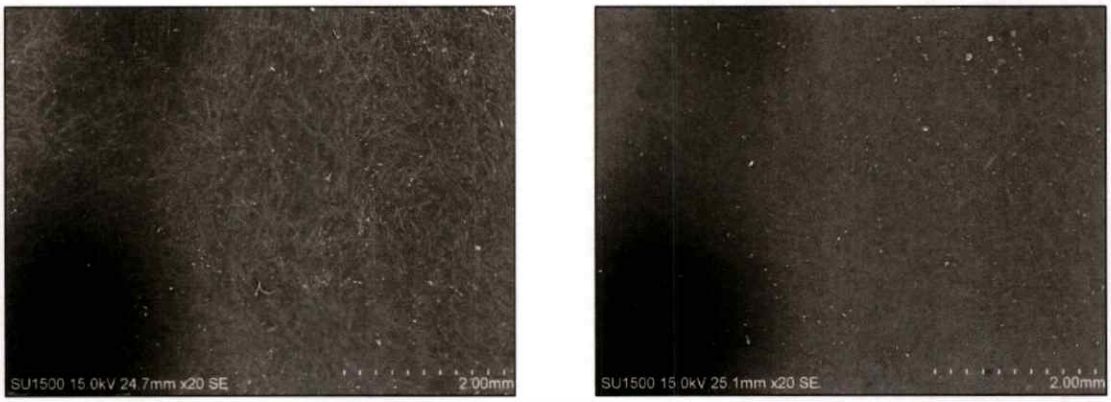

a) Experiment No.1 (without induction heating)

b) Experiment No.4 (with induction heating)

Figure 4.14 SEM images of PC (a) experiment no.1 without induction heating and (b) experiment no.4 with induction heating at the area where V-notch of weld line occur.

4.4 Effect Of Processing Parameters On Gloss Property

4.4.1 Polycarbonate (PC)

Figure 4.15 shows the measured gloss of PC material at the angle of 60°. It was found that the experiment No.1, which is the combination of low injection speed (25 mm/s), low packing pressure (1200 kgf/cm²), low heating temperature (30°C) and low water temperature (30°C), was the glossiest with gloss value of 105.5 GU. Comparing to experiment No.5, it is improved by 2.2% and 97.1%, respectively, as shown in Table 4.12.

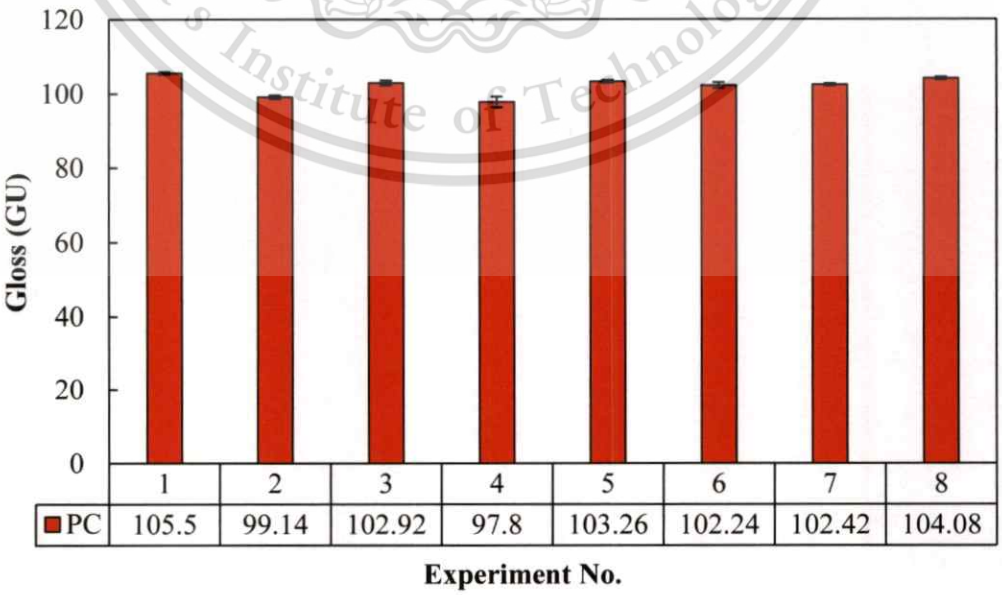

Figure 4.15 The measured gloss of PC specimen.

Table 4.14 Percentage of the improvement and the calculated S/N ratio for the measured gloss of PC specimens.

Exp.	Factor Combination				Average Gloss (GU)	Improvement comparing to Exp.5 (%)	S/N ratio
	A	B	C	D			
1	25	1200	30	30	105.5	2.2	40.46
2	25	1200	165	80	99.14	-4.0	39.92
3	75	1300	30	30	102.92	-0.3	40.25
4	75	1300	165	80	97.8	-5.3	39.80
5	25	1300	80	80	103.26	-	40.28
6	25	1300	165	30	102.24	-1.0	40.19
7	75	1200	80	80	102.42	-0.8	40.21
8	75	1200	165	30	104.08	0.8	40.35

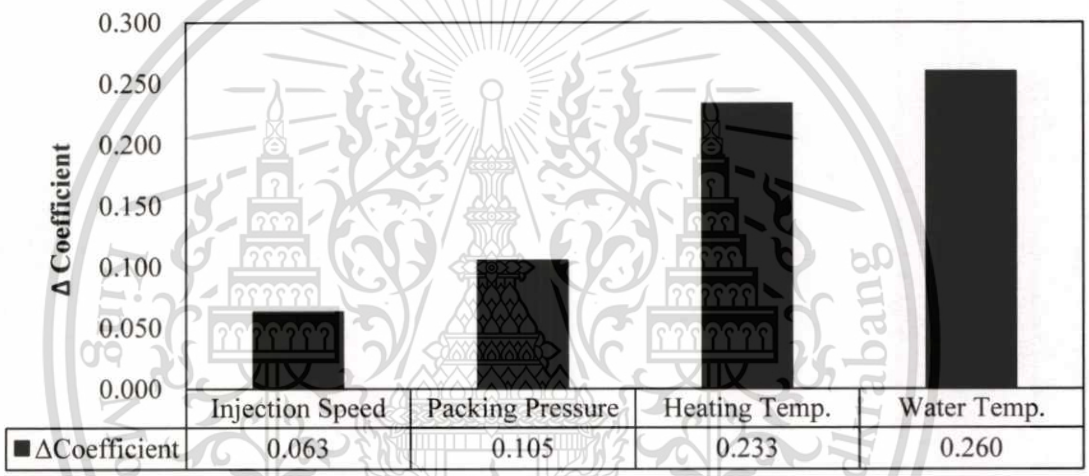

Figure 4.16 The relationship between the difference of regression coefficient values and process parameters affecting on the gloss property of PC specimens.

The regression analysis was employed to analyze the measured values to investigate the effect of each molding parameter on gloss property. Due to this study focus on the glossier surface providing the good surface quality, so the larger-the-better quality characteristic of S/N ratio as Eq. 2 is carried out to identify the optimum setting and ranking in the increase of the gloss value. The calculated S/N ratios are listed in Table 4.14. The results of regression analysis showed that the optimum parameter setting of the highest gloss can be obtained from the experiment No.1 which is the combination of low injection speed (25 mm/s), low packing pressure (1200 kgf/cm²), low heating temperature (30°C), and low water temperature (30°C). The ranking of each parameter affecting the gloss property is obtained from the difference between the maximum and minimum value

coefficient from regression analysis. The effect of each parameter depends on how large that difference value is. In the other words, the parameter with the highest difference value is the most effective parameter affecting the gloss as shown in Figure4.16. Table 4.15 reveals the most effective parameter resulting in the optimal gloss is the water temperature, followed by heating temperature, packing pressure, and injection speed, respectively.

Table 4.15 The best parameter combination and ranking of the effect for producing parts with the optimal gloss of V-notch on PC specimens.

Parameter	PC	
	Best Combination	**Factor Ranking**
Injection Speed (mm/s)	25	4
Packing Pressure(kgf/cm²)	1200	3
Heating Temperature (°C)	30	2
Water Temperature (°C)	30	1

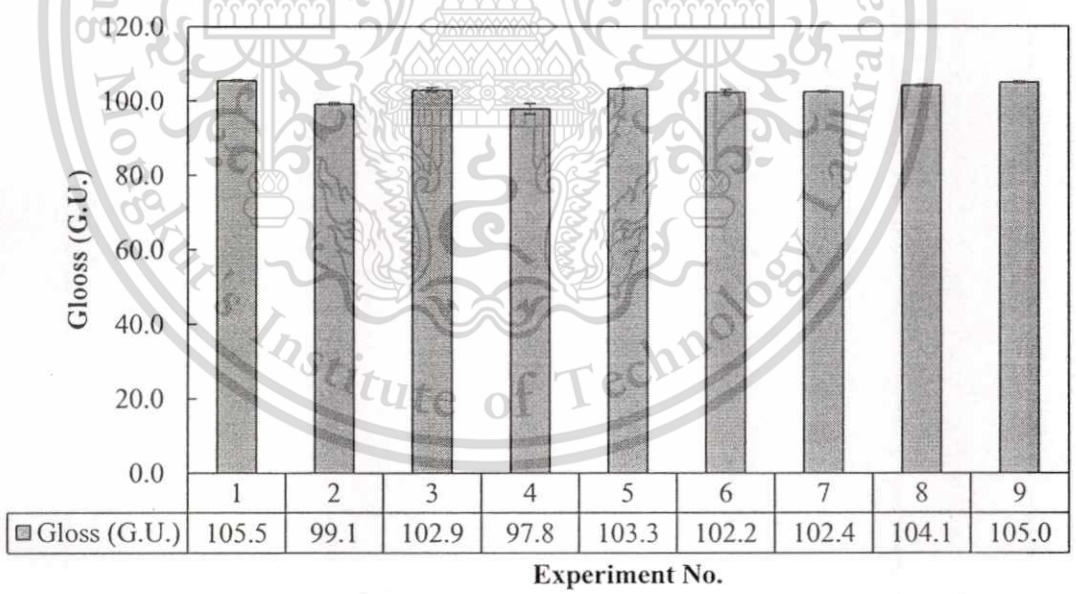

Figure 4.17 Validation of surface gloss property for PC

To validate the best combination, experiment No.1 was repeated in the injection molding and surface gloss property testing. It was found that experiment No.1, as experiment No.9 in Figure 4.12, has the high gloss value and closely to that of the original experiment No.1.

4.4.2 Polycarbonate/Acrylonitrile Butadiene Styrene (PC/ABS)

Figure 4.18 exhibits the measured gloss of PC/ABS material at the angle of 60°. It was found that the specimens of the experiment No.8 which were the combination of low injection speed (25 mm/s), low packing pressure (1200 kgf/cm²), low heating temperature (30°C), and low water temperature (30°C) were the glossiest (95.50 GU). However, the gloss values of experiment No.2-9 are not much different to each other.

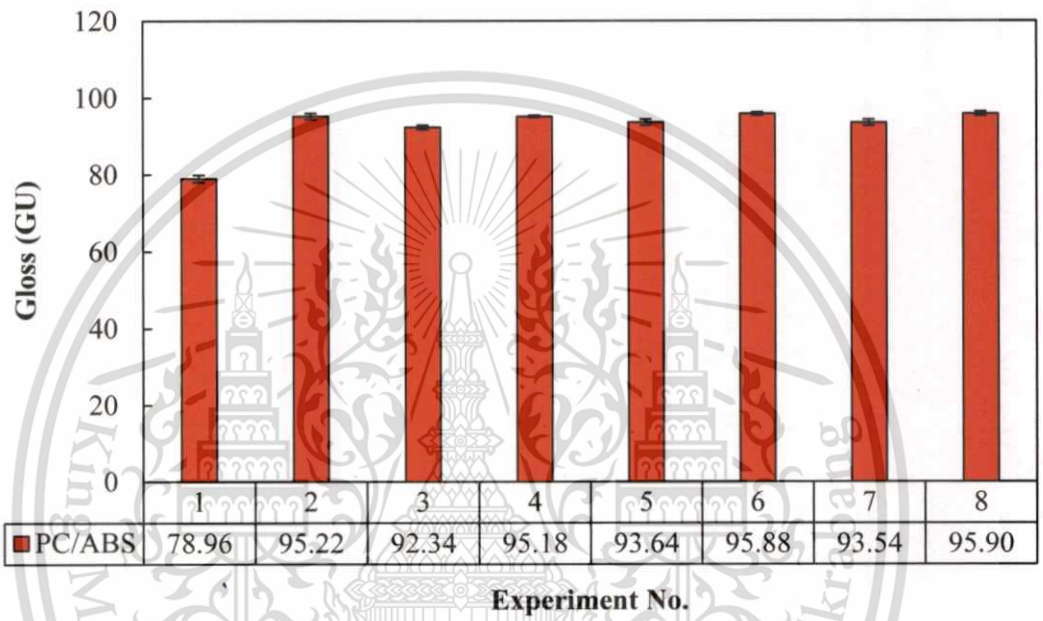

Figure 4.18 The measured gloss of PC/ABS specimen

Table 4.16 Percentage of the improvement and the calculated S/N ratio for the measured gloss of PC/ABS specimens.

Exp.	Factor Combination				Average Gloss (GU)	Improvement comparing to Exp.5 (%)	S/N ratio
	A	B	C	D			
1	25	1200	30	30	78.96	-15.7	37.95
2	25	1200	160	80	95.22	1.7	39.57
3	100	1300	30	30	92.34	-1.4	39.31
4	100	1300	160	80	95.18	1.6	39.57
5	25	1300	80	80	93.64	-	39.43
6	25	1300	160	30	95.88	2.4	39.63
7	100	1200	80	80	93.54	-0.1	39.42
8	100	1200	160	30	95.9	2.4	39.64

In regression analysis, the larger-the-better quality characteristic of S/N ratio as Eq. 2 is carried out to identify the optimum setting and ranking

in the increase of the gloss value. The calculated S/N ratios are listed in Table 4.16. The results of regression analysis showed that the optimum parameter setting of the optimal gloss can be obtained from the experiment No.4 which is the combination of high injection speed (100 mm/s), high packing pressure (1300 kgf/cm²), high heating temperature (160°C), and high water temperature (80°C) as Table 4.17. The parameter with the highest difference value is the most effective parameter affecting the weld line visibility as in Figure4.19. Table 4.17 shows that the most effective parameter resulting in the optimal gloss is the heating temperature followed by, water temperature, packing pressure, and injection speed, respectively.

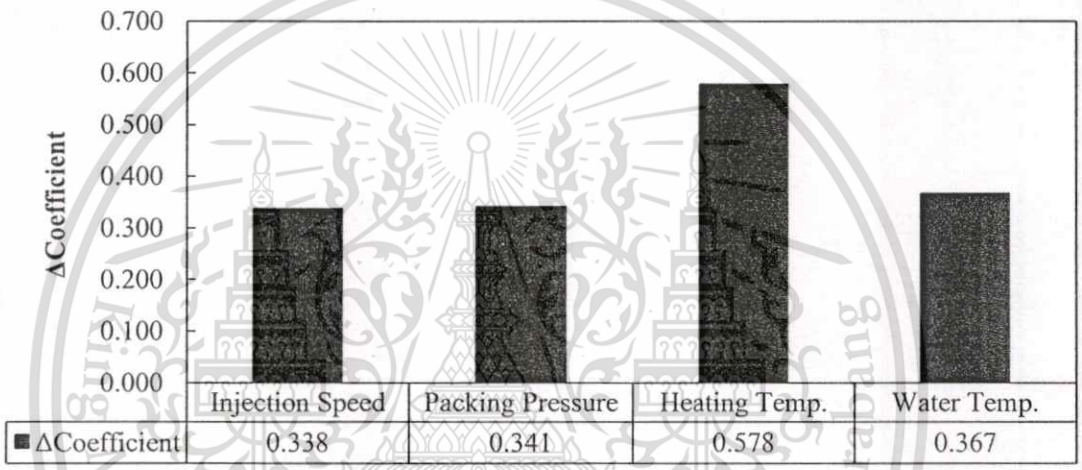

Figure 4.19 The relationship between the difference of regression coefficient values and process parameters affecting on the gloss property of PC/ABS specimens.

Table 4.17 The best parameter combination and ranking of the effect for producing parts with the optimal gloss of V-notch on PC specimens.

Parameter	PC/ABS	
	Best Combination	Factor Ranking
Injection Speed (mm/s)	100	4
Packing Pressure (kgf/cm²)	1300	3
Heating Temperature (°C)	160	1
Water Temperature (°C)	80	2

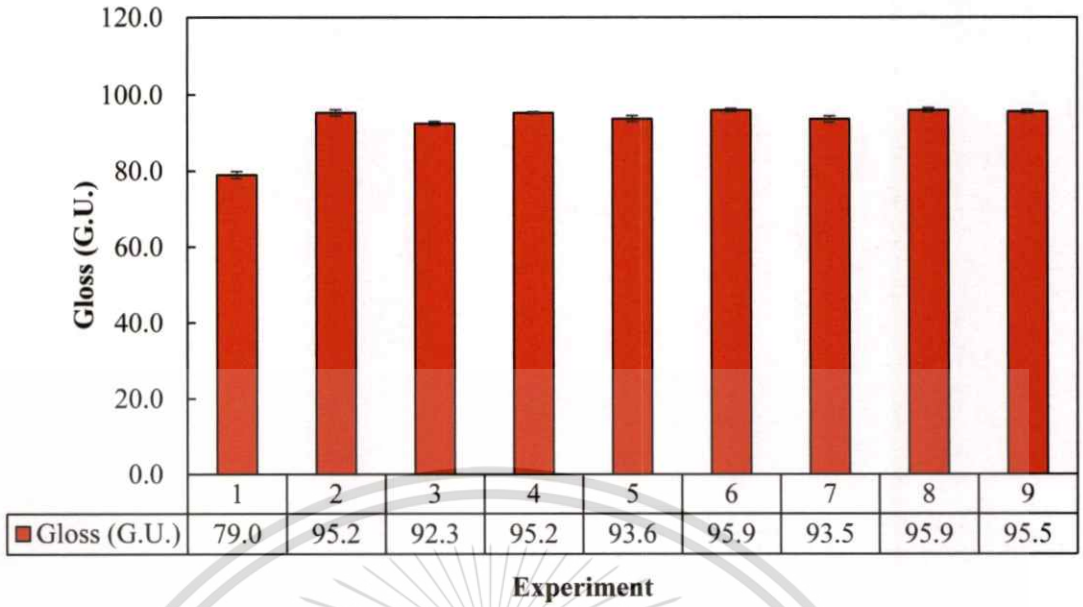

Figure 4.20 Validation of surface gloss property for PC

To validate the best combination, experiment No.4 was repeated in the injection molding and surface gloss property testing. It was found that experiment No.4, as experiment No.9 in Figure 4.20, is still provided the high gloss value.

4.4.3 Nylon 6 with 30% Glass-Fiber Filled (PA6GF30)

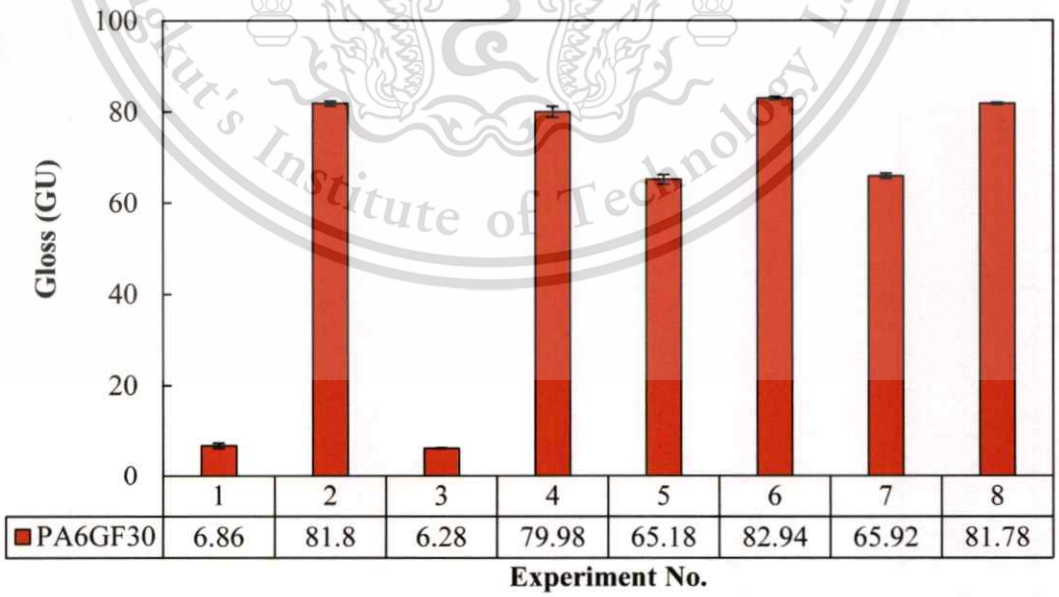

Figure 4.21 The measured gloss of PA6GF30 specimen.

Figure 4.21 shows the measured gloss of PA6GF2 material at the angle of 60°. It was found that the specimens were obviously glossier when the mold temperature increased. The specimens of the experiment No.6 which were the combination of low injection speed (25 mm/s), high packing pressure (1300 kgf/cm²), high heating temperature (160°C), and low water temperature (30°C) were the glossiest (82.94 GU).

For the regression analysis, the larger-the-better quality characteristic of S/N ratio as Eq. 2 is carried out to identify the optimum setting and ranking in the increase of the gloss value. The calculated S/N ratios are listed in Table 4.18. The parameter with the highest difference value of coefficient is the most effective parameter affecting the weld line visibility as in Figure4.22. Table 4.19 shows that the most effective parameter resulting in the optimal gloss is the heating temperature followed by, water temperature, injection speed and, packing pressure, respectively. The results of regression analysis showed that the optimum parameter setting of the optimal gloss can be obtained from the experiment No.2 which is the combination of high injection speed (25 mm/s), high packing pressure (1200 kgf/cm²), high heating temperature (160°C), and high water temperature (80°C) as Table 4.19.

Table 4.18 Percentage of the improvement and the calculated S/N ratio for the measured gloss of PA6GF30 specimens.

Exp.	Factor Combination				Average Gloss (GU)	Improvement comparing to Exp.5 (%)	S/N ratio
	A	B	C	D			
1	25	1200	30	30	6.86	-89.5	16.62
2	25	1200	160	80	81.8	25.5	38.25
3	75	1300	30	30	6.28	-90.4	15.96
4	75	1300	160	80	79.98	22.7	38.06
5	25	1300	80	80	65.18	-	36.28
6	25	1300	160	30	82.94	27.2	38.38
7	75	1200	80	80	65.92	1.1	36.38
8	75	1200	160	30	81.78	25.5	38.25

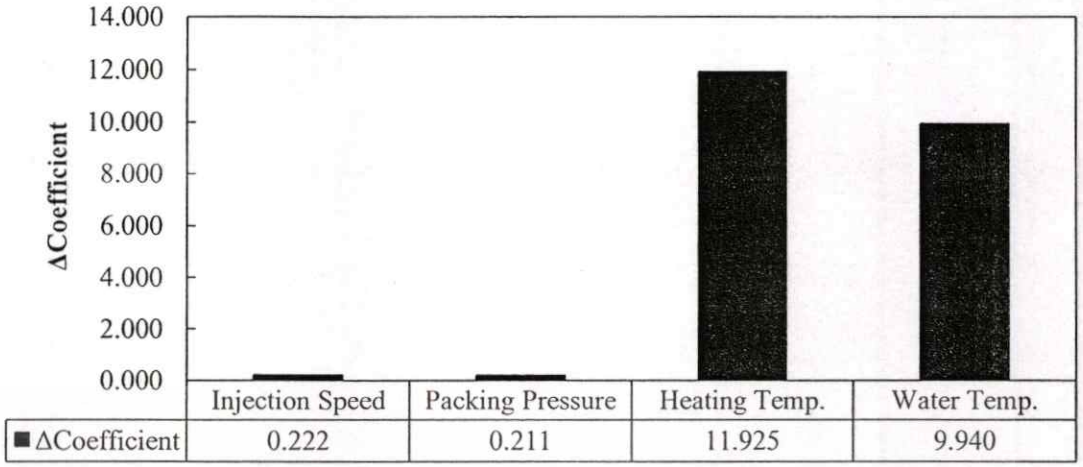

Figure 4.22 The relationship between the difference of regression coefficient values and process parameters affecting on the gloss property of PA6GF30 specimens.

Table 4.19 The best parameter combination and ranking of the effect for producing parts with the optimal gloss of V-notch on PA6GF30 specimens.

Parameter	PA6GF30	
	Best Combination	Factor Ranking
Injection Speed (mm/s)	25	3
Packing Pressure (kgf/cm²)	1200	4
Heating Temperature (°C)	160	1
Water Temperature (°C)	80	2

To validate the best combination, experiment No.2 was repeated in the injection molding and surface gloss property testing. It was found that experiment No.2, as experiment No.9 in Figure 4.23, is still provided the high gloss value that is not apparently different from that of experiment No.6.

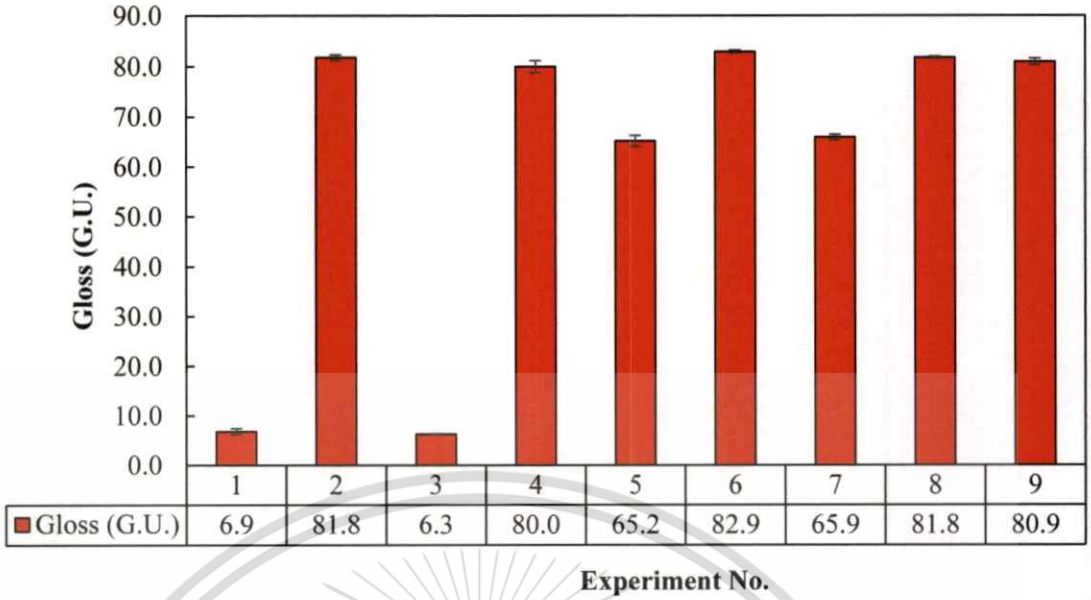

Figure 4.23 Validation of surface gloss property for PA6GF30

4.5 Effect Of Processing Parameters On Flexural Strength Property

4.5.1 Polycarbonate (PC)

Figure 4.24 shows the flexural strength of weldline. It was found that the flexural strength values of each experiment were not apparently different to that of each other. The experiment No.1 had the highest flexural strength of weldline whereas that of the experiment No.7 had the least.

The regression analysis was employed to analyze the measured values to investigate the effect of each molding parameter on flexural strength property of weldline. Due to this study focus on the more the flexural strength, the better the quality. Therefore, the larger-the-better quality characteristic of S/N ratio as Eq. 2 is carried out to identify the optimum setting and ranking of process parameter affecting the flexural strength property. The calculated S/N ratios are listed in Table 4.20. The ranking of each parameter affecting the flexural strength of weld line is obtained from the difference between the maximum and minimum value coefficient from regression analysis. The effect of each parameter depends on how large that difference value is. In the other words, the parameter with the highest difference value is the most effective parameter affecting flexural strength. From Figure 4.25, it can be concluded that the packing pressure is the most influencing parameter on the flexural strength of weldline followed by

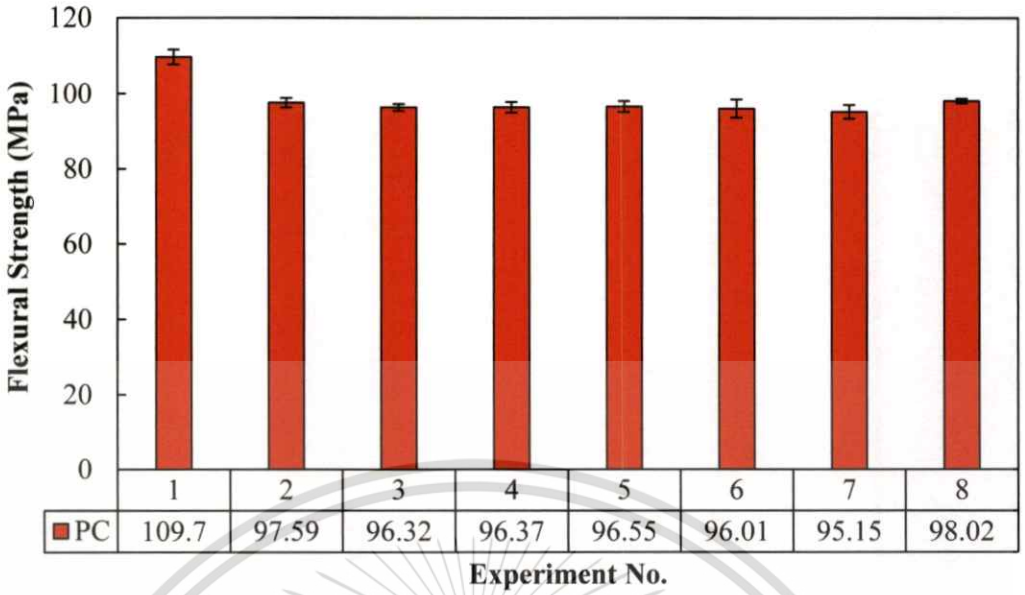

Figure 4.24 The measured flexural strength of PC specimens.

water temperature, injection speed, and heating temperature, respectively. Table 4.21 summarizes the optimum process setting and ranking of process parameter for flexural strength of weldline. The results of regression analysis showed that the optimum parameter setting for the flexural strength of weldline property can be obtained from the experiment no.1 which is the combination of low injection speed (25 mm/s), low packing pressure (1200 kgf/cm²), low heating temperature (30°C), and low water temperature (30°C).

Table 4.20 Percentage of the improvement and the calculated S/N ratio for the measured flexural strength of PC specimens.

Exp.	Factor Combination				Average flexural strength (MPa)	Improvement comparing to Exp.5 (%)	S/N ratio
	A	B	C	D			
1	25	1200	30	30	109.7	13.6	40.80
2	25	1200	165	80	97.59	1.1	39.79
3	75	1300	30	30	96.32	-0.2	39.67
4	75	1300	165	80	96.37	-0.2	39.68
5	25	1300	80	80	96.55	-	39.69
6	25	1300	165	30	96.01	-0.6	39.64
7	75	1200	80	80	95.15	-1.5	39.56
8	75	1200	165	30	98.02	1.5	39.83

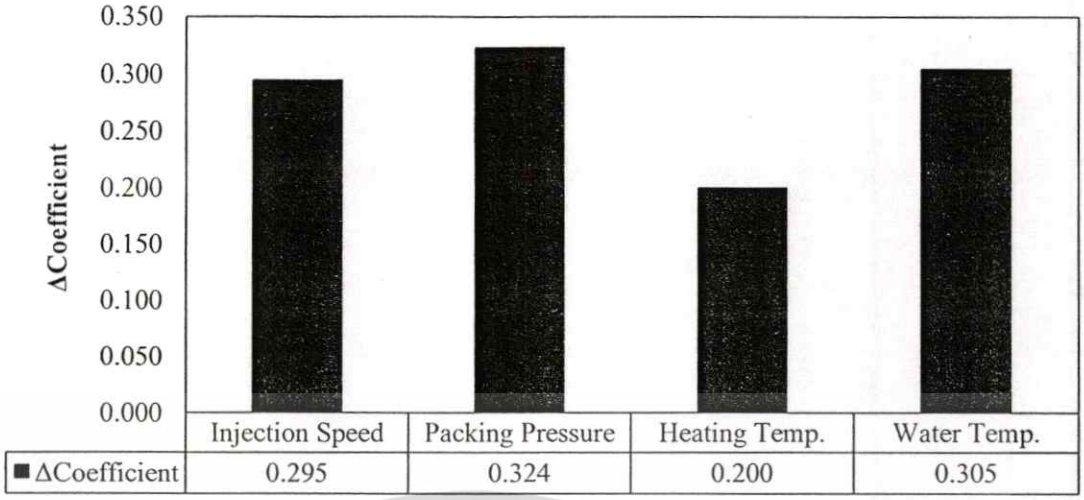

Figure 4.25 The relationship between the difference of regression coefficient values and process parameters on the flexural strength property of PC specimens.

Table 4.21 The best parameter combination and ranking of the effect for producing parts with the optimal flexural strength on PC specimens.

Parameter	PC	
	Best Combination	Factor Ranking
Injection Speed (mm/s)	25	3
Packing Pressure (kgf/cm²)	1200	1
Heating Temperature (°C)	30	4
Water Temperature (°C)	30	2

To validate the best combination, experiment No.1 was repeated in the injection molding and flexural strength of weldline property testing. It was found that experiment No.1, as experiment No.9 in Figure 4.26, is still provided the high flexural strength of weldline among other experiments.

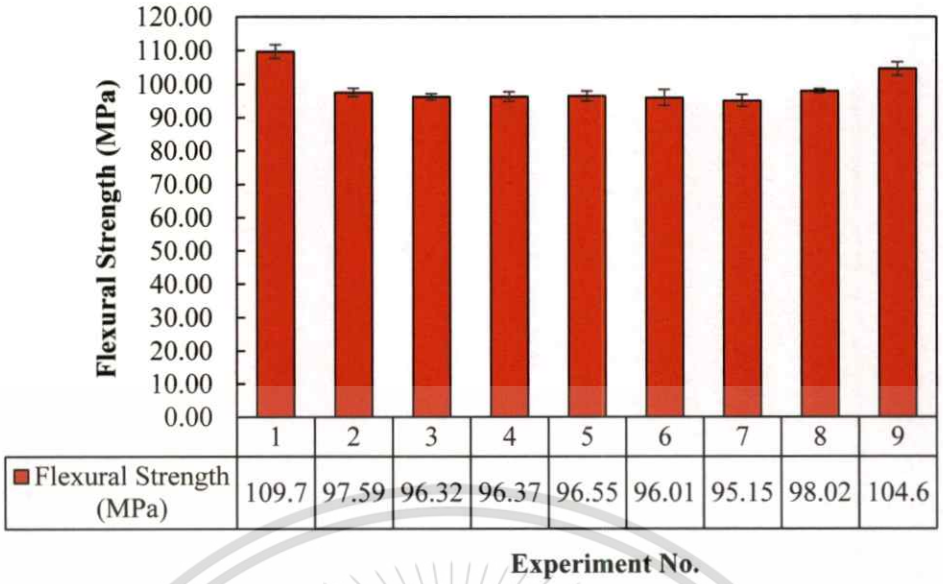

Figure 4.26 Validation of flexural strength of weldline property for PC

4.5.2 Polycarbonate/Acrylonitrile Butadiene Styrene (PC/ABS)

The flexural strength of weldline of PC/ABS specimen was shown in Figure 4.27. It was found that the flexural strength values of each experiment were not apparently different to that of each other. The experiment no.1 had the highest flexural strength of weldline whereas that of the experiment no.2 had the least.

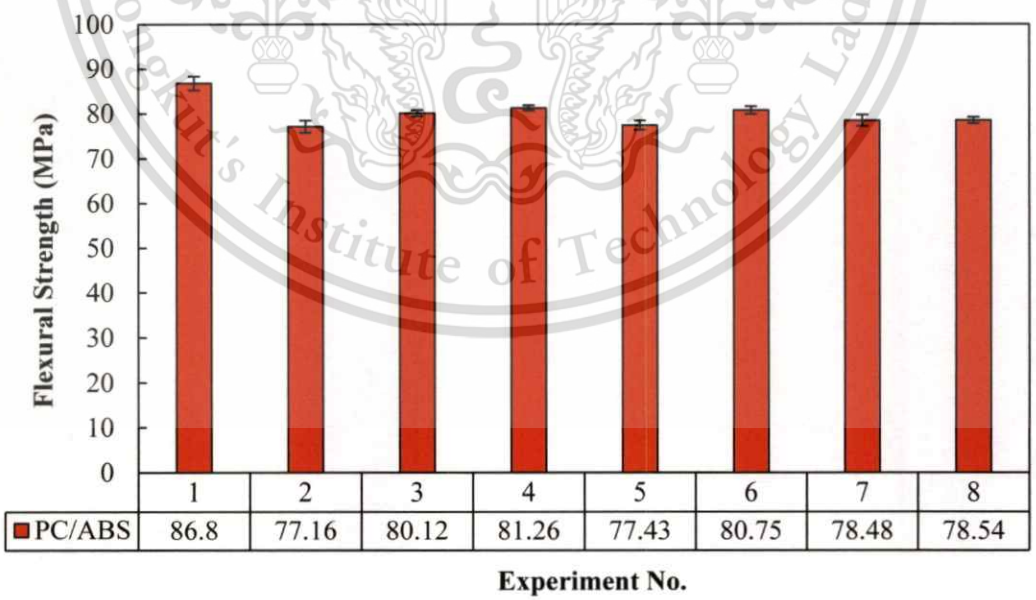

Figure 4.27 The measured flexural strength of PC/ABS specimens.

For the regression analysis, the larger-the-better quality characteristic of S/N ratio as Eq. 2 is carried out to identify the optimum setting and

Table 4.22 Percentage of the improvement and the calculated S/N ratio for the measured flexural strength of PC/ABS specimens.

Exp.	Factor Combination				Average flexural strength (MPa)	Improvement comparing to Exp.5 (%)	S/N ratio
	A	B	C	D			
1	25	1200	30	30	86.8	12.1	38.77
2	25	1200	160	80	77.16	-0.3	37.74
3	100	1300	30	30	80.12	3.5	38.07
4	100	1300	160	80	81.26	4.9	38.20
5	25	1300	80	80	77.43	-	37.78
6	25	1300	160	30	80.75	4.3	38.14
7	100	1200	80	80	78.48	1.4	37.89
8	100	1200	160	30	78.54	1.4	37.90

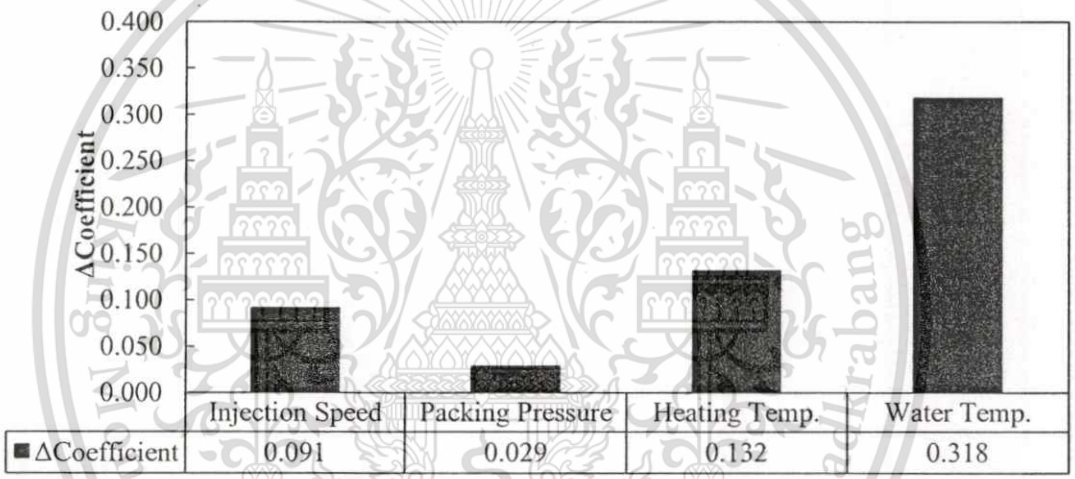

Figure 4.28 The relationship between the difference of regression coefficient values and process parameters on the flexural strength property of PC/ABS specimens.

ranking in the increase of the flexural strength of weldline property. The calculated S/N ratios are listed in Table 4.22. The parameter with the highest difference value of coefficient is the most effective parameter affecting flexural strength of weldline. Figure 4.28 shows that the water temperature is the most influencing parameter on the flexural strength of weldline followed by heating temperature, injection speed, and packing pressure, respectively. Table 4.23 summarizes the optimum process setting and ranking of process parameter for flexural strength of weldline. The results of regression analysis showed that the optimum parameter setting for the flexural strength property can be obtained from the experiment no.1 which is the combination of low injection speed (25 mm/s), low packing

pressure (1200 kgf/cm²), low heating temperature (30°C), and low water temperature (30°C).

Table 4.23 The best parameter combination and ranking of the effect for producing parts with the optimal flexural strength on PC/ABS specimens.

Parameter	PC/ABS	
	Best Combination	Factor Ranking
Injection Speed (mm/s)	25	3
Packing Pressure (kgf/cm²)	1200	4
Heating Temperature (°C)	30	2
Water Temperature (°C)	30	1

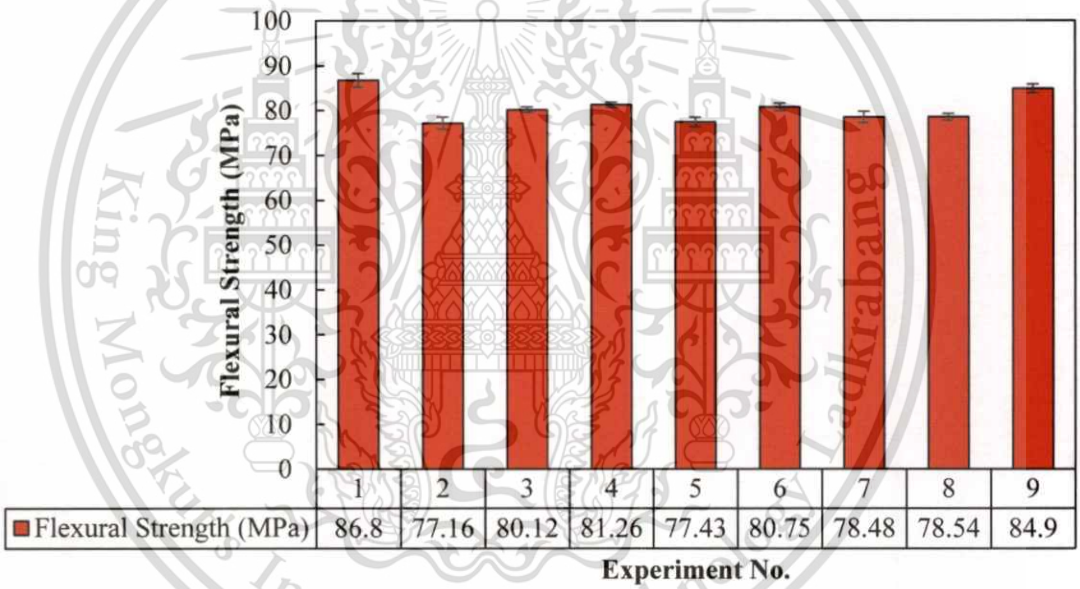

Figure 4.29 Validation of flexural strength of weldline property for PC/ABS.

To validate the best combination, experiment No.1 was repeated in the injection molding and flexural strength of weldline property testing. It was found that experiment No.1, as experiment No.9 in Figure 4.29, is still provided the high flexural strength of weldline among other experiments.

4.5.3 Nylon 6 with 30% Glass-Fiber Filled (PA6GF30)

Figure 4.30 shows the flexural strength of weldline of PA6GF30 material. It was found that the flexural strength values of each experiment were not apparently different to that of each other. The experiment No.1

had the highest flexural strength of weldline whereas that of the experiment no.6 had the least.

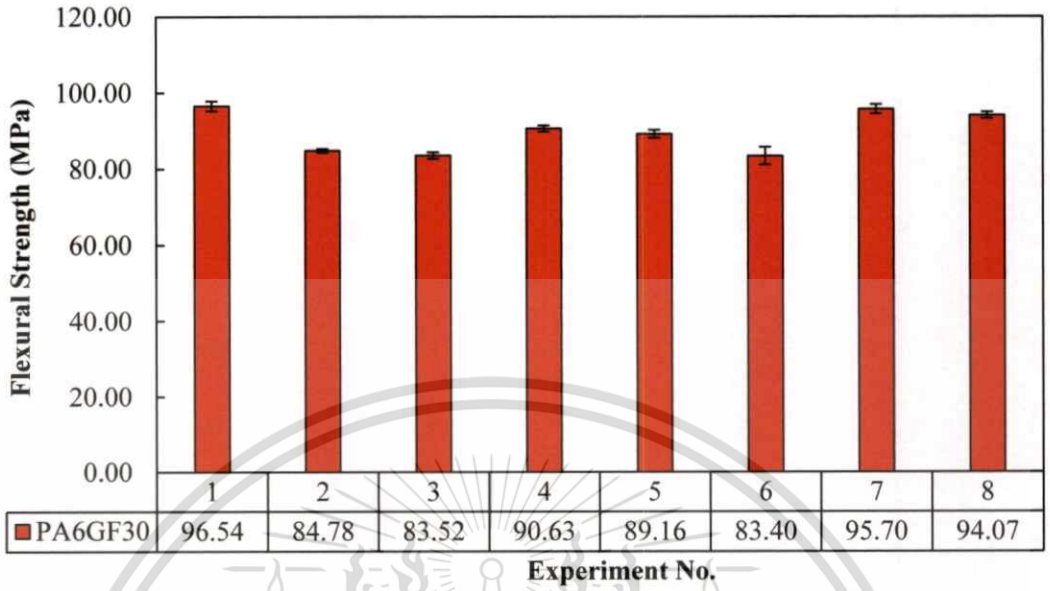

Figure 4.30 The measured flexural strength of PA6GF30 specimens.

For the regression analysis, the larger-the-better quality characteristic of S/N ratio as Eq. 2 is carried out to identify the optimum setting and, ranking in the increase of the flexural strength of weldline property. The calculated S/N ratios are listed in Table 4.24. The parameter with the highest difference value of coefficient is the most effective parameter affecting flexural strength of weldline. Figure 4.31 shows that the packing pressure is the most influencing parameter on the flexural strength of weldline followed by heating temperature, water temperature, and injection speed, and respectively. Table 4.25 summarizes the optimum process setting and ranking of process parameter for flexural strength of weldline. The results of regression analysis showed that the optimum parameter setting for the flexural strength property can be obtained from the experiment No.7 which is the combination of high injection speed (100 mm/s), low packing pressure (1200 kgf/cm^2), low heating temperature (80°C), and high water temperature (80°C).

To validate the best combination, experiment No.7 was repeated in the injection molding and flexural strength of weldline property testing. It was found that experiment No.1, as experiment No.9 in Figure 4.32, is still provided the high flexural strength of weldline.

Table 4.24 Percentage of the improvement and the calculated S/N ratio for the measured flexural strength of PA6GF30 specimens.

Exp.	Factor Combination				Average flexural strength (MPa)	Improvement comparing to Exp.5 (%)	S/N ratio
	A	B	C	D			
1	25	1200	30	30	96.54	8.3	39.69
2	25	1200	160	80	84.78	-4.9	38.57
3	75	1300	30	30	83.52	-6.3	38.43
4	75	1300	160	80	90.63	1.6	39.14
5	25	1300	80	80	89.16	-	39.00
6	25	1300	160	30	83.4	-6.5	38.42
7	75	1200	80	80	95.7	7.4	39.62
8	75	1200	160	30	94.07	5.5	39.47

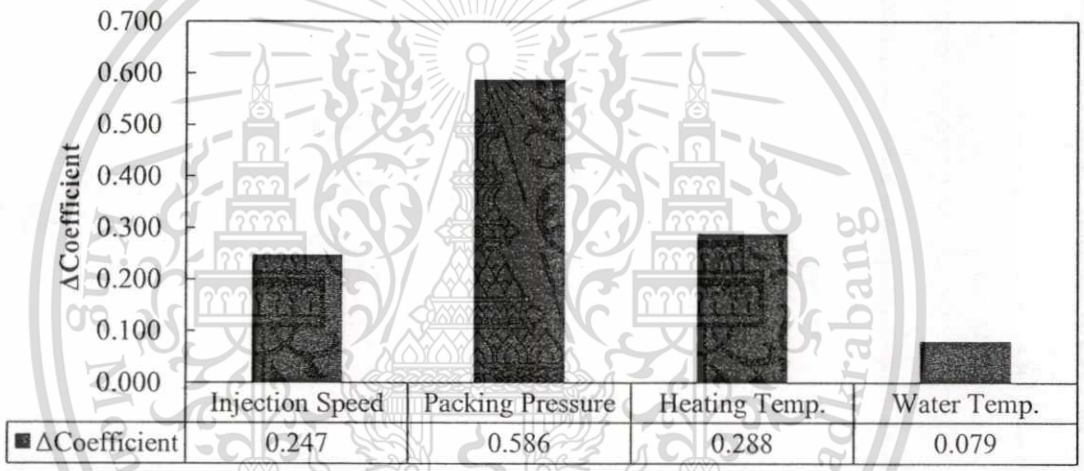

Figure 4.31 The relationship between the difference of regression coefficient values and process parameters on the flexural strength property of PA6GF30 specimens

Table 4.25 The best parameter combination and ranking of the effect for producing parts with the optimal flexural strength on PA6GF30 specimens.

Parameter	PA6GF30	
	Best Combination	Factor Ranking
Injection Speed (mm/s)	100	3
Packing Pressure (kgf/cm²)	1200	1
Heating Temperature (°C)	80	2
Water Temperature (°C)	80	4

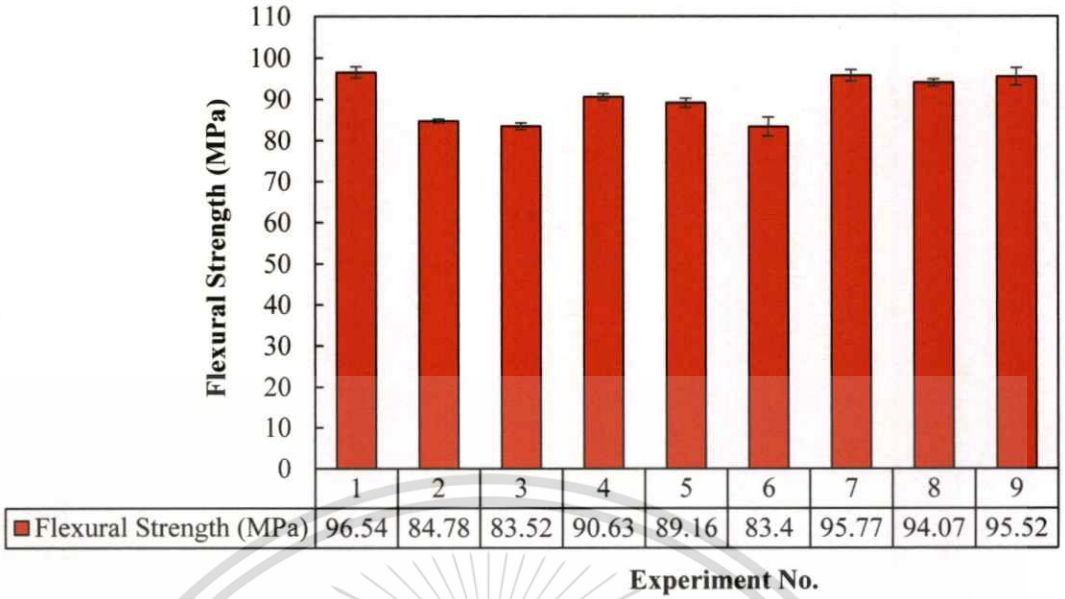

Figure 4.32 Validation of flexural strength of weldline property for PA6GF30

4.6 Effect Of Processing Parameters On Roughness Property

4.6.1 Polycarbonate (PC)

The surface average roughness (Ra) values in two direction (parallel and perpendicular to the gate) of the tested parts are exhibited in Figure 4.33. It was observed that experiment No. 6 showed the least average roughness values whereas experiment No. 1 provided the most average roughness values. It was revealed that the average roughness values was decreased when the mold surface temperature before injection was high to 80°C and 160°C. This was the result from the high mold temperature slowed down the freezing of the melt resulting in the molecular mobility of the melt is higher. Consequently, the molecules of the melt have enough time in flowing along the mold surface. They can replicate the feather of the cavity-side mold surface better. Therefore, the parts were smoother or less roughness.

The regression analysis was employed to analyze the measured values to investigate the effect of each molding parameter on surface average roughness of weldline. Due to this study focus on the smoother the surface average roughness, the better the part quality. Therefore, the smaller-the-better quality characteristic of S/N ratio as Eq. 1 is carried out to identify the optimum setting and ranking of process parameter affecting the surface average roughness. The calculated S/N ratios are listed in Table 4.26.

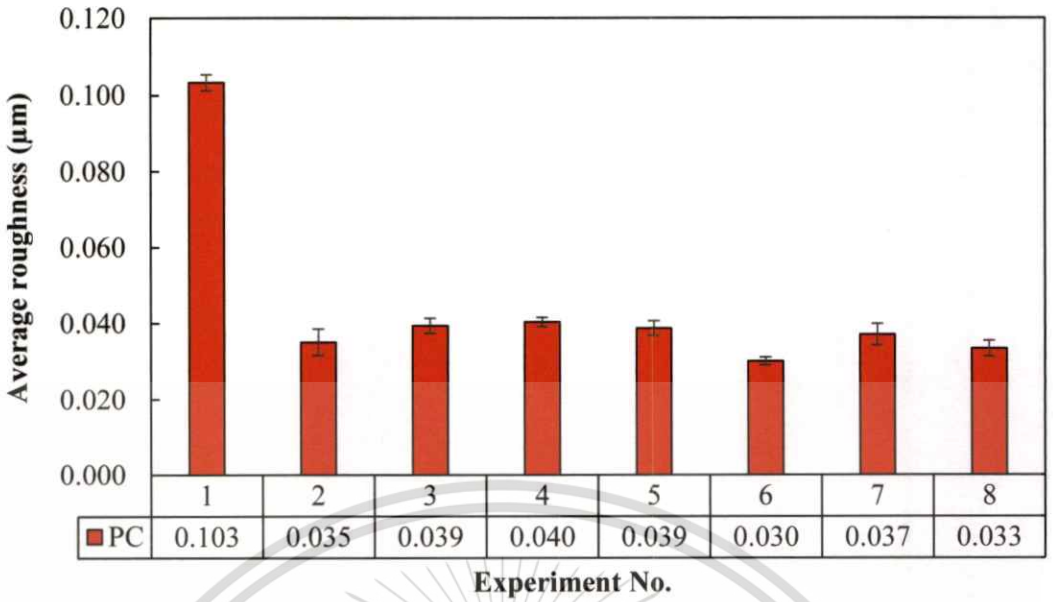

Figure 4.33 The measured surface average roughness in two direction of PC specimen.

Table 4.26 Percentage of the improvement and the calculated S/N ratio for the measured surface average roughness of PC specimens.

Exp.	Factor Combination				Average Roughness (µm)	Improvement comparing to Exp.5 (%)	S/N ratio
	A	B	C	D			
1	25	1200	30	30	0.10	-167.2	19.71
2	25	1200	165	80	0.04	9.5	29.08
3	75	1300	30	30	0.04	-1.7	28.09
4	75	1300	165	80	0.04	-4.3	27.88
5	25	1300	80	80	0.04	-	28.24
6	25	1300	165	30	0.03	22.4	30.45
7	75	1200	80	80	0.04	4.3	28.61
8	75	1200	165	30	0.03	13.8	29.53

The ranking of each parameter affecting the surface average roughness is obtained from the difference between the maximum and minimum value coefficient from regression analysis. The effect of each parameter depends on how large that difference value is. In the other words, the parameter with the highest difference value is the most effective parameter affecting surface average roughness. From Figure 4.34, it can be concluded that the heating temperature is the most influencing parameter on the surface average roughness followed by packing pressure, injection speed, and water temperature, respectively. Table 4.27 summarizes the optimum process setting and ranking of process parameter for surface average

roughness. The results of regression analysis revealed that the optimum parameter setting for the surface average roughness can be obtained from the experiment no.4 which is the combination of high injection speed (75 mm/s), high packing pressure (1300 kgf/cm²), high heating temperature (165°C), and high water temperature (80°C).

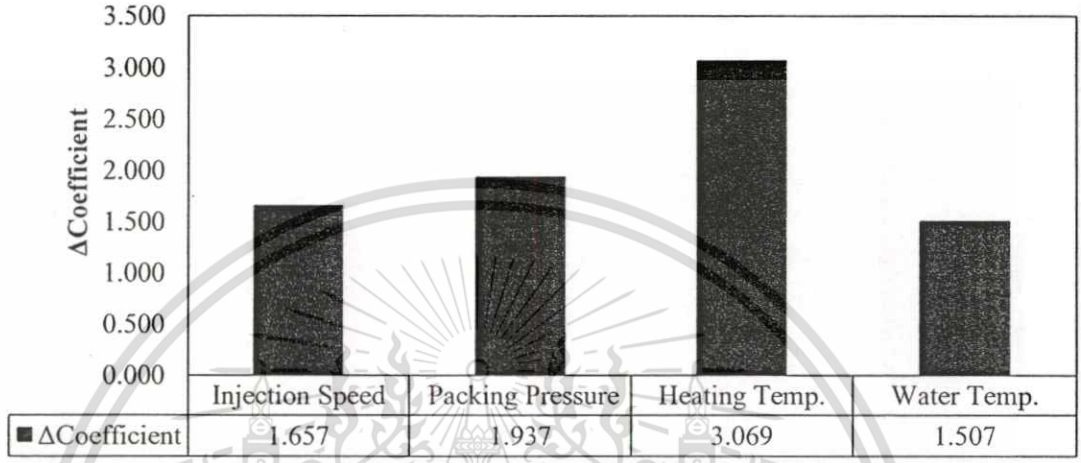

Figure 4.34 The relationship between the difference of regression coefficient values and process parameters on surface average roughness of PC specimens.

Table 4.27 The best parameter combination and ranking of the effect for producing parts with the optimal surface average roughness of PC specimens.

Parameter	PC	
	Best Combination	**Factor Ranking**
Injection Speed (mm/s)	75	3
Packing Pressure (kgf/cm²)	1300	2
Heating Temperature (°C)	165	1
Water Temperature (°C)	80	4

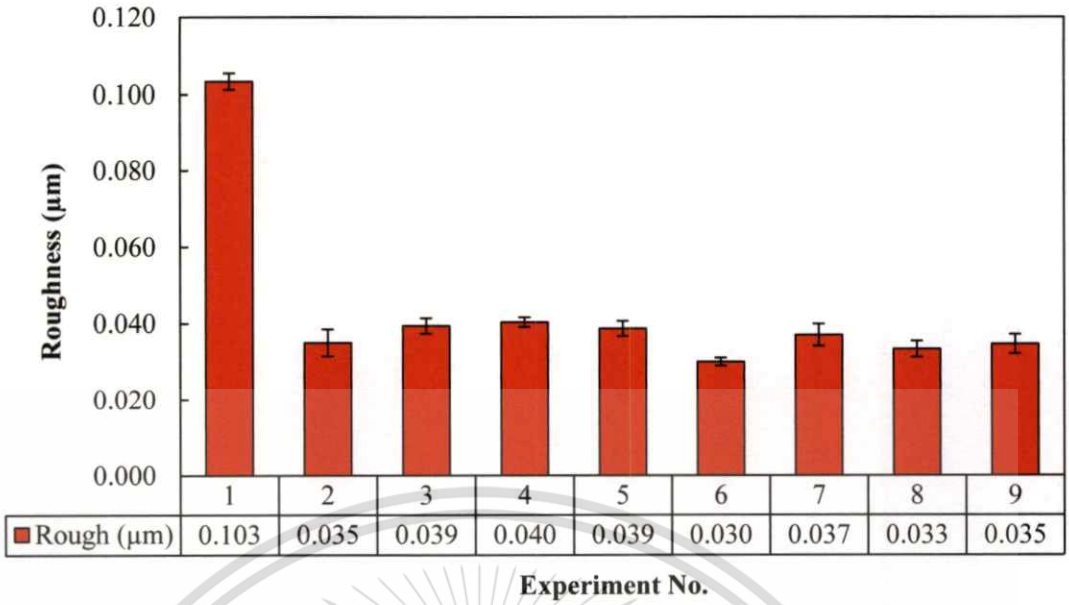

Figure 4.35 Validation of roughness property for PC

To validate the best combination, experiment No.4 was repeated in the injection molding and surface gloss property testing. It was found that experiment No.1, as experiment No.9 in Figure 4.32, has low surface average roughness at 0.035µm.

4.6.2 Polycarbonate/Acrylonitrile Butadiene Styrene (PC/ABS)

The surface average roughness (Ra) values in two direction (parallel and perpendicular to the gate) of the tested parts are exhibited in Figure 4.36. It was observed that experiment No. 6 showed the least average roughness values whereas experiment No. 1 provided the most average roughness values. It was revealed that the average roughness values was decreased when the mold surface temperature before injection was high to 80°C and 160°C. This was the result from the high mold temperature slowed down the freezing of the melt resulting in the molecular mobility of the melt is higher. (Consequently), the molecules of the melt have enough time in flowing along the mold surface. They can replicate the feather of the cavity-side mold surface better. Therefore, the parts were smoother or less roughness.

For the regression analysis, the smaller-the-better quality characteristic of S/N ratio as Eq. 1 is carried out to identify the optimum setting and, ranking in the decrease of the roughness property. The calculated S/N ratios are listed in Table 4.28. The parameter with the highest difference value of coefficient is the most effective parameter

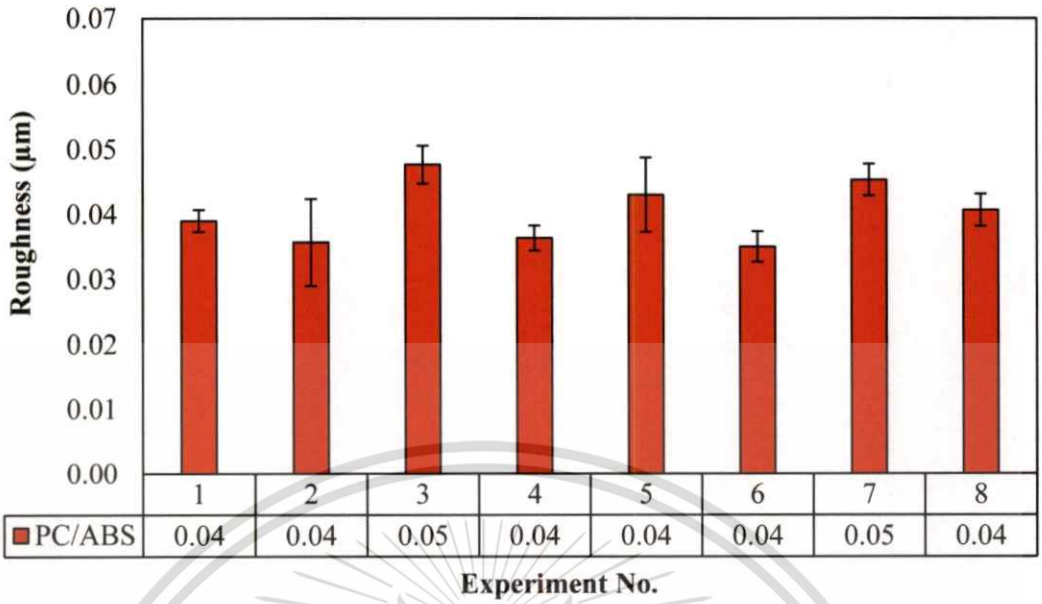

Figure 4.36 The measured surface average roughness in two direction of PC/ABS specimen.

Table 4.28 Percentage of the improvement and the calculated S/N ratio for the measured surface average roughness of PC specimens.

Exp.	Factor Combination				Average Roughness (µm)	Improvement comparing to Exp.5 (%)	S/N ratio
	A	B	C	D			
1	25	1200	30	30	0.04	9.3	28.17
2	25	1200	160	80	0.04	17.1	28.80
3	100	1300	30	30	0.05	-10.9	26.42
4	100	1300	160	80	0.04	15.5	28.78
5	25	1300	80	80	0.04	-	27.25
6	25	1300	160	30	0.04	18.6	29.10
7	100	1200	80	80	0.05	-5.4	26.86
8	100	1200	160	30	0.04	5.4	27.80

affecting surface average roughness. Figure 4.37 shows that the heating temperature is the most influencing parameter on the surface average roughness followed by injection speed, water temperature, and packing pressure, respectively. Table 4.29 summarizes the optimum process setting and ranking of process parameter on surface average roughness. The results of regression analysis showed that the optimum parameter setting for surface average roughness property can be obtained from the experiment No.2 which is the combination of low injection speed (25

mm/s), low packing pressure (1200 kgf/cm²), high heating temperature (160°C), and high water temperature (80°C).

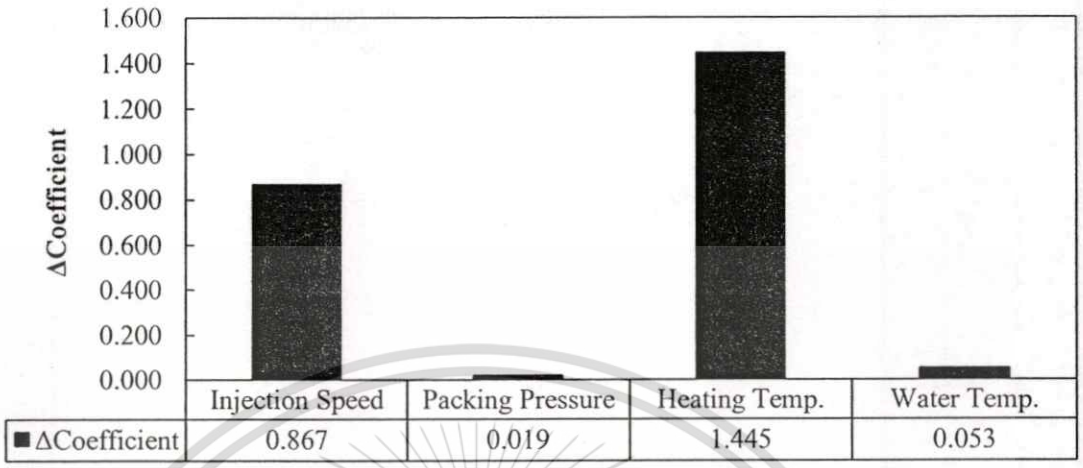

Figure 4.37 The relationship between the difference of regression coefficient values and process parameters on surface average roughness of PC/ABS specimens.

Table 4.29 The best parameter combination and ranking of the effect for producing parts with the optimal surface average roughness of PC/ABS specimens.

Parameter	PC/ABS	
	Best Combination	Factor Ranking
Injection Speed (mm/s)	25	2
Packing Pressure (kgf/cm²)	1200	4
Heating Temperature (°C)	160	1
Water Temperature (°C)	80	3

To validate the best combination, the experiment No.2 was repeated in the injection molding and surface gloss property testing. It was found that experiment No.2, as experiment No.9 in Figure 4.38, has low surface average roughness at 0.035μm.

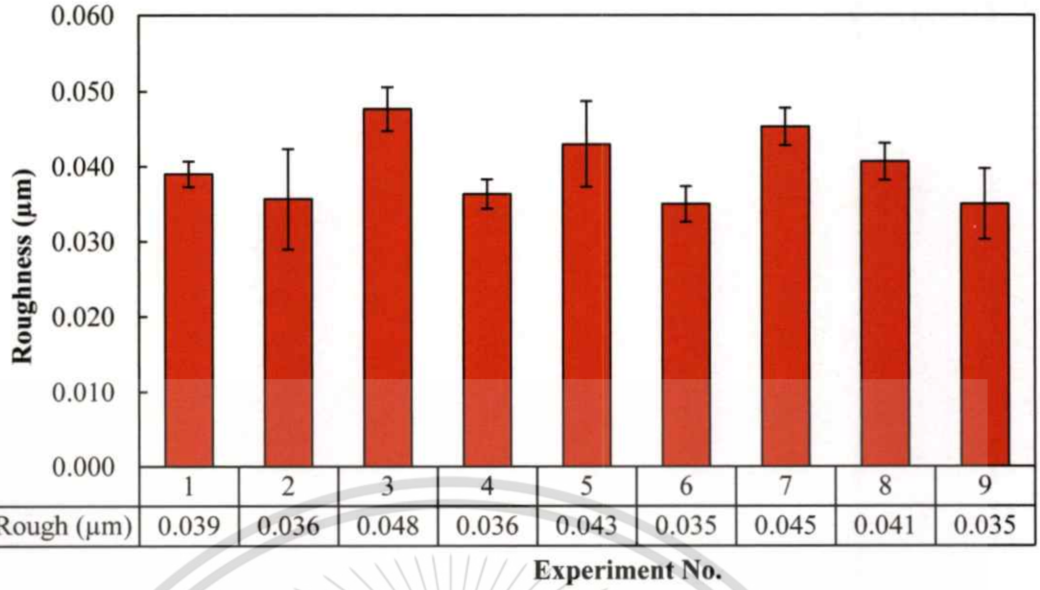

Figure 4.38 Validation of roughness property for PA6GF30.

4.6.3 Nylon 6 with 30% Glass-Fiber Filled (PA6GF30)

The surface average roughness (Ra) values in two direction (parallel and perpendicular to the gate) of the tested parts are exhibited in Figure 4.39. It was observed that experiment No. 8 showed the least average roughness values whereas experiment No. 1 provided the most average roughness values followed by the experiment No.3 which also has high average roughness values. The surface average roughness of the experiment No.1 and 3 were very high due to the cavity surface temperature is low resulting in the lower molecular mobility of melt. Therefore, the glass fibers float on the part surface. The melt cannot can replicate or move along the feather of the cavity-side mold surface. Therefore, the part surface was rougher.

For the regression analysis, the smaller-the-better quality characteristic of S/N ratio as Eq. 1 is carried out to identify the optimum setting and, ranking in the decrease of the surface average roughness property. The calculated S/N ratios are listed in Table 4.30. The parameter with the highest difference value of coefficient is the most effective parameter affecting the surface average roughness. Figure 4.40 shows that the heating temperature is the most influencing parameter on the surface average roughness followed by water temperature, injection speed, and packing pressure, respectively. Table 4.31 concludes the optimum process setting and ranking of process parameter on surface average roughness. The results of regression analysis showed that the optimum parameter

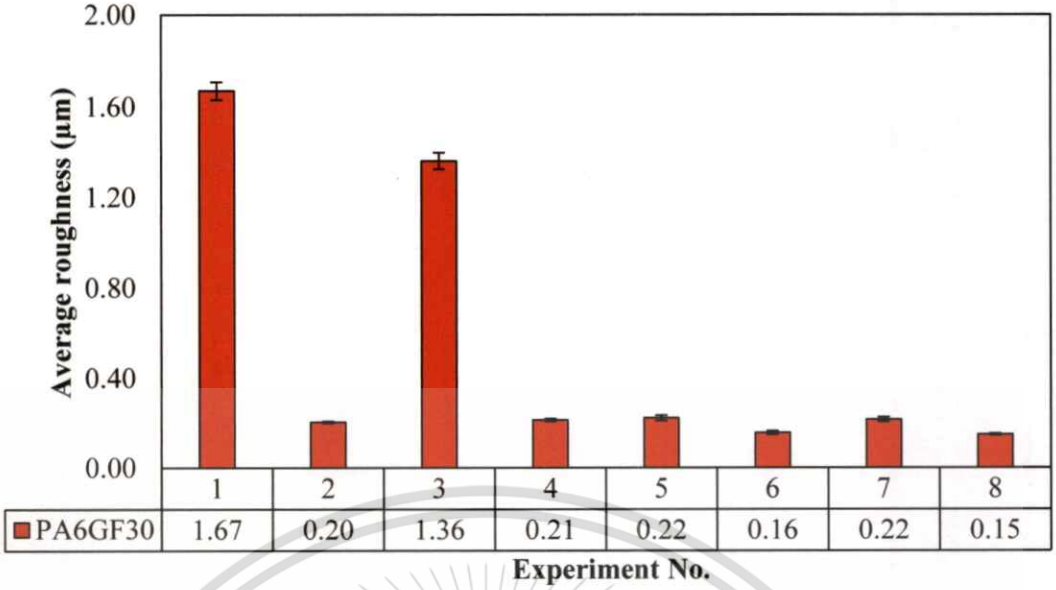

Figure 4.39 The measured surface average roughness in two direction of PA6GF30 specimen.

Table 4.30 The measured surface average roughness in two direction of PA6GF30 specimen.

Exp.	Factor Combination				Average Roughness (µm)	Improvement comparing to Exp.5 (%)	S/N ratio
	A	B	C	D			
1	25	1200	30	30	1.67	-649.9	-4.45
2	25	1200	160	80	0.20	8.4	13.81
3	75	1300	30	30	1.36	-511.7	-2.69
4	75	1300	160	80	0.21	4.2	13.41
5	25	1300	80	80	0.22	-	13.03
6	25	1300	160	30	0.16	29.9	16.13
7	75	1200	80	80	0.22	3.1	13.31
8	75	1200	160	30	0.15	33.4	16.57

setting for the surface average roughness property can be obtained from the experiment No.4 which is the combination of high injection speed (100 mm/s), high packing pressure (1300 kgf/cm^2), high heating temperature (160°C), and high water temperature (80°C).

To validate the best combination, the experiment No.4 was repeated in the injection molding and surface gloss property testing. It was found that experiment No.4, as experiment No.9 in Figure 4.38, has low surface average roughness at 0.198 µm.

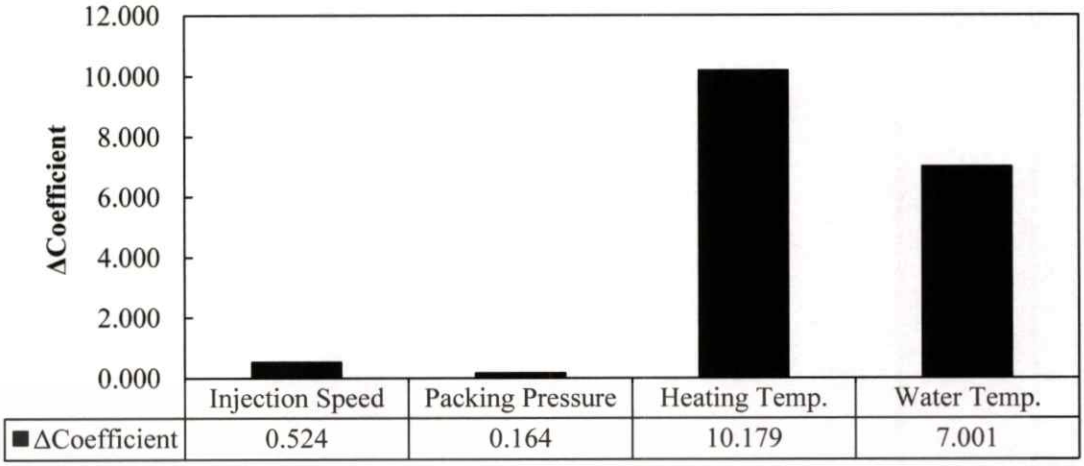

Figure 4.40 The relationship between the difference of regression coefficient values and process parameters on surface average roughness of PA6GF30 specimens.

Table 4.31 The best parameter combination and ranking of the effect for producing parts with the optimal surface average roughness of PA6GF30 specimens.

Parameter	PA6GF30	
	Best Combination	Factor Ranking
Injection Speed (mm/s)	100	3
Packing Pressure (kgf/cm²)	1300	4
Heating Temperature (°C)	160	1
Water Temperature (°C)	80	2

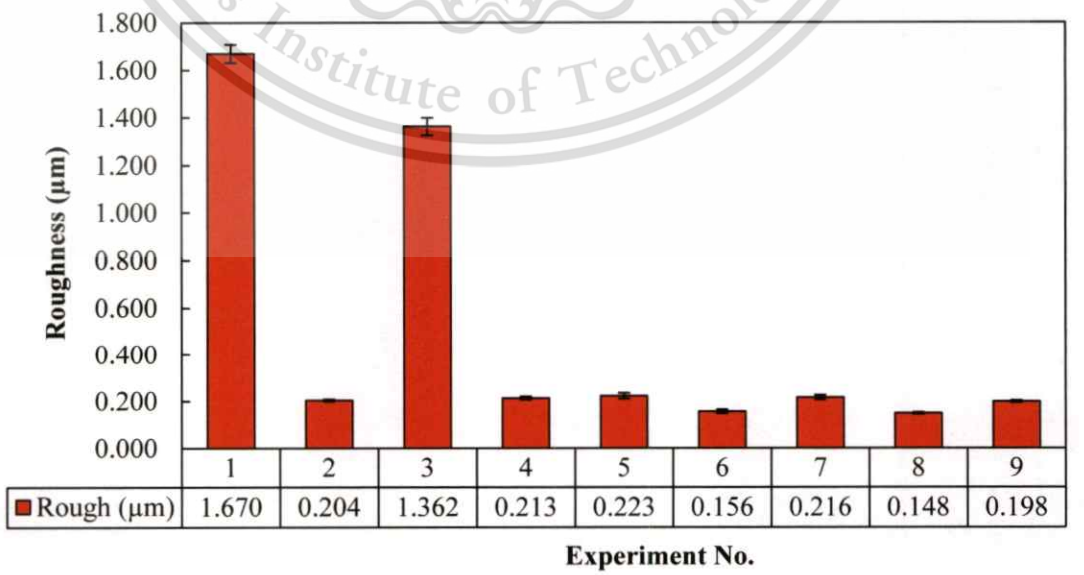

Figure 4.41 Validation of roughness property for PA6GF30.

4.7 Effect Of Processing Parameters On Warpage Property

4.7.1 Polycarbonate (PC)

For the measurement of displacement, the positive value represents the displacement that shifting up from the reference point. The negative displacement represents the displacement that shifting down from the reference point. Table 4.32 presents the displacement in Z-axis on the given points and the range of displacement. The difference of maximum and minimum displacement of each experiment was shown in Figure 4.42 and 4.43. According to the result, it was found that the specimens in every experiment were concave from the interested surface side or heated mold side as shown in Figure 4.44. The largest displacement range obtained from the experiment No.4 was -1.424 to 0.775 mm, that is the difference was 2.199 mm. The displacement range tended to be larger when the mold temperature was higher.

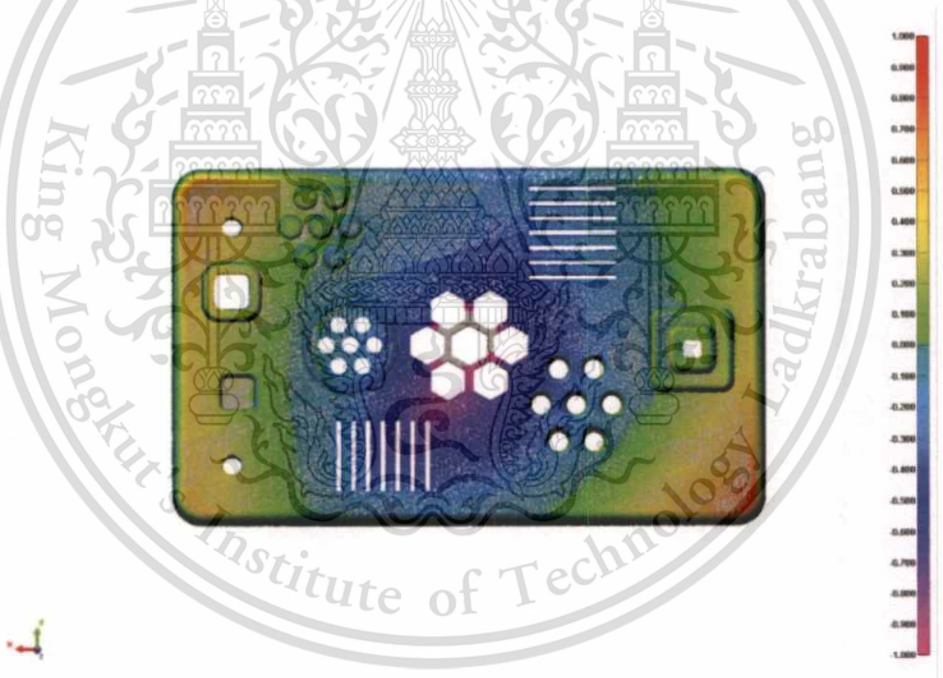

Figure 4.42 Z-Displacement of PC specimen.

The regression analysis was employed to analyze the measured values to investigate the effect of each molding parameter on warpage. Due to this study focus on reducing warpage, the smaller-the-better quality characteristic of S/N ratio as Eq. 1 is carried out to identify the optimum setting and ranking of process parameter affecting the warpage. The calculated S/N ratios are listed in Table. 4.32. The ranking of each parameter affecting warpage is obtained from the difference between the maximum and minimum value coefficient from regression analysis. The

Table 4.32 Z-Displacement of each given point in mm unit of PC specimens

Exp.	A1	A2	A3	B1	B2	B3	B4	C1	C2	C3	Displacement range
1	0.049	-0.046	0.107**	0.052	-0.316*	-0.135	-0.003	0.067	-0.050	0.080	-0.316 to 0.107
2	0.486	-0.153	0.172	0.297	-0.888*	-0.638	0.142	0.290	-0.206	0.489**	-0.888 to 0.489
3	0.126	-0.001	-0.002	0.085	-0.451*	-0.144	0.064	0.099	-0.074	0.171**	-0.451 to 0.171
4	0.605	-0.207	0.341	0.356	-1.424*	-1.023	0.284	0.462	-0.256	0.775**	-1.424 to 0.775***
5	0.212**	-0.213	0.163	0.108	-0.512*	-0.452	-0.024	0.091	-0.243	0.122	-0.512 to 0.212
6	-0.020	-0.022	0.128**	-0.044	-0.360*	-0.266	-0.061	0.026	-0.122	0.073	-0.360 to 0.128
7	0.492	-0.145	0.146	0.283	-1.055*	-0.653	0.264	0.236	-0.215	0.597**	-1.055 to 0.597
8	0.209	-0.056	0.250	0.128	-0.514*	-0.250	0.077	0.315**	-0.094	0.285	-0.514 to 0.315

* Lowest displacement ** Highest displacement *** Largest range of displacement

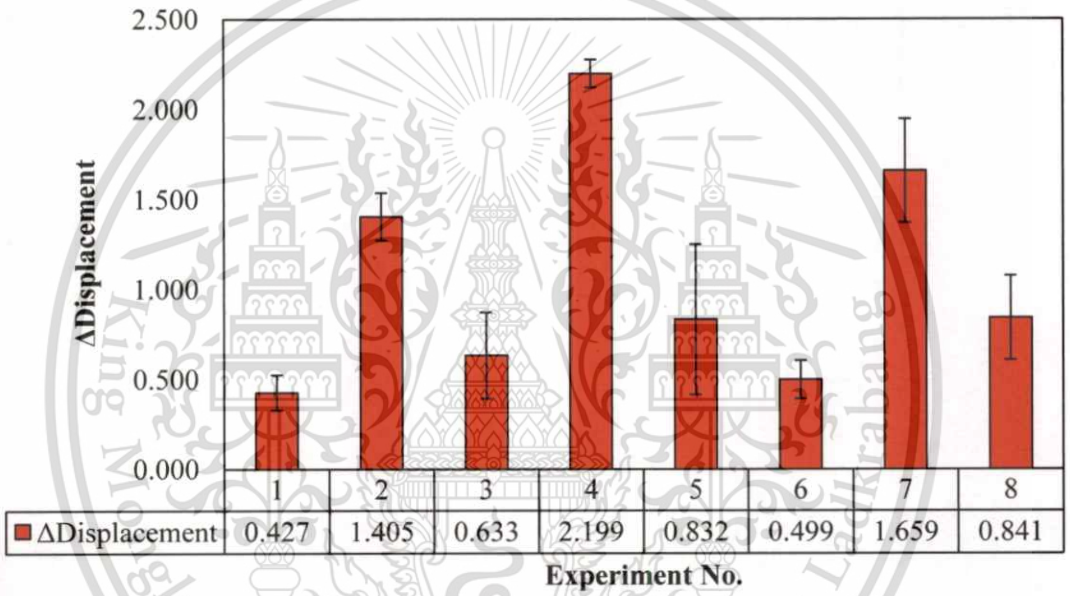

Figure 4.43 The difference of maximum and minimum values of displacement of PC.

effect of each parameter depends on how large that difference value is. In the other words, the parameter with the highest difference value is the most effective parameter affecting warpage. Figure 4.30 it can be concluded that the water temperature is the most influencing parameter on the warpage followed by injection speed, heating temperature, and, packing pressure, respectively. The water temperature was the most effective parameter on warpage may due to the cavity side heated by induction heating caused the more difference of the temperature between cavity side and core side. The water temperature is the important parameter in transfer the heat from mold. The polymer with higher temperature exhibited more shrinkage than the polymer with lower temperature during the cooling stage. The

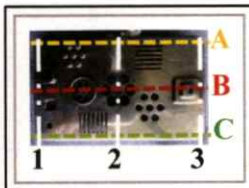

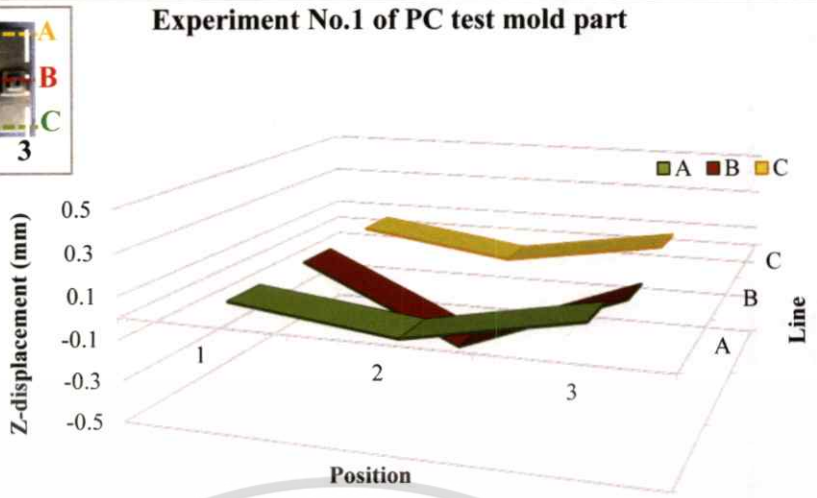

	1	2	3
A	0.049	-0.046	0.107
B	0.052	-0.316	-0.003
C	0.067	-0.050	0.080

Figure 4.44 Z-Displacement of PC specimens including the displacement of A, B, and C point groups.

Table 4.33 Percentage of the improvement and the calculated S/N ratio for the warpage of PC specimens.

Exp.	Factor Combination				Average difference of displacement range (mm)	Improvement comparing to Exp.5 (%)	S/N ratio
	A	B	C	D			
1	25	1200	30	30	0.43	48.7	7.17
2	25	1200	165	80	1.40	-68.8	-2.99
3	75	1300	30	30	0.63	23.9	3.39
4	75	1300	165	80	2.20	-164.2	-6.85
5	25	1300	80	80	0.83	-	0.62
6	25	1300	165	30	0.50	40.1	5.85
7	75	1200	80	80	1.66	-99.3	-4.52
8	75	1200	165	30	0.84	-1.1	1.18

difference of shrinkage caused bending moment. This leads to the distortion and finally, warpage. The specimens were concave from the hotter side and convex to the cooler side of the mold. With the lower water temperature, the heat transfer from mold to cooling channel is better resulting in the less difference of the temperature between cavity and core side. Therefore, warpage was reduced. Table 4.34 summarizes the

optimum process setting and ranking of process parameter for warpage. The results of regression analysis revealed that the optimum parameter setting for the warpage was low injection speed (25 mm/s), high packing pressure (1300 kgf/cm²), low heating temperature (30°C), and low water temperature (30°C), which is the new experiment besides the eight experiments designed from Taguchi method.

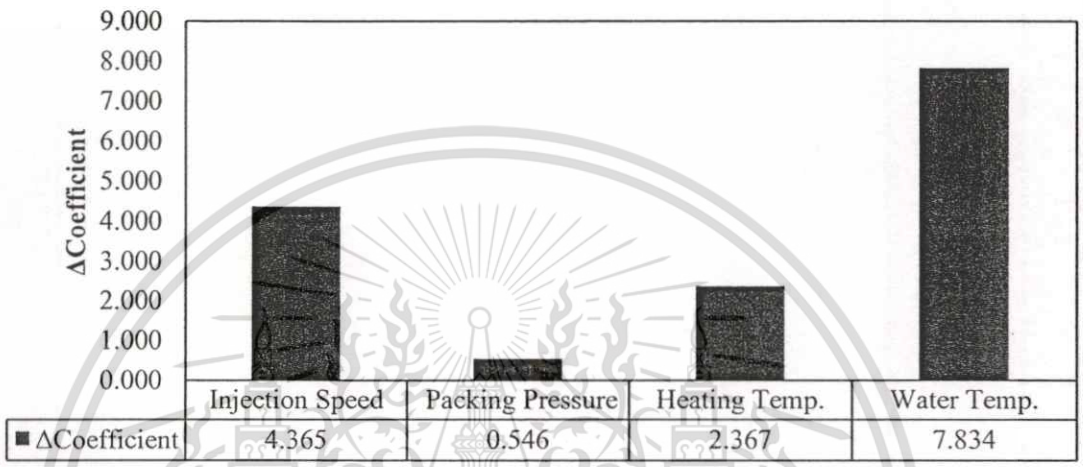

Figure 4.45 The relationship between the difference of regression coefficient values and process parameters on warpage of PC specimens.

Table 4.34 The best parameter combination and ranking of the effect for producing parts with the optimal warpage of PC specimens.

Parameter	PC	
	Best Combination	**Factor Ranking**
Injection Speed (mm/s)	25	2
Packing Pressure (kgf/cm²)	1300	4
Heating Temperature (°C)	30	3
Water Temperature (°C)	30	1

To validate the best combination, the new experiment, the experiment No.9 in Figure4.46, was conducted by injection molding and surface gloss property testing. It was found that new experiment has the lowest difference of displacement at 0.291.

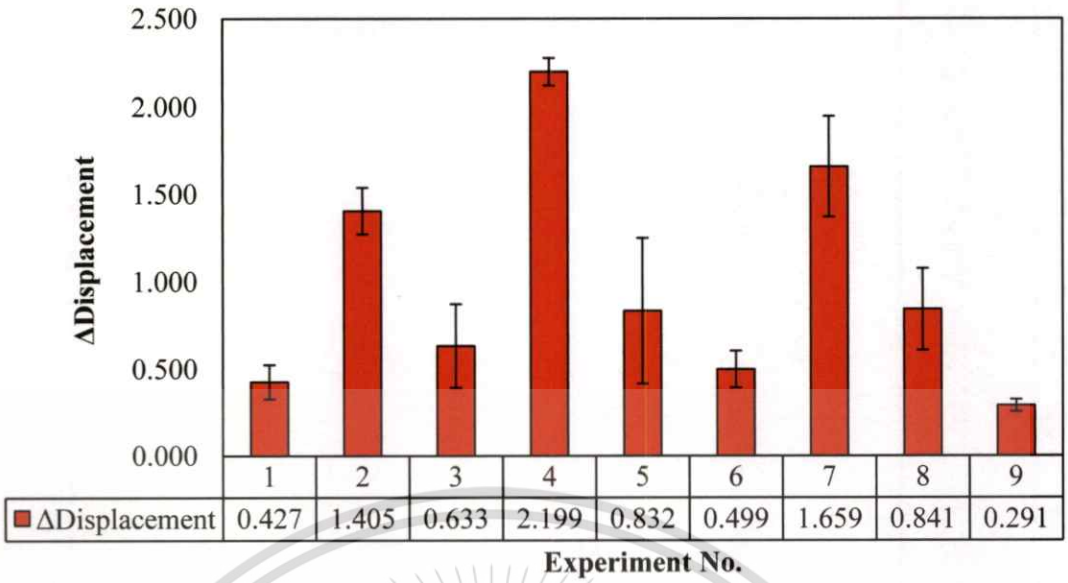

Figure 4.46 Validation of flexural strength of weldline property for PC

4.7.2 Polycarbonate/Acrylonitrile Butadiene Styrene (PC/ABS)

Table 4.35 presents the displacement in Z-axis on the given points and the range of displacement. According to the result, it was found that the specimens in every experiment were concave from the interested surface side or heated mold side as shown in Figure 4.47 and 4.49. The largest displacement range obtained from the experiment No.4 was -2.790 to 1.238 mm., which the difference was 4.032 mm. The displacement range tended to be larger when the mold temperature was higher.

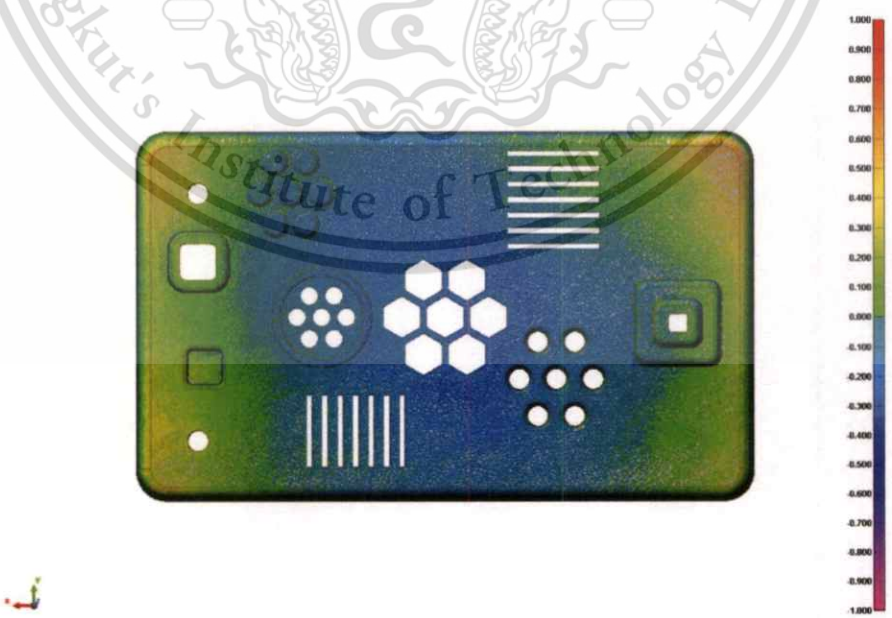

Figure 4.47 Z-Displacement of PC/ABS specimen.

Table 4.35 Z-Displacement of each given point in mm unit of PC/ABS specimens.

Exp.	A1	A2	A3	B1	B2	B3	B4	C1	C2	C3	Displacement range
1	0.118	-0.031	0.067	0.076	-0.504*	-0.319	0.071	0.077	-0.055	0.238**	-0.504 to 0.238
2	0.566	-0.122	0.252	0.313	-1.145*	-0.758	0.256	0.367	-0.213	0.566**	-1.145 to 0.566
3	0.093	-0.056	0.134	0.043	-0.336*	-0.162	0.013	0.087	-0.122	0.182**	-0.336 to 0.182
4	0.932	-0.327	0.290	0.523	-2.790*	-2.307	0.477	0.502	-0.472	1.238**	-2.790 to 1.238***
5	0.234	-0.155	0.119	0.303	-0.850*	-0.518	0.182	0.106	-0.147	0.413**	-0.850 to 0.413
6	0.204	-0.164	0.238	0.068	-0.637*	-0.571	-0.006	0.299**	-0.244	0.282	-0.637 to 0.299
7	0.485	-0.261	0.112	0.287	-1.968*	-1.589	0.273	0.157	-0.361	0.738**	-1.968 to 0.738
8	0.338	-0.243	0.345	0.149	-0.552*	-0.500	0.077	0.464**	-0.313	0.405	-0.552 to 0.464

* Lowest displacement ** Highest displacement *** Largest range of displacement

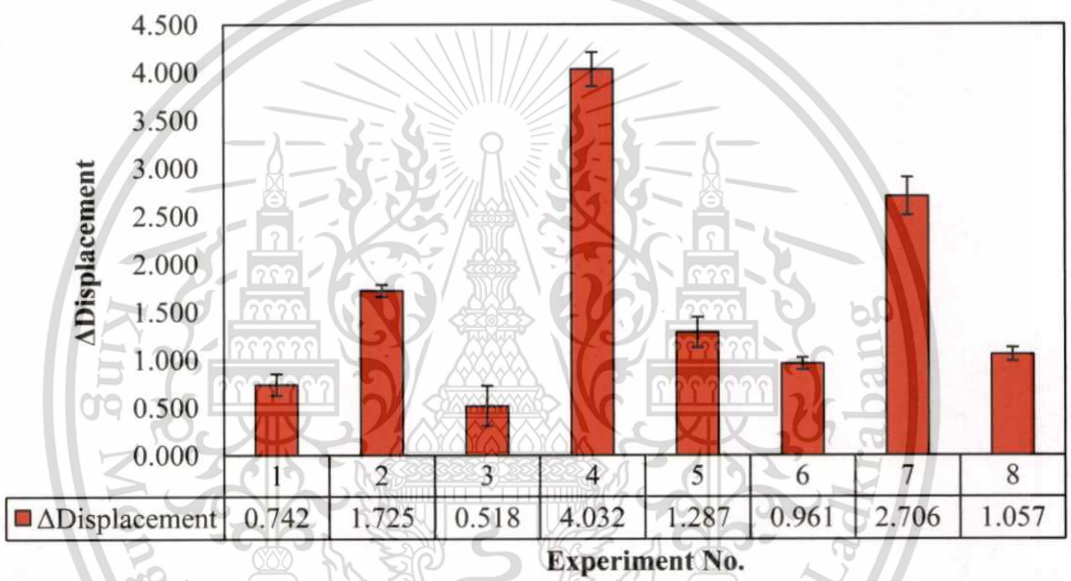

Figure 4.48 The difference of maximum and minimum values of displacement.

For the regression analysis, the smaller-the-better quality characteristic of S/N ratio as Eq. 1 is carried out to identify the optimum setting and ranking of process parameter affecting the reduction of warpage. The calculated S/N ratios are listed in Table 4.36. The parameter with the highest difference of coefficient value is the most effective parameter affecting the reduction of warpage. From Figure 4.50, it can be concluded that the water temperature is the most influencing parameter on the reduction of warpage followed by heating temperature, and injection speed, and packing pressure, respectively. The reason why the water temperature is the main parameter is the same with PC. Table 4.37 summarizes the optimum process setting and ranking of process parameter for the reduction of warpage. The results of regression analysis revealed

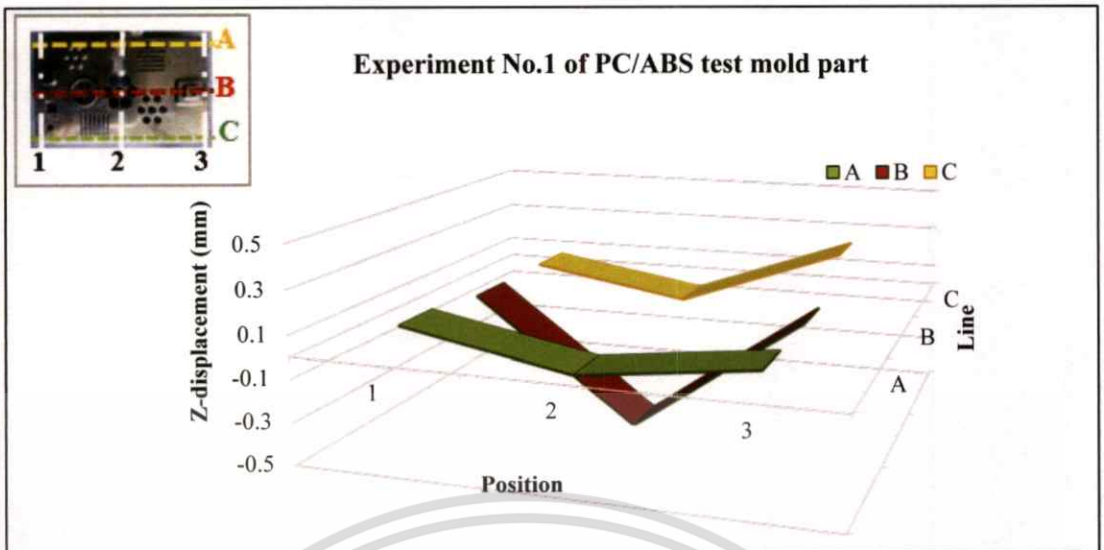

	1	2	3
A	0.118	-0.031	0.067
B	0.076	-0.504	0.071
C	0.077	-0.055	0.238

Figure 4.49 Z-Displacement of PC/ABS specimens including the displacement of A, B, and C point groups.

Table 4.36 Percentage of the improvement and the calculated S/N ratio for the warpage of PC/ABS specimens.

Exp.	Factor Combination				Average difference of displacement range (mm)	Improvement comparing to Exp.5 (%)	S/N ratio
	A	B	C	D			
1	25	1200	30	30	0.74	42.4	2.50
2	25	1200	160	80	1.72	-34.0	-4.74
3	100	1300	30	30	0.52	59.8	5.04
4	100	1300	160	80	4.03	-213.3	-12.12
5	25	1300	80	80	1.29	-	-2.26
6	25	1300	160	30	0.96	25.4	0.33
7	100	1200	80	80	2.71	-110.3	-8.67
8	100	1200	160	30	1.06	17.9	-0.50

that the optimum parameter setting for the reduction of warpage was low injection speed (25 mm/s), high packing pressure (1300 kgf/cm²), low heating temperature (30°C), and low water temperature (30°C), which is the new experiment besides the eight experiments designed from Taguchi method.

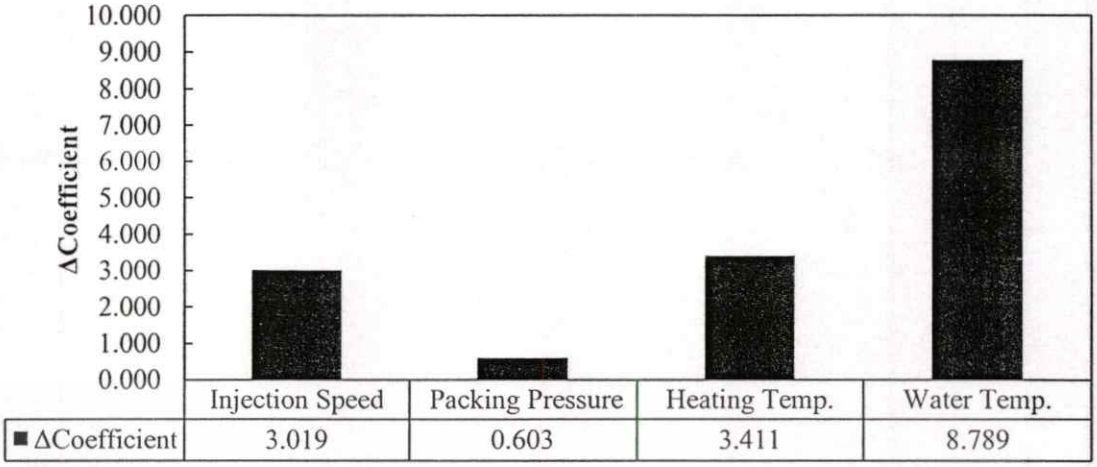

Figure 4.50 The relationship between the difference of regression coefficient values and process parameters on warpage of PC specimens.

Table 4.37 The best parameter combination and ranking of the effect for producing parts with the optimal warpage of PC/ABS specimens.

Parameter	PC/ABS	
	Best Combination	Factor Ranking
Injection Speed (mm/s)	25	3
Packing Pressure (kgf/cm²)	1300	4
Heating Temperature (°C)	30	2
Water Temperature (°C)	30	1

To validate the best combination, the new experiment, the experiment No.9 in Figure4.51, was conducted by injection molding and surface gloss property testing. It was found that new experiment has the lowest difference of displacement at 0.372.

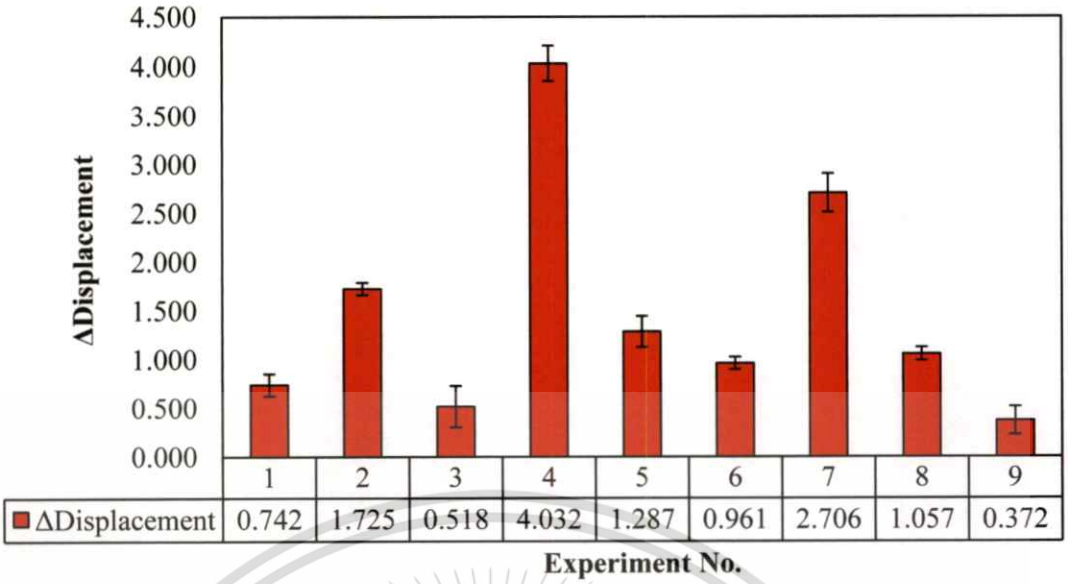

Figure 4.51 Validation of flexural strength of weldline property for PC/ABS

4.7.3 Nylon 6 with 30% Glass-Fiber Filled (PA6GF30)

Table 4.35 presents the displacement in Z-axis on the given points and the range of displacement. According to the result, it was found that the specimens in every experiment were concave from the interested surface side or heated mold side as shown in Figure 4.52 and 4.54. The largest displacement range obtained from the experiment No.3 was -0.839 to 0.307 mm., which the difference was 1.146 mm.

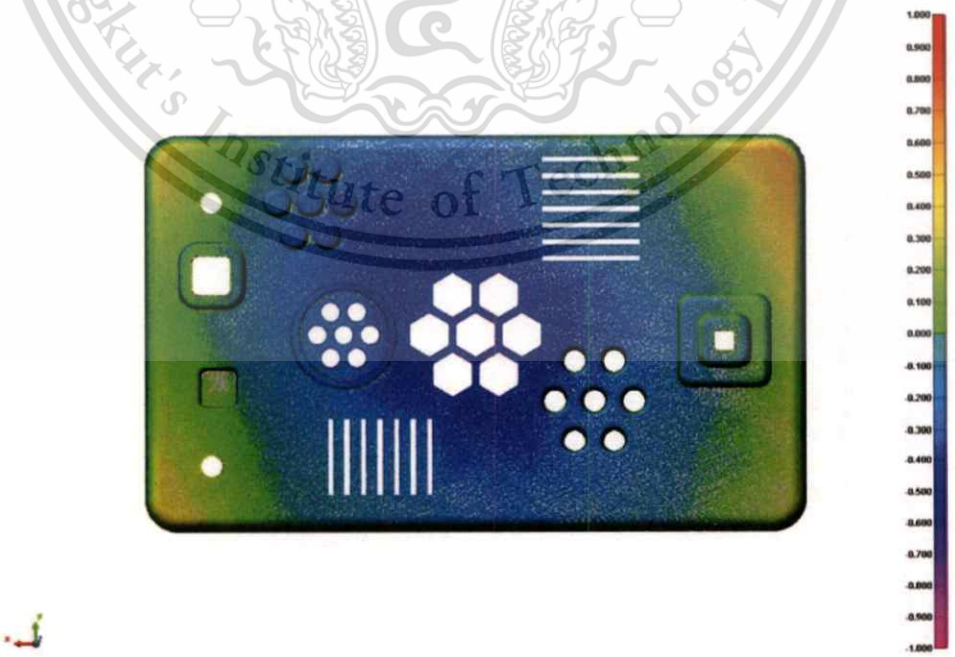

Figure 4.52 Z-Displacement of PA6GF30 specimen.

Table 4.38 Z-Displacement of each given point in mm unit of PA6GF30 specimens.

Exp.	A1	A2	A3	B1	B2	B3	B4	C1	C2	C3	Displacement range
1	0.311	-0.155	0.376**	0.147	-0.416*	-0.212	0.101	0.134	-0.075	0.198	-0.416 to 0.376
2	0.305	-0.363	0.577**	0.196	-0.375*	-0.360	0.203	0.320	-0.223	0.181	-0.375 to 0.577
3	0.307**	-0.162	0.245	0.151	-0.839*	-0.635	0.097	0.052	-0.114	0.282	-0.839 to 0.307***
4	0.251	-0.324	0.479**	0.096	-0.405	-0.410*	0.080	0.305	-0.279	0.177	-0.410 to 0.479
5	0.113	-0.238	0.201**	0.035	-0.336	-0.386*	-0.098	0.048	-0.256	-0.036	-0.386 to 0.201
6	0.283	-0.207	0.300**	0.092	-0.326	-0.346*	0.112	0.149	-0.148	0.209	-0.346 to 0.300
7	0.305	-0.231	0.410**	0.095	-0.356*	-0.282	0.118	0.151	-0.181	0.224	-0.356 to 0.410
8	0.297	-0.270	0.425**	0.051	-0.355*	-0.242	0.082	0.171	-0.195	0.194	-0.355 to 0.425

* Lowest displacement ** Highest displacement *** Largest range of displacement

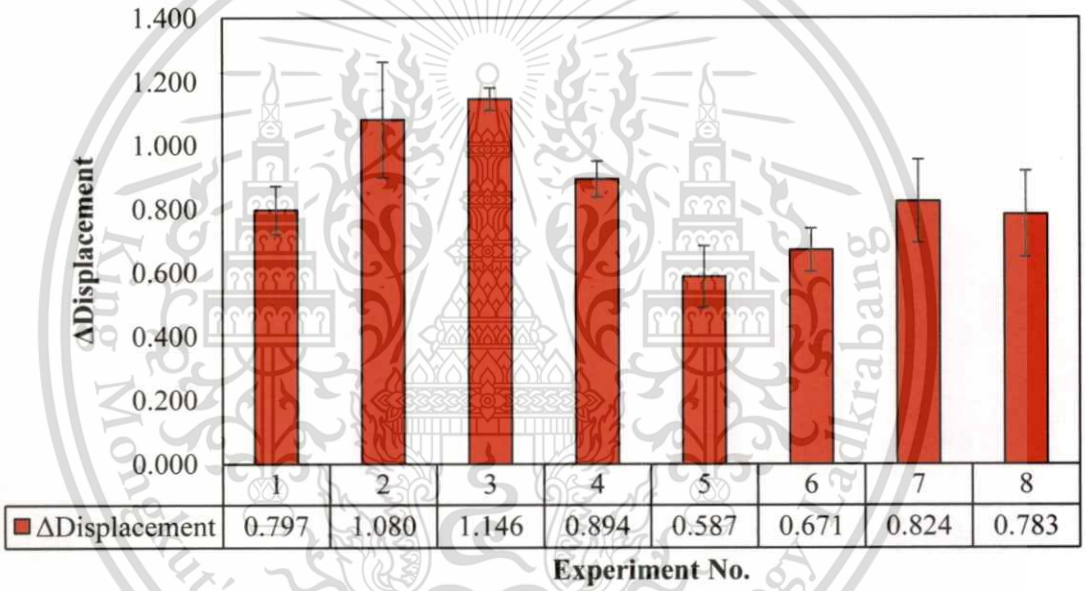

Figure 4.53 The difference of maximum and minimum values of displacement.

For the regression analysis, the smaller-the-better quality characteristic of S/N ratio as Eq. 1 is carried out to identify the optimum setting and ranking of process parameter affecting the reduction of warpage. The calculated S/N ratios are listed in Table 4.39. The parameter with the highest difference of coefficient value is the most effective parameter affecting the reduction of warpage. From Figure 4.55, it can be concluded that the injection speed is the most influencing parameter on the reduction of warpage followed by packing pressure, heating temperature, and water temperature, respectively. Table 4.40 summarizes the optimum process setting and ranking of process parameter for the reduction of warpage. The

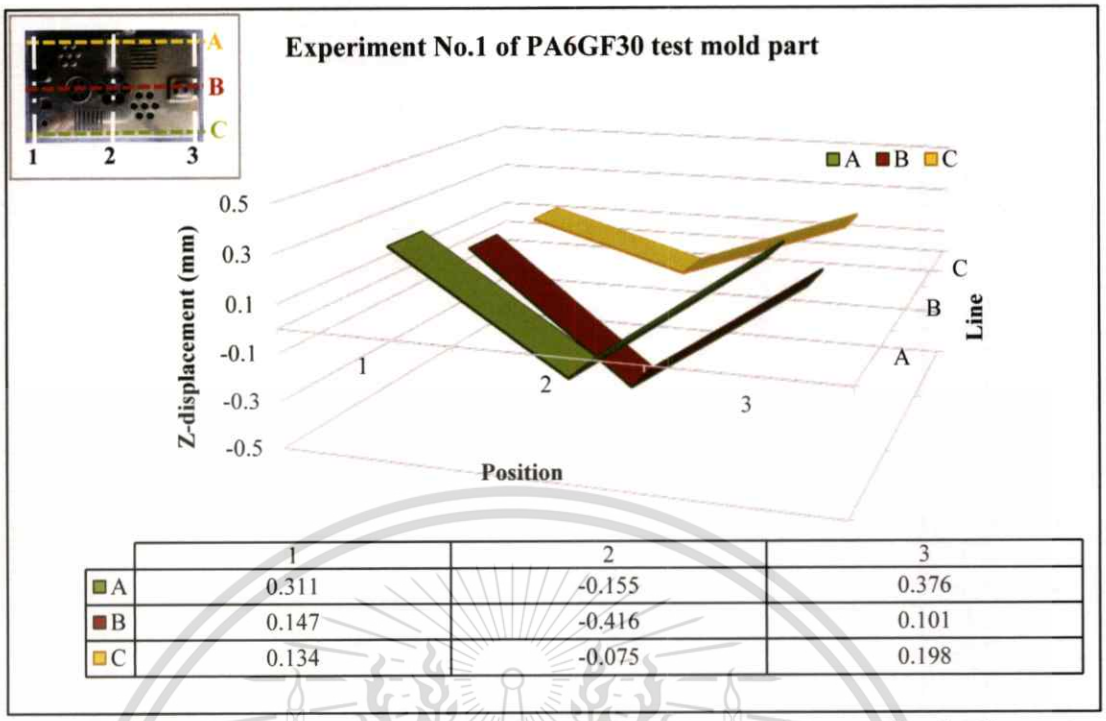

	1	2	3
A	0.311	-0.155	0.376
B	0.147	-0.416	0.101
C	0.134	-0.075	0.198

Figure 4.54 Z-Displacement of PA6GF30 specimens including the displacement A, B, and C point groups.

Table 4.39 Percentage of the improvement and the calculated S/N ratio for the warpage of PA6GF30 specimens.

Exp.	Factor Combination				Average difference of displacement range (mm)	Improvement comparing to Exp.5 (%)	S/N ratio
	A	B	C	D			
1	25	1200	30	30	0.80	-35.8	1.93
2	25	1200	160	80	1.08	-83.9	-0.79
3	75	1300	30	30	1.15	-95.1	-1.19
4	75	1300	160	80	0.89	-52.2	0.96
5	25	1300	80	80	0.59	-	4.51
6	25	1300	160	30	0.67	-14.3	3.42
7	75	1200	80	80	0.82	-40.3	1.57
8	75	1200	160	30	0.78	-33.4	1.99

results of regression analysis revealed that the optimum parameter setting for the reduction of warpage was low injection speed (25 mm/s), high packing pressure (1300 kgf/cm²), low heating temperature (30°C), and high water temperature (80°C), that is the experiment No.5.

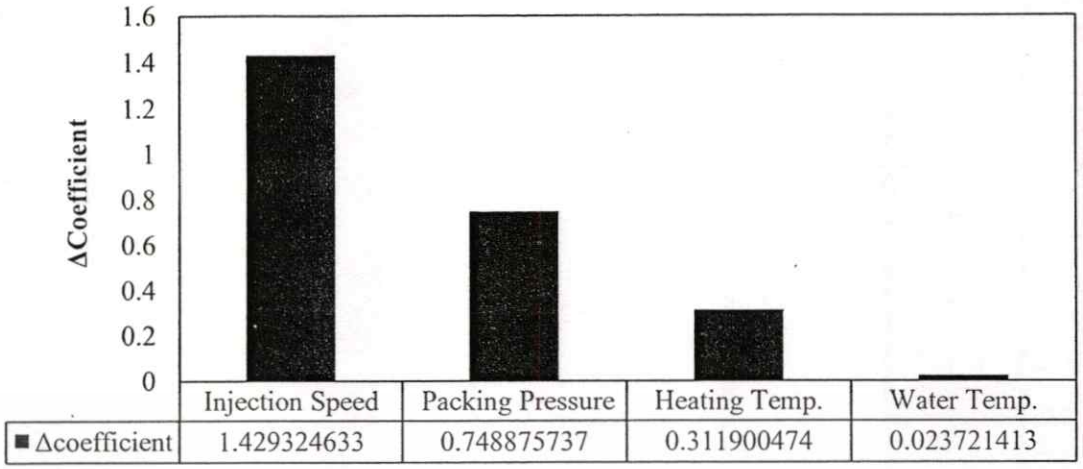

Figure 4.55 The relationship between the difference of regression coefficient values and process parameters on warpage of PA6GF30 specimens.

Table 4.40 The best parameter combination and ranking of the effect for producing parts with the optimal warpage of PA6GF30 specimens.

Parameter	PA6GF30	
	Best Combination	Factor Ranking
Injection Speed (mm/s)	25	1
Packing Pressure (kgf/cm²)	1300	2
Heating Temperature (°C)	80	3
Water Temperature (°C)	80	4

To validate the best combination, the experiment No.5 was repeated with injection molding and surface gloss property testing. It was found that the experiment No.5, as the experiment No.9 in Figure 4.56, has the lowest difference of displacement at 0.598 that closely to the original experiment No.5.

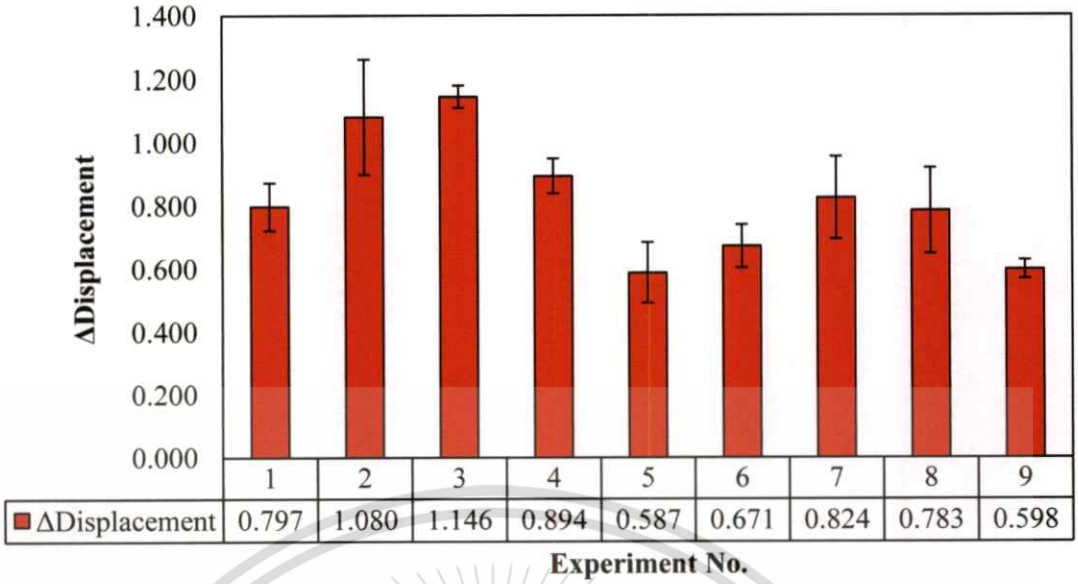

Figure 4.56 Validation of flexural strength of weldline property for PA6GF30

CHAPTER 5
CONCLUSION AND SUGGESTIONS

5.1 Conclusion

To solve the surface defects of automotive parts, such as weldline, gloss and roughness, caused by the conventional injection molding process, it requires a method having high efficiency in heating and cooling the mold. Induction heating is the interesting method in heating and cooling the mold rapidly which tends to make lowest overall cost of production in term of mold making cost, equipment cost, and running cost. This research is examination the performance of induction heating system before applying it to further produce the real automotive parts. Therefore, a new special test mold namely test mold was designed and produced for this study.

A preliminary study was carried out to obtain the optimal condition of induction heating system. It was found that the optimal condition is the use of SKD61 as mold insert with 80% power and gap of 17.5 mm that provided the heating rate at 10 °C/s. This condition was used in the injection molding stage to examine the performance of induction heating with other molding process parameter on properties of test mold parts.

The main experiment of test mold was conducted. The experimental layout of each different material, which is polycarbonate (PC), polycarbonate/acrylonitrile butadiene styrene (PC/ABS), and nylon 6 with 30% glass-fiber filled (PA6GF30), was based on Taguchi method's L8 orthogonal array. Table 5.1 summarizes the effective parameter on each property of each material analyzed by regression analysis. It revealed that the induction heat is the efficient technology to solve weldline issue. It also improves the surface roughness and gloss issues. It proved that the mold surface temperature is the key parameter to enhance the surface appearance or quality for injection molding. Thus, the induction heating dominate the surface quality of molded part. While the flexural strength of weldline and warpage are not enhanced by induction heating.

Finally, PC/ABS and PA6GF30 is the most proper plastic material to use with induction heating to improve properties followed by PC.

Table 5.1 The effective parameter on each property for PC, PC/ABS, and PA6GF30 materials.

Property	Effective parameter		
	PC	PC/ABS	PA6GF30
1. Weldline	T_{IH}	T_{IH}	T_{IH}
2. Surface gloss	T_{w}	T_{IH}	T_{IH}
3. Flexural strength of weldline	P_{pack}	T_{w}	P_{pack}
4. Surface roughness	T_{IH}	T_{IH}	T_{IH}
5. Warpage	T_{w}	T_{w}	V_{inj}

5.2 Suggestion

For the induction heating, to improve the electrical energy conversion efficiency or coil efficiency, a magnetic flux concentrator or magnetic shield should be located around the coil. In addition, the larger power supply should be used next time to improve the heating rate.

For the most precision in detect the mold surface temperature, the thermocouple should be fitted inside the mold to measure the temperature at mold surface.

Due to the limited area of the test mold part, the weldline strength only could be tested as flexural strength. To investigate the weldline strength, it should be tested by tensile testing with a tensile specimen.

REFERENCES

[1] "Plastic Injection Moulding Explained," Patterson and Rothwell Ltd, [Online]. Available: http://www.patterson-rothwell.co.uk/services/plastic-injection-moulding-explained.htm. [Accessed 05 April 2016].

[2] "About Injection Molding," Xcentric Mold & Engineering, [Online]. Available:https://www.xcentricmold.com/about-injection-molding.php. [Accessed 05 April 2016].

[3] B. A. Olmsted and M. E. Davis, Eds., Practical Injection Molding, New York: Taylor & Francis Inc, 2001.

[4] S. H. Masood and N. N. Trang, "Thermal analysis of conformal cooling channels in injection moulding," in *Proceedings of the 3rd BSME-ASME International Conference on Thermal Engineering*, Dhaka, Bangladesh, 2006.

[5] A. J. Ryan, Polymer Processing and Structure Development, W. N. Arthur and A. J. Ryan, Eds., Boston: Kluwer Academic Publishers, 1998.

[6] G. Wang, G. Zhao, H. Li and Y. Guan, "Research of thermal response simulation and mold structure optimization for rapid heat cycle molding processes, respectively, with steam heating and electric heating," *Materials and Design,* vol. 31, no. 1, pp. 382-395, 2010.

[7] J. Q. Li, S. F. Jiang and C. Chen, "Survey and Trend of Rapid Heat Cycle Molding," *Advanced Materials Research,* Vols. 189-193, pp. 2543-2546, 2011.

[8] G. Wang, G. Zhao and X. Wang, "Effects of cavity surface temperature on mechanical properties of specimens with and without a weld line in rapid heat cycle molding," *Materials and Design,* vol. 44, pp. 509-520, 2013.

[9] G. Wang, G. Zhao, H. Li and Y. Guan, "Research on optimization design of the heating/cooling channels for rapid heat cycle molding based on response surface methodology and constrained particle swarm optimization," *Expert Systems with Applications,* vol. 38, no. 6, pp. 6705-6719, 2011.

[10] "Theory of Heating by Induction," [Online]. Available: www.asminternational.org/document. [Accessed 07 July 2016].

[11] "About Induction Heating," [Online]. Available: http://pdfo. ambrell.com/411-0169-10.pdf. [Accessed 05 July 2016].

[12] G. E. Totten , New York, United States: CRC Press, 2006.

[13] "Induction Heating Work Coils," [Online]. Available: http://pdfo.ambrell.com/411-0168-10.pdf. [Accessed 05 July 2016].

[14] "Introduction to PlasticWeld Systems, Inc.," [Online]. Available: http://www.plasticweldsystems.com/pdf/pws-induction-forming-seminar.pdf. [Accessed 07 July 2016].

[15] F. W. Curtis, High-frequency induction heating, New York,: McGraw-Hill, 1950.

[16] J. Lux , "Wheeler Formulas for Inductance," 26 1 2004. [Online]. Available:http://home.earthlink.net/~jimlux/hv/wheeler.htm. [Accessed 8 7 2016].

[17] K. Chatterjee and V. Ramanarayanan, "Computer-Aided Design of Pancake Coils for Induction Heaters," *Journal of The Indian Institute of Science,* vol. 72, no. 2, pp. 111-119, 1992.

[18] S. S. Aung, H. P. Wai and N. N. Soe, "Design Calculation and Performance Testing of Heating Coil in Induction Surface Hardening Machine," *International Journal of Electrical, Computer, Energetic, Electronic and Communication Engineering,* vol. 2, no. 6, pp. 1134-1138, 2008.

[19] "D2S3-8," MATSUI MFG. CO., LTD, 2013. [Online]. Available: http://www.caemolding.org/newsevents/news/cmsa2014/file/CMSA2014-pdf/D2S3/D2S3-8.pdf. [Accessed 07 July 2016].

[20] G. Taguchi, Introduction to quality engineering: designing quality into products and processes, Tokyo: The Organization, 1990.

[21] S. C. Nian, S. W. Tsai, M. S. Huang, R. C. Huang and C. H. Chen, "Key parameters and optimal design of a single-layered induction coil for external rapid mold surface heating," *International Communications in Heat and Mass Transfer,* vol. 57, pp. 109-117, 2014.

[22] H. Shen, Z. Q. Yao, Y. J. Shi and J. Hu, "Study on temperature field induced in high frequency induction heating," *Acta Metallurgica Sinica,* vol. 19, no. 3, pp. 190-196, 2006.

[23] M. H. Tavakoli, H. Karbaschi and F. Samavat, "Influence of workpiece height on the induction heating process," *Mathematical and Computer Modelling,* vol. 54, pp. 50-58, 2011.

[24] C. G. Kang, P. K. Seo and H. K. Jung, "Numerical analysis by new proposed coil design method in induction heating process for semi-solid forming and its experimental verification with globalization evaluation," *Materials Science and Engineering,* vol. 341, pp. 121-138, 2003.

[25] T. Todaka and M. Enokizono, "Optimal design method with the boundary element for high-frequency quenching coil," *IEEE Transactions on Magnetics,* vol. 32, no. 3, pp. 1262-1265, 1996.

[26] S. C. Chen, Y. W. Lin, R. D. Chien and H. M. Li, "Variable mold temperature to improve surface quality of microcellular injection molded parts using induction heating technology," *Advances in Polymer Technology,* vol. 27, no. 4, pp. 224-232, 2008.

[27] M.-S. Huang and Y.-L. Huang, "Effect of multi-layered induction coils on efficiency and uniformity of surface heating," *International Journal of Heat and Mass Transfer,* vol. 53, no. 11, pp. 2414-2423, 2010.

[28] S. C. Nian, M. S. Huang and T. H. Tsai , "Enhancement of induction heating efficiency on injection mold surface using a novel magnetic shielding method," *International Communications in Heat and Mass Transfer,* vol. 50, pp. 52-60, 2014.

[29] S. C. Chen, W. R. Jong and J. A. Chang, "Dynamic mold surface temperature control using induction heating and its effects on the surface appearance on weld line," *Journal of Applied Polymer Science,* vol. 101, no. 2, pp. 1174- 1180, 2006.

[30] S. Kim, C. S. Shiau, B. H. Kim and D. Yao, "Injection Molding Nanoscale Features with the Aid of Induction Heating," *Polymer-Plastics Technology and Engineering,* vol. 46, pp. 1031-1037, 2007.

[31] Y. T. Sung and S. J. Hwang, "Design of an insert type induction heating and cooling system for injection moulding processes," *Technical gazette,* vol. 21, no. 3, pp. 651-656, 2014.

[32] U. Hinzpeter and E. Wrona, "Use of Induction Heating in Plastic Injection Molding," in *Advances in Induction and Microwave Heating of Mineral and Organic Materials*, S. Grundas, Ed., InTech, 2011, pp. 339-344.

[33] R. Foad, "Rapid Temperature Cycling for Medical Mouldings," MedTech Communications Ltd, 08 March 2013. [Online]. Available: http://www.med-techinnovation.com/Articles/articles/article/73. [Accessed 2016 April 07].

[34] M. C. Jeng, S. C. Chen, P. S. Minh, J. A. Chang and C. s. Chung, "Rapid mold temperature control in injection molding by using steam heating," *International Communications in Heat and Mass Transfer,* vol. 37, no. 9, pp. 1295-1304, 2010.

[35] H.-L. Lina, S.-C. Chen, M.-C. Jenga, P.-S. Minh, J.-A. Chang and J.-R. Hwang, "Induction heating with the ring effect for injection molding plates," *International Communications in Heat and Mass Transfer,* vol. 39, no. 4, pp. 514-522, 2012.

[36] M.-S. Huang and N.-S. Ta, "Experimental rapid surface heating by induction for micro-injection molding of light-guided plates," *Journal of Applied Polymer Science ,* vol. 113, no. 2, pp. 1345-1354, 2009.

[37] K. Park, D.-H. Sohn and K.-H. Cho, "Eliminating weldlines of an injection-molded part with the aid of high-frequency induction heating,," *Journal of Mechanical Science and Technology,* vol. 24, no. 1, pp. 149-152, 2010.

APPENDIX A

REGRESSION ANALYSIS BY MICROSOFT EXCEL

1. Regression Analysis of Weldline Property

1.1 PC

SUMMARY OUTPUT

Regression Statistics	
Multiple R	0.963037992
R Square	0.927442173
Adjusted R Square	0.830698405
Standard Error	3.669723497
Observations	8

ANOVA

	df	*SS*	*MS*	*F*	*Significance F*
Regression	4	516.4050918	129.1013	9.586583	0.046734288
Residual	3	40.40061164	13.46687		
Total	7	556.8057034			

	Coefficients	*Standard Error*	*t Stat*	*P-value*	*Lower 95%*	*Upper 95%*	*Lower 95.0%*	*Upper 95.0%*
Intercept	-27.57227624	2.901171159	-9.50384	0.00247	-36.80509768	-18.3394548	-36.80509768	-18.33945481
speed H	8.966357353	2.59488637	3.455395	0.040776	0.708270812	17.22444389	0.708270812	17.22444389
pack H	1.64822263	2.59488637	0.635181	0.570445	-6.609863911	9.906309171	-6.609863911	9.906309171
heating H	12.20596196	2.59488637	4.703852	0.01818	3.947875415	20.4640485	3.947875415	20.4640485
water H	5.109289246	2.59488637	1.968984	0.143589	-3.148797295	13.36737579	-3.148797295	13.36737579

RESIDUAL OUTPUT

Observation	*Predicted S/N*	*Residuals*
1	-27.57227624	3.753823734
2	-10.25702504	-1.940953056
3	-16.95769626	-1.940953056
4	0.35755494	3.753823734
5	-20.81476437	-0.31543433
6	-13.71809166	-1.497436348
7	-13.49662965	-1.497436348
8	-6.399956936	-0.31543433

1.2 PC/ABS

SUMMARY OUTPUT

Regression Statistics	
Multiple R	0.998530262
R Square	0.997062685
Adjusted R Square	0.993146265
Standard Error	1.155513417
Observations	8

ANOVA

	df	*SS*	*MS*	*F*	*Significance F*
Regression	4	1359.700168	339.925	254.5852	0.000397283
Residual	3	4.005633769	1.335211		
Total	7	1363.705802			

	Coefficients	*Standard Error*	*t Stat*	*P-value*	*Lower 95%*	*Upper 95%*	*Lower 95.0%*	*Upper 95.0%*
Intercept	-21.95999325	0.913513566	-24.039	0.000158	-24.86720113	-19.0527854	-24.86720113	-19.05278538
speed H	11.80536033	0.817071373	14.44838	0.000719	9.205074555	14.4056461	9.205074555	14.4056461
pack H	0.787930351	0.817071373	0.964335	0.406014	-1.81235542	3.388216123	-1.81235542	3.388216123
heating H	22.42107384	0.817071373	27.44078	0.000106	19.82078806	25.02135961	19.82078806	25.02135961
water H	6.095749773	0.817071373	7.460486	0.004986	3.495464002	8.696035544	3.495464002	8.696035544

RESIDUAL OUTPUT

Observation	*Predicted S/N*	*Residuals*
1	-21.95999325	1.119383362
2	6.556830354	-0.535878005
3	-9.366702576	-0.535878005
4	19.15012103	1.119383362
5	-15.07631313	0.090604017
6	1.249010933	-0.674109375
7	-4.058883154	-0.674109375
8	12.26644091	0.090604017

2. Regression Analysis of Gloss Property

2.1 PC

SUMMARY OUTPUT

Regression Statistics	
Multiple R	0.909222327
R Square	0.826685239
Adjusted R Square	0.595598892
Standard Error	0.138280985
Observations	8

ANOVA

	df	*SS*	*MS*	*F*	*ignificance F*
Regression	4	0.273621874	0.068405	3.577387	0.16162433
Residual	3	0.057364892	0.019122		
Total	7	0.330986766			

	Coefficients	*Standard Error*	*t Stat*	*P-value*	*Lower 95%*	*Upper 95%*	*Lower 95.0%*	*Upper 95.0%*
Intercept	40.51393429	0.109320717	370.597	4.33E-08	40.166027	40.8618416	40.16602698	40.8618416
speed H	-0.06287068	0.097779422	-0.64298	0.566001	-0.3740484	0.24830708	-0.37404844	0.24830708
pack H	-0.1051862	0.097779422	-1.07575	0.36085	-0.416364	0.20599156	-0.41636396	0.20599156
heating H	-0.23322148	0.097779422	-2.38518	0.097163	-0.5443992	0.07795628	-0.54439924	0.07795628
water H	-0.2596186	0.097779422	-2.65515	0.076656	-0.5707964	0.05155916	-0.57079636	0.05155916

RESIDUAL OUTPUT

Observation	*Predicted S/N*	*Residuals*
1	40.51393429	-0.049021099
2	40.02109421	-0.096411611
3	40.34587741	-0.096411611
4	39.85303733	-0.049021099
5	40.14912948	0.129323964
6	40.17552661	0.016108746
7	40.19144501	0.016108746
8	40.21784213	0.129323964

2.2 PC/ABS

SUMMARY OUTPUT

Regression Statistics	
Multiple R	0.791484201
R Square	0.62644724
Adjusted R Square	0.128376893
Standard Error	0.52744772
Observations	8

ANOVA

	df	*SS*	*MS*	*F*	*Significance F*
Regression	4	1.399628067	0.349907	1.257749	0.442849304
Residual	3	0.834603291	0.278201		
Total	7	2.234231357			

	Coefficients	*Standard Error*	*t Stat*	*P-value*	*Lower 95%*	*Upper 95%*	*Lower 95.0%*	*Upper 95.0%*
Intercept	38.50221065	0.416984035	92.33498	2.8E-06	37.17518135	39.82924	37.1751813	39.82924
speed H	0.337607943	0.372961859	0.905208	0.432083	-0.84932315	1.52453903	-0.84932315	1.52453903
pack H	0.341479529	0.372961859	0.915588	0.427399	-0.84545156	1.52841062	-0.84545156	1.52841062
heating H	0.578410967	0.372961859	1.550858	0.218725	-0.60852012	1.76534206	-0.60852012	1.76534206
water H	0.366970565	0.372961859	0.983936	0.397698	-0.81996053	1.55390166	-0.81996053	1.55390166

RESIDUAL OUTPUT

Observation	*Predicted S/N*	*Residuals*
1	38.50221065	-0.555888896
2	39.44759218	0.126022976
3	39.18129812	0.126022976
4	40.12667965	-0.555888896
5	39.21066074	0.217674839
6	39.42210114	0.212191081
7	39.20678916	0.212191081
8	39.41822956	0.217674839

2.3 PA6GF30

SUMMARY OUTPUT

Regression Statistics	
Multiple R	0.838264558
R Square	0.70268747
Adjusted R Square	0.306270763
Standard Error	8.24678933
Observations	8

ANOVA

	df	*SS*	*MS*	*F*	*Significance F*
Regression	4	482.2142633	120.5536	1.772598	0.332986676
Residual	3	204.0286028	68.00953		
Total	7	686.242866			

	Coefficients	*Standard Error*	*t Stat*	*P-value*	*Lower 95%*	*Upper 95%*	*Lower 95.0%*	*Upper 95.0%*
Intercept	21.55631684	6.519659417	3.306356	0.045516	0.807850818	42.3047829	0.80785082	42.3047829
speed H	-0.222055152	5.831360658	-0.03808	0.972017	-18.7800473	18.335937	-18.7800473	18.335937
pack H	-0.211215972	5.831360658	-0.03622	0.973382	-18.7692082	18.3467762	-18.7692082	18.3467762
heating H	11.92502553	5.831360658	2.044982	0.133406	-6.63296665	30.4830177	-6.63296665	30.4830177
water H	9.940169866	5.831360658	1.704606	0.186815	-8.61782232	28.498162	-8.61782232	28.498162

RESIDUAL OUTPUT

Observation	*Predicted S/N*	*Residuals*
1	21.55631684	-4.931535617
2	43.42151224	-5.166997697
3	21.12304572	-5.166997697
4	42.98824112	-4.931535617
5	31.28527074	4.993566111
6	33.2701264	5.104967203
7	31.27443155	5.104967203
8	33.25928722	4.993566111

3. Regression Analysis of Flexural Strength of Weldline Property

3.1 PC

SUMMARY OUTPUT

Regression Statistics	
Multiple R	0.762149096
R Square	0.580871244
Adjusted R Square	0.022032904
Standard Error	0.395169152
Observations	8

ANOVA

	df	*SS*	*MS*	*F*	*ignificance F*
Regression	4	0.649261641	0.162315	1.039426	0.507769
Residual	3	0.468475977	0.156159		
Total	7	1.117737618			

	Coefficients	*tandard Error*	*t Stat*	*P-value*	*Lower 95%*	*Upper 95%*	*Lower 95.0%*	*Upper 95.0%*
Intercept	40.39420492	0.312408646	129.2993	1.02E-06	39.399981	41.3884287	39.3999812	41.3884287
speed H	-0.29476484	0.279426787	-1.05489	0.368922	-1.184026	0.5944959	-1.1840256	0.5944959
pack H	-0.32350245	0.279426787	-1.15774	0.330774	-1.212763	0.5657583	-1.2127632	0.5657583
heating H	-0.20034825	0.279426787	-0.717	0.525157	-1.089609	0.6889125	-1.089609	0.6889125
water H	-0.30487908	0.279426787	-1.09109	0.355026	-1.19414	0.58438167	-1.1941398	0.58438167

RESIDUAL OUTPUT

Observation	*Predicted S/N*	*Residuals*
1	40.39420492	0.406521922
2	39.88897759	-0.10292333
3	39.77593763	-0.10292333
4	39.2707103	0.406521922
5	39.76582339	-0.07338166
6	39.87035422	-0.23021693
7	39.794561	-0.23021693
8	39.89909182	-0.07338166

3.2 PC/ABS

SUMMARY OUTPUT

Regression Statistics	
Multiple R	0.580120518
R Square	0.336539816
Adjusted R Square	-0.54807376
Standard Error	0.409820649
Observations	8

ANOVA

	df	*SS*	*MS*	*F*	*Significance F*
Regression	4	0.255582148	0.063896	0.380437	0.813212202
Residual	3	0.503858894	0.167953		
Total	7	0.759441042			

	Coefficients	*Standard Error*	*t Stat*	*P-value*	*Lower 95%*	*Upper 95%*	*Lower 95.0%*	*Upper 95.0%*
Intercept	38.34690973	0.323991671	118.3577	1.33E-06	37.31582364	39.3779958	37.3158236	39.37799583
speed H	-0.0914568	0.28978696	-0.3156	0.772987	-1.01368824	0.83077464	-1.0136882	0.830774641
pack H	-0.02878947	0.28978696	-0.09935	0.927129	-0.95102091	0.89344197	-0.9510209	0.893441974
heating H	-0.13157916	0.28978696	-0.45405	0.680626	-1.0538106	0.79065228	-1.0538106	0.790652284
water H	-0.31825276	0.28978696	-1.09823	0.352344	-1.2404842	0.60397868	-1.2404842	0.603978679

RESIDUAL OUTPUT

Observation	*Predicted S/N*	*Residuals*
1	38.34690973	0.420366399
2	37.89707781	-0.152528624
3	38.22666346	-0.152528624
4	37.77683155	0.420366399
5	37.9998675	-0.223607291
6	38.18654111	-0.044230484
7	37.93720017	-0.044230484
8	38.12387378	-0.223607291

3.3 PA6GF30

SUMMARY OUTPUT

Regression Statistics	
Multiple R	0.71458521
R Square	0.510632022
Adjusted R Square	-0.14185862
Standard Error	0.561809677
Observations	8

ANOVA

	df	*SS*	*MS*	*F*	*Significance F*
Regression	4	0.98803467	0.247009	0.782589	0.60454863
Residual	3	0.94689034	0.31563		
Total	7	1.93492501			

	Coefficients	*Standard Error*	*t Stat*	*P-value*	*Lower 95%*	*Upper 95%*	*Lower 95.0%*	*Upper 95.0%*
Intercept	39.31632635	0.444149548	88.52047	3.18E-06	37.9028443	40.729808	37.9028443	40.7298084
speed H	0.246930985	0.397259433	0.621586	0.578249	-1.01732583	1.5111878	-1.01732583	1.5111878
pack H	-0.58639562	0.397259433	-1.4761	0.236399	-1.85065243	0.6778612	-1.85065243	0.67786119
heating H	-0.28788883	0.397259433	-0.72469	0.521051	-1.55214564	0.976368	-1.55214564	0.97636799
water H	0.079389069	0.397259433	0.199842	0.854384	-1.18486774	1.3436459	-1.18486774	1.34364588

RESIDUAL OUTPUT

Observation	*Predicted S/N*	*Residuals*
1	39.31632635	0.37586834
2	39.10782659	-0.542503025
3	38.97686171	-0.542503025
4	38.76836196	0.37586834
5	38.8093198	0.192804945
6	38.4420419	-0.026170261
7	39.6426464	-0.026170261
8	39.27536851	0.192804945

4. Regression Analysis of Roughness Property

4.1 PC

SUMMARY OUTPUT

Regression Statistics	
Multiple R	0.68330889
R Square	0.46691104
Adjusted R Square	-0.2438742
Standard Error	3.72041569
Observations	8

ANOVA

	df	*SS*	*MS*	*F*	*ignificance F*
Regression	4	36.36961018	9.092403	0.656895	0.66182335
Residual	3	41.52447879	13.84149		
Total	7	77.89408896			

	Coefficients	*Standard Error*	*t Stat*	*P-value*	*Lower 95%*	*Upper 95%*	*Lower 95.0%*	*Upper 95.0%*
Intercept	23.6147353	2.941246858	8.028818	0.004034	14.2543751	32.975096	14.2543751	32.9750955
speed H	1.65693915	2.630731165	0.62984	0.573502	-6.7152215	10.0291	-6.7152215	10.0290998
pack H	1.93667635	2.630731165	0.736174	0.514964	-6.4354843	10.308837	-6.4354843	10.308837
heating H	3.06904351	2.630731165	1.166612	0.327671	-5.3031172	11.441204	-5.3031172	11.4412042
water H	1.50652395	2.630731165	0.572664	0.606976	-6.8656367	9.8786846	-6.8656367	9.87868462

RESIDUAL OUTPUT

Observation	*redicted S/N*	*Residuals*
1	23.6147353	-3.901351418
2	28.1903028	0.885220087
3	27.2083508	0.885220087
4	31.7839183	-3.901351418
5	27.0579356	1.184369973
6	28.6204552	1.831761358
7	26.7781984	1.831761358
8	28.340718	1.184369973

4.2 PC/ABS

SUMMARY OUTPUT

Regression Statistics	
Multiple R	0.91393886
R Square	0.83528425
Adjusted R Square	0.61566324
Standard Error	0.61129665
Observations	8

ANOVA

	df	*SS*	*MS*	*F*	*ignificance F*
Regression	4	5.684921139	1.42123	3.803299	0.1506086
Residual	3	1.121050786	0.373684		
Total	7	6.805971924			

	Coefficients	*Standard Error*	*t Stat*	*P-value*	*Lower 95%*	*Upper 95%*	*Lower 95.0%*	*Upper 95.0%*
Intercept	27.5927937	0.483272436	57.09573	1.18E-05	26.054805	29.130782	26.0548052	29.1307823
speed H	-0.8671135	0.432252007	-2.00604	0.138514	-2.242732	0.5085053	-2.2427323	0.50850526
pack H	-0.0192857	0.432252007	-0.04462	0.967217	-1.394904	1.3563331	-1.3949045	1.35633314
heating H	1.44479539	0.432252007	3.342484	0.044306	0.0691766	2.8204142	0.06917659	2.82041419
water H	0.05262148	0.432252007	0.121738	0.910803	-1.322997	1.4282403	-1.3229973	1.42824028

RESIDUAL OUTPUT

Observation	*redicted S/N*	*Residuals*
1	27.5927937	0.577673244
2	29.0902106	-0.286801083
3	26.7063945	-0.286801083
4	28.2038114	0.577673244
5	27.6261295	-0.371556455
6	29.0183035	0.080684293
7	26.7783017	0.080684293
8	28.1704756	-0.371556455

4.3 PA6GF30

SUMMARY OUTPUT

Regression Statistics	
Multiple R	0.78466441
R Square	0.61569824
Adjusted R Square	0.10329589
Standard Error	7.9775092
Observations	8

ANOVA

	df	*SS*	*MS*	*F*	*Significance F*
Regression	4	305.8802352	76.47006	1.201591	0.45825947
Residual	3	190.921959	63.64065		
Total	7	496.8021942			

	Coefficients	*Standard Error*	*t Stat*	*P-value*	*Lower 95%*	*Upper 95%*	*Lower 95.0%*	*Upper 95.0%*
Intercept	0.95509715	6.30677478	0.15144	0.889239	-19.115875	21.0260693	-19.115875	21.0260693
speed H	0.52434612	5.64095085	0.092953	0.9318	-17.427677	18.4763693	-17.427677	18.4763693
pack H	0.16432321	5.64095085	0.02913	0.97859	-17.7877	18.1163464	-17.7877	18.1163464
heating H	10.1793243	5.64095085	1.80454	0.16891	-7.7726989	28.1313475	-7.7726989	28.1313475
water H	7.00139516	5.64095085	1.241173	0.302749	-10.950628	24.9534183	-10.950628	24.9534183

RESIDUAL OUTPUT

Observation	*Predicted S/N*	*Residuals*
1	0.95509715	-5.410005308
2	18.1358166	-4.330344316
3	1.64376649	-4.330344316
4	18.8244859	-5.410005308
5	8.12081552	4.913388037
6	11.2987446	4.826961587
7	8.48083843	4.826961587
8	11.6587675	4.913388037

5. Regression Analysis of Warpage Property

5.1 PC

SUMMARY OUTPUT

Regression Statistics	
Multiple R	0.99774121
R Square	0.99548751
Adjusted R Square	0.98947086
Standard Error	0.51073619
Observations	8

ANOVA

	df	*SS*	*MS*	*F*	*ignificance F*
Regression	4	172.6371788	43.15929	165.4554	0.00075576
Residual	3	0.782554381	0.260851		
Total	7	173.4197332			

	Coefficients	*Standard Error*	*t Stat*	*P-value*	*Lower 95%*	*Upper 95%*	*Lower 95.0%*	*Upper 95.0%*
Intercept	7.49070665	0.403772415	18.5518	0.000342	6.20572262	8.77569067	6.20572262	8.775690674
speed H	-4.36492335	0.361145027	-12.0863	0.001219	-5.514248	-3.2155987	-5.514248	-3.21559869
pack H	0.54632774	0.361145027	1.512766	0.227542	-0.6029969	1.6956524	-0.6029969	1.695652397
heating H	-2.36680129	0.361145027	-6.5536	0.007224	-3.5161259	-1.2174766	-3.5161259	-1.21747664
water H	-7.83363333	0.361145027	-21.6911	0.000214	-8.982958	-6.6843087	-8.982958	-6.68430868

RESIDUAL OUTPUT

Observation	*Predicted S/N*	*Residuals*
1	7.49070665	-0.321614809
2	-2.70972798	-0.280591969
3	3.67211104	-0.280591969
4	-6.52832359	-0.321614809
5	0.20340105	0.418965068
6	5.67023309	0.183241709
7	-4.70785004	0.183241709
8	0.758982	0.418965068

5.2 PC/ABS

SUMMARY OUTPUT

Regression Statistics	
Multiple R	0.925756
R Square	0.85702417
Adjusted R Square	0.66638974
Standard Error	3.30746796
Observations	8

ANOVA

	df	*SS*	*MS*	*F*	*ignificance F*
Regression	4	196.7175014	49.17938	4.495642	0.12356118
Residual	3	32.81803294	10.93934		
Total	7	229.5355343			

	Coefficients	*Standard Error*	*t Stat*	*P-value*	*Lower 95%*	*Upper 95%*	*Lower 95.0%*	*Upper 95.0%*
Intercept	4.75622797	2.614783011	1.818976	0.166491	-3.5651786	13.077635	-3.5651786	13.0776345
speed H	-3.01904703	2.338733024	-1.29089	0.287221	-10.461939	4.4238452	-10.461939	4.42384524
pack H	0.60261655	2.338733024	0.257668	0.813327	-6.8402757	8.0455088	-6.8402757	8.04550883
heating H	-3.4107849	2.338733024	-1.45839	0.240813	-10.853677	4.0321074	-10.853677	4.03210737
water H	-8.789056	2.338733024	-3.75804	0.032934	-16.231948	-1.346164	-16.231948	-1.3461637

RESIDUAL OUTPUT

Observation	*Predicted S/N*	*Residuals*
1	4.75622797	-2.25872184
2	-7.44361292	2.703663126
3	2.33979749	2.703663126
4	-9.8600434	-2.25872184
5	-3.43021147	1.173668936
6	1.94805963	-1.61861022
7	-7.05187506	-1.61861022
8	-1.67360396	1.173668936

5.3 PA6GF30

SUMMARY OUTPUT

Regression Statistics	
Multiple R	0.45683533
R Square	0.20869852
Adjusted R Square	-0.8463701
Standard Error	2.61323506
Observations	8

ANOVA

	df	*SS*	*MS*	*F*	*Significance F*
Regression	4	5.403256776	1.350814	0.197806	0.9242586
Residual	3	20.48699249	6.828997		
Total	7	25.89024927			

	Coefficients	*Standard Error*	*t Stat*	*P-value*	*Lower 95%*	*Upper 95%*	*Lower 95.0%*	*Upper 95.0%*
Intercept	2.03459576	2.065943716	0.984826	0.397324	-4.5401592	8.60935071	-4.5401592	8.609350707
speed H	-1.4293246	1.847836234	-0.77351	0.495579	-7.3099642	4.45131496	-7.3099642	4.451314963
pack H	0.74887574	1.847836234	0.405272	0.712447	-5.1317639	6.62951533	-5.1317639	6.629515333
heating H	-0.3119005	1.847836234	-0.16879	0.876699	-6.1925401	5.56873912	-6.1925401	5.568739122
water H	0.02372141	1.847836234	0.012837	0.990564	-5.8569182	5.90436101	-5.8569182	5.90436101

RESIDUAL OUTPUT

Observation	*Predicted S/N*	*Residuals*
1	2.03459576	-0.10607039
2	1.7464167	-2.53930391
3	1.35414687	-2.53930391
4	1.06596781	-0.10607039
5	2.80719291	1.700296996
6	2.47157103	0.945077301
7	0.62899254	0.945077301
8	0.29337065	1.700296996

APPENDIX B

CONFERENCE PROCEEDING

The 6th TSME International Conference on Mechanical Engineering
16-18 December 2015

AMM029

Elimination of Weld lines in Injection-Molded Parts by means of the Induction Heated Mold

Sineenat Tongjoy[1,*], Patcharee Larpsuriyakul[2], Dumrong Thanomjitr[2], Natcha Prakymoramas[2], Preechar Karin[1], Takushi Saito[3], Isao Satoh[3]

[1] International College, King Mongkut's Institute of Technology Ladkrabang, Bangkok, 10520, Thailand
[2] National Metal and Materials Technology Center (MTEC), Klong Luang, Pathumthani, 12120, Thailand
[3] Department of Mechanical and Control Engineering, Tokyo Institute of Technology, 12-1, O-okayama 2, Meguro-ku, Tokyo 152-8552, Japan
* Corresponding Author: sineenat.tongjoy@gmail.com, 66-870913912

Abstract

Weld line is one of the most common injection molding problems where two separated melt fronts join together. It affects both the appearance and strength of plastic products. In this study, elimination of weld lines in injection-molded parts by means of the induction heated mold was accomplished using the induction heated mold and with polycarbonate/acrylonitrile-butadiene-styrene (PC/ABS) as the molding material. The effect of the injection molding parameters; injection speed, holding pressure, heating temperature, and water temperature, on the occurrence or visibility of a weld line was studied; thereby the exact number of the molding conditions was designed by employing Taguchi's 2-level L8 orthogonal array. The depth and width of a V-notch characterizing the degree of visibility of a weld line were thoroughly investigated by means of the 3D measuring laser microscope. From the results, the optimal combination and ranking of each processing parameter affecting the weld line visibility were obtained upon performing the S/N ratio analysis. It was found that the visibility of weld line was effectively decreased by increasing the mold heating temperature to above the melt's glass transition temperature (Tg) prior to the melt filling stage. In addition, the weld line was almost invisible at the heating temperature of 160°C. The S/N ratio analysis of the results revealed that the optimal parameter setting resulting in the smallest depth and width of V-notch was high injection speed, high holding pressure, high heating temperature, and high water temperature. Two parameters mostly affecting the depth and width of a V-notch were the heating temperature and injection speed, respectively.

Keywords: weld line, induction heating, injection molding, Taguchi method

1. Introduction

Nowadays plastics have been being popular in a wide variety of industrial applications. Injection molding is one of the most widely used process for manufacturing plastic products because of its advantages such as short cycle times, high production rate, high quality of part surface, easy to produce the complex geometry parts, good mechanical properties and low cost. Although injection molding has many advantages, some defects frequently occur in the injection-molded parts. Weld line is one of the common injection molding defects. It is generated when the two separated melt fronts meet each other after the holes or from two or multi-gates. Weld lines can be caused by melt fronts flowing around holes or inserts in the cavity, multiple gates or mold of variable depth where hesitation can occur. Weld lines reduce the surface quality and mechanical strength of the injection-molded parts [1-3].

The effect of processing parameter on weld line has been investigated in numerous studies [4-6]. Previous studies have indicated that the mold temperature is the key parameter on the reduction of the depth and width of weld lines [6]. Weld line can be sufficiently reduced when the mold temperature is higher than the glass transition temperature of molded material prior to the injection. However the higher mold temperature results in the mold heating and cooling time increment. Therefore the rapid heat cycle molding technology (RHCM) have been studied and developed to heat and cool the mold rapidly. Induction heating is one of RHCMs. Induction heating occurs due to electromagnetic force fields producing Eddy current on the mold surface. The resistance to the flow of the Eddy current results in a rapid temperature rise on the mold surface [7]. Chen et al. [8] studied the improvement the surface appearance of weld lines by means of the induction heating. Huang and Tai [9] used induction heating to heat the mold surfaces rapidly resulting in improvement of the replication rate of the height of the microstructure of light guided plates (LGP) in the injection molding process. Park et al. [10] applied high-frequency induction heating to eliminate weld lines in an injection-molded plastic part.

The objective of this study is to eliminate the weld line by applying induction heating to heat the mold surface over the melt's glass transition temperature (Tg) prior the injection. To investigate the effect of the induction heating conditions on the occurrence or visibility of a weld line, the experimental layout was designed by Taguchi method. The injection molding with induction heating was then performed. The optimal combination and ranking of each processing parameter affecting the depth and width of weld line's

The 6th TSME International Conference on Mechanical Engineering
16-18 December 2015

AMM029

V-notch were obtained upon performing the S/N regression analysis.

2. Taguchi Method

Taguchi method is a form of the design of experiment (DOE) techniques that are the powerful tool to optimize the design for performance, quality and cost and reduce the sensitivity of the system performance to source of variation. Taguchi method is appropriate to study the effect of several parameters on the desired characteristic. Taguchi method utilizes the specifically designed tables known as "orthogonal array" to design the experimental layout. With the orthogonal array, the number of experimental trials can be reduced to study the entire system. The experimental results based on orthogonal array are converted into a form of signal to noise (S/N) ratio. In terms of S/N ratio, signal or S represents the desired value (mean) from the control factors for the outcome characteristic and noise or N represents the undesired value from uncontrollable factor for the outcome characteristic. S/N ratio can be categorized into three quality characteristic i.e. smaller-the-better, larger-the-better, and nominal-the-best. Calculation of the S/N ratio depends on the desired quality characteristics or experimental objective as follows [11]:

- For smaller-the-better:

$$S/N = -10\,log_{10}\left(\frac{1}{n}\sum_{i=0}^{n} y_i^2\right) \quad (1)$$

- For larger-the-better:

$$S/N = -10\,log_{10}\left(\frac{1}{n}\sum_{i=0}^{n}\frac{1}{y_i^2}\right) \quad (2)$$

- For nominal-the-best:

$$S/N = 10\,log_{10}\left(\frac{\mu_y^2}{\sigma_y^2}\right) \quad (3)$$

where y_i is the measured data or output for the ith trial, n is the number of trials, and μ_y and σ_y represent the mean and standard deviation of the response variable Y, respectively.

The larger S/N ratio provides better quality characteristics, regardless of the category of the quality characteristic. Thus, the optimal level of the process parameters is the level with the largest S/N ratio. The S/N ratio for each level of process parameters is calculated based on the S/N analysis. To determine the effect of each parameter and the optimal parameter combination on the output, the signal to noise (S/N) ratio is employed by Taguchi method.

3. Experimental

3.1 Material and Molding

Polycarbonate/acrylonitrile-butadiene-styrene (PC/ABS) (Bayblend® T85XF was used as the molding material. An injection molding machine (FANUC ROBOSHOT S-2000i 100B) together with a single layer multi turn of induction coil was employed to implement the experiments.

3.2 Experimental Design

In this study, the four control factors; injection speed (A), holding pressure (B), heating temperature or the mold surface temperature before the filling stage (C), and water temperature (D), with two levels were chosen. Thus, the experiments were performed according to Taguchi's 2-level L8 orthogonal array as shown in Table. 1. Table. 2 listing 8 experiments based on a L8 orthogonal array was required to further determine the optimum parameter setting of the levels of these factors. Noted that 'no heating' means the mold surface has relatively the same temperature as the water temperature of each condition used.

Table. 1 Factors and levels for the Taguchi experiments

Factor	Level	
	1	2
A: Injection Speed (mm/s)	25	100
B: Holding Pressure (kgf/cm²)	1200	1300
C: Heating Temperature (°C)	no heating*	160
D: Water Temperature (°C)	30	80

Table. 2 Experimental layout based on a L_8 orthogonal array

Experiment	Factor			
	A	B	C	D
1	1	1	1	1
2	1	1	2	2
3	2	2	1	1
4	2	2	2	2
5	1	2	1	2
6	1	2	2	1
7	2	1	1	2
8	2	1	2	1

3.3 Weld line Measurement

The depth and width of a V-notch characterizing the degree of visibility of a weld line were thoroughly investigated by means of the 3D measuring laser microscope (Olympus LEXT OLS4100) as shown in Fig.1. For all measurements, a total magnification of 50X was used to investigate the weld line thereby three samples per experiment were analyzed.

4. Results and Discussion

The experimental results showed that during the induction heating and cooling, it took 16 s to bring the cavity surface temperature from 80 to 160°C and 65 s to return to 80°C.

The 6th TSME International Conference on Mechanical Engineering
16-18 December 2015

AMM029

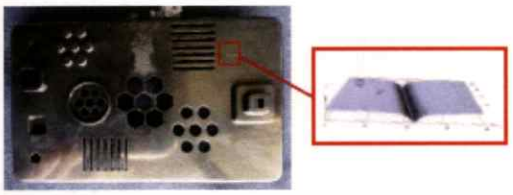

Fig. 1 The position of weld line's V-notch investigated by means of the 3D laser measuring microscope

Fig. 2 shows the top view of V-notch of weld line for each experiment at a total magnification of 50X. It was found that weld line is smaller and less visible when the heating temperature was higher. According to the Taguchi experimental design, the experiments were performed and the results of the measured depth and width of V-notch were obtained as shown in Table. 3. To investigate the effect of each molding parameter on the depth and width of a V-notch, the S/N ratio analysis was employed to analyze the measured values. Due to V-notch structure of weld lines cause the poor surface quality of the injection-molded parts so the smaller depth and width of V-notch can improve this issue. Therefore, the smaller-the-better quality characteristic of S/N ratio as Eq. 1 is carried out to identify the optimum setting and ranking in eliminating the weld line. The calculated S/N ratios are listed in Table. 3. Table. 4 and Table. 5 show the mean S/N ratios of each level of the parameter for the depth and width of V-notch, respectively. By considering the smallest depth and width, the level with highest mean S/N ratio for each parameter are selected as the optimum parameter setting. This optimum parameter setting of the smallest depth and width can be obtained from No.4 of experiments which is the combination of high injection speed (100 mm/s), high holding pressure (1300 kgf/cm²), high heating temperature (160°C), and high water temperature (80°C). The ranking of each parameter affecting the weld line visibility is obtained from the difference between the maximum and minimum value (Max-Min) of mean S/N ratio for each parameter. The effect of parameter depends on how large the Max-Min value is. In the other words, the parameter with the highest Max-Min value is the most effective parameter affecting the weld line visibility.

Table. 4 shows that the most effective parameter resulting in the smallest depth of v-notch is the heating temperature, followed by injection speed, water temperature, and holding pressure, respectively. Table. 5 points out that the most effective parameter promoting the smallest width of v-notch is the injection speed, followed by heating temperature, water temperature, and holding pressure, respectively.

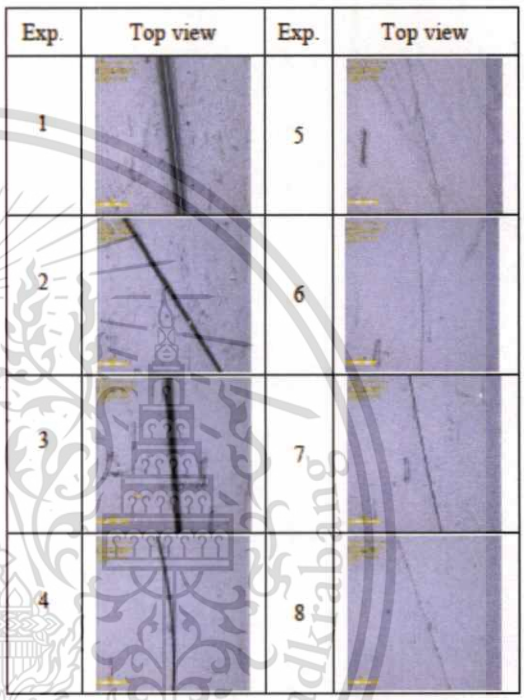

Fig. 2 The top view of V-notch of weld line for each experiment at a total magnification of 50X

According to the results, it was found that when the mold surface temperature exceeded the melt's glass transition temperature the depth was obviously decreased from 5.610 μm of experiment No.5 (heating temperature and injection speed of 80°C and 25 mm/s, respectively) to 0.096 μm of experiment No.4 (heating temperature and injection speed of 160°C and 100 mm/s, respectively). This resulted from the high mold surface temperature before the filling stage that then

Table. 3 Calculated S/N ratio for the measured depth and width of V-notch

Exp.	Factor Combination				V-notch							
					Depth (μm)				Width (μm)			
	A	B	C	D	1	2	3	S/N ratio	1	2	3	S/N ratio
1	25	1200	30	30	10.899	10.922	11.225	-20.84	100.414	103.210	106.938	-40.30
2	25	1200	160	80	0.537	0.437	0.520	6.02	40.081	42.792	44.233	-32.55
3	100	1300	30	30	3.396	2.801	3.156	-9.90	30.675	31.522	40.505	-30.76
4	100	1300	160	80	0.093	0.116	0.078	20.27	2.203	2.288	2.288	-7.08
5	25	1300	80	80	5.384	5.540	5.907	-14.99	74.230	76.009	79.653	-37.69
6	25	1300	160	30	1.093	0.903	0.786	0.57	48.131	49.571	51.859	-33.96
7	100	1200	80	80	1.632	1.685	1.850	-4.73	34.658	39.742	37.454	-31.44
8	100	1200	160	30	0.236	0.225	0.261	12.36	24.658	20.422	21.862	-27.00

AMM029

again prohibited or slowed down the freezing of the melt. Consequently, the molecular mobility is higher resulting in the increase in the diffusion of molecules across the weld line interface. The high temperature and high injection speed also prevented the premature melt freezing. This leads to the smaller depth and width of V-notch.

Table. 4 S/N ratio for the depth of V-notch by factor level

Parameter	Mean S/N ratio			Rank
	Level 1	Level 2	Max-Min	
V_{inj}	-7.31	4.50*	11.81	2
$P_{holding}$	-1.80	-1.01*	0.79	4
$T_{heating}$	-12.62	9.81*	22.43	1
T_{water}	-4.45	1.64*	6.09	3

*Optimum Level

Table. 5 S/N ratio for the width of V-notch by factor level

Parameter	Mean S/N ratio			Rank
	Level 1	Level 2	Max-Min	
V_{inj}	-36.13	-24.07*	12.06	1
$P_{holding}$	-32.82	-27.37*	5.45	4
$T_{heating}$	-35.05	-25.15*	9.90	2
T_{water}	-33.01	-27.19*	5.82	3

*Optimum Level

5. Conclusion

This study applied the induction heating to heat the mold surface aiming to study the elimination of weld line. The effects of the processing parameters including injection speed, holding pressure, heating temperature, and water temperature on the occurrence or visibility of a weld line were investigated by employing Taguchi method together with the regression analysis. The results showed that the heating temperature or the mold surface temperature before the filling stage and injection speed were the main driving parameters responsible for the smaller depth and width of V-notch. Furthermore, the optimum parameter setting was obtained as follows: high injection speed, high holding pressure, and high heating temperature.

6. Acknowledgement

This study was financially supported by National Metal and Materials Technology Center (MTEC), T. Krungthai Industries Public., Ltd. and NSTDA-University-Industry Research Collaboration.

7. References

[1] Brahimi, B., Ait-Kadi, A. and Ajji, A. (1994). Weld line and mechanical properties of injection molded Polyethylene/ Polystylene/Copolymer blends, *Polymer Engineering & Science*, vol.34(15), August 1994, pp. 1202 - 1210.

[2] Nadkarni, V. M. and Ayodhya, S. R. (1993). The influence of knit-lines on the tensile properties of fiberglass reinforced thermoplastics, *Polymer Engineering & Science*, vol.33(6), March 1993, pp. 358 - 367.

[3] Tomari, K. et al. (1990). The V-notch at weld lines in polystyrene injection moldings, Polymer Engineering & Science, vol.30(15), August 1990, pp. 931 - 936.

[4] Malguarnera, S. C., and Manisali, A. (1981).The effects of processing parameters on the tensile properties of weld lines in injection molded thermoplastics, *Polymer Engineering & Science*, vol.21(10), July 1981, pp. 586 - 593.

[5] Selden, R. (1997). Effect of processing on weld line strength in five thermoplastics, *Polymer Engineering & Science*, vol.37(1), January 1997, pp. 205 - 218.

[6] Tosello, G., Gava, A., Hansen, H. N., Lucchetta, G. and Marinello, F. (2009).Characterization and analysis of weld lines on micro-injection moulded parts using atomic force microscopy(AFM), *Wear*, vol.266(5-6), March 2009, pp. 534 - 538.

[7] Haimbaugh, R.E. (2001). Practical Induction Heat Treating, 1st edition, ISBN: 0-87170-743-8, ASM International, United States of America.

[8] Chen, S.C., Jong, W.R. and Chang, J.A. (2006). Dynamic mold surface temperature control using induction heating and its effects on the surface appearance of weld line, *Journal of Applied Polymer Science*, vol.101(2), July 2006, pp. 1174 - 1180.

[9] Huang, M.S. and Tai, N.S. (2009). Experimental rapid surface heating by induction for micro-injection molding of light-guided plates, *Journal of Applied Polymer Science*, vol.113(2), July 2009, pp. 1345 - 1354.

[10] Park, K., Sohn, D.H. and Cho, K.H. (2010). Eliminating weldlines of an injection-molded part with the aid of high-frequency induction heating, *Journal of Mechanical Science and Technology*, vol.24(1), January 2010, pp. 149 - 152.

[11]Taguchi, G. (1990). Introduction to quality engineering: designing quality into products and processes, Asian Productivity Organization, ISBN: 9-28331-084-5, The Organization, Tokyo.

AUTHOR BIOGRAPHY

NAME: Sineenat Tongjoy

DATE OF BIRTH: April 2nd, 1991

ADDRESS: 692/24 Phichaironnarong Songkram Road, Pak Phriao, Muang, Saraburi 18000

EDUCATIONAL BACKGROUND:

2009-2012	B.Eng. in Petrochemicals and Polymeric Materials, Silpakorn University
2013-2015	M.Eng. in Automotive Engineering (International program), International College, King Mongkut's Institute of Technology Ladkrabang (KMITL)

SCHOLARSHIP:

2013 - 2015	Full scholarship for study in the master degree from National Science and Technology Development Agency (NSTDA)
2014-2016	NUI-RC Scholarship (NSTDA-University-Industry Research Collaboration)